THE EFFECT OF CHEMICAL COMPOSITION VARIATIONS ON THE BRITTLE-DUCTILE TRANSITION TEMPERATURES OF STEELS.

A thesis presented for the degree
of Master of Science in Engineering
in the University of Cape Town

by

L.A. ERASMUS

January 1971

SYNOPSIS.

The development and use of a wide range of new constructional materials has taken place in the last decade. Steel remains however the most widely used and cheapest material available to the engineer. Despite a long record of service, failures still occur in major steel structures due to a lack of understanding of its basic properties. Sudden and catastrophic failure by cleavage fracture is one of the properties of steel which is still not widely appreciated.

In this investigation the brittle to ductile transition has been examined from theoretical considerations and related to a detailed study of the effects of carbon, manganese, nickel, chromium and some of the lesser known elements such as oxygen, nitrogen, aluminium and silicon on the propensity of steel to cleavage fracture.

Using the standard Charpy test to determine the ductile transition temperature of a wide range of experimental steels, the variation in transition temperature brought about by the above elements has been examined using multiple linear regression techniques. It has been shown that the temperature at

which the transition from ductile to brittle cleavage fracture occurs can be predicted by a semi-analytical equation based on the chemical composition and grain size of the steel, as follows:-

$$T_{20} = 264(\%C) - 11.8(d^{-\frac{1}{2}}) + 28(\%Mn) - 140{,}000(F') + 3850(\%N_R) + 18(\%Cr) + 50(\%Al_R) + 68(\%Si) + \text{constant}$$

where F' is a variable dependent on dislocation locking strength.

The equation has been shown to be applicable to a wide range of experimental steels, commercial steels and to steels used in published research papers.

A modification of the above equation has been produced for the comparison of steels in the normalised condition where grain size measurements are not available.

ACKNOWLEDGEMENTS.

The support of Professor D.C. Stevenson, Head of Department of Mechanical Engineering, University of Canterbury, and Emeritus Professor R.J. Rastrick, former Head of the Department, is gratefully acknowledged.

This research project was started whilst the author was in the Research Department of Steel Peech and Tozer Ltd., (now B.S.C.) Sheffield, England. My grateful thanks go to the Directors of Steel Peech and Tozer Ltd., for their continual interest and support in providing materials for the project, and to former colleagues, particularly Mrs. E. Portman of the Metallurgical Services Department, and Mr. P.B. Dunnill, Chief Chemist, for their valuable assistance.

Many members of the technical staff of the Department of Mechanical Engineering, University of Canterbury, assisted with the testing programme and preparation of the thesis, especially Miss B. Barclay, Mrs. V. Grey, and Messrs E.D. Retallick and D. Somerville. Their willing assistance and the meticulous typing of Mrs. N. Newman, is gratefully acknowledged.

Much of the success of the computer analysis of data is due to a colleague, Mr. J.S. Smaill, who contributed many weekend hours to this project.

The continued encouragement and sacrifices of my wife and family over the last year have made this thesis possible.

CONTENTS.

LIST OF FIGURES.

CHAPTER 1

INTRODUCTION

1.1 Scope of Thesis:

Sudden, catastrophic failure of structures due to unexpected brittle fractures has been a problem and of concern to engineers ever since the introduction of low carbon steel as a structural material. This problem was raised in an acute form during the Second World War following the occurrence of brittle fractures in welded Liberty ships and T-2 tankers. These calamities focused attention on the fact that normally ductile steels can become brittle under certain conditions. Three basic factors are known to contribute to this change to the brittle cleavage-type fracture in any one steel:-

a) a triaxial state of stress

b) low temperatures, and

c) a high strain rate or rapid rate of loading.

In most steels this transition from ductile to brittle behaviour occurs over a very limited range of temperature, called the transition temperature. Changes in this transition temperature of over 100°C. can be producted by changes in the chemical composition or microstructure of low carbon structural steels. Although these effects have

long been established on a qualitative basis[1]* (see Table 1.1) few attempts have been made to assess the effect of chemical composition and microstructure quantitatively. The purpose of this thesis is therefore to make a quantitative study of the effects of carbon, manganese, nickel, chromium and some of the lesser known elements in steel, such as nitrogen, oxygen, aluminium and silicon, on the brittle - ductile transition temperature.

1.2 Classification of Fractures:

Fracture can be defined as the separation, or fragmentation of a solid body into two or more parts under the action of stress. Fracture in steels can be broadly classified into the two categories of ductile and brittle fractures. Ductile fractures are characterised by the occurrence of appreciable amounts of plastic deformation, both prior to and during the fracture process, and in the vicinity of the actual fracture; whereas brittle fractures show none of this gross deformation.

Although this classification of fractures is commonly used to describe fractures in steels and other metals used in engineering a further sub-classification becomes

---

* Numbers in parenthesis indicate references

Table 1.1

Effect of metallurgical factors on the transition temperature behaviour of steel structures.

Factors which lower the transition temperature	Factors which raise the transition temperature
1. Deoxidation practice	Rimming practice
Aluminium residual	High rolling temperatures
Silicon (below 0.25%)	Large section sizes
Small ferritic grain size	Carbon
	Nitrogen
2. Alloy content	Oxygen
High Mn-to-C ratio	Phosphorus
Low carbon	Boron
Low phosphorus	Molybdenum
Nickel	Silicon (over 0.25%)
	Annealing
3. Heat treatment	Notches
Normalising	Temper brittleness
Quench and temper	Cold deformation
Chromium has little effect.	

From reference 1.

necessary to adequately describe all fractures. Fatigue fractures, produced by fluctuating stress conditions, appear on a macroscopic scale to be brittle, since the two halves of the fracture can be fitted together without any noticeable plastic deformation. It is almost certain however that most fatigue fractures occur by one or other of a series of plastic blunting processes,[2,3] where the plastic deformation is localised at the tip of the advancing fatigue crack, and can only be seen on a micro scale.[4]

Brittle fractures can also be classified into transgranular (cleavage) and intergranular (stress corrosion etc) sub-groups, and ductile fractures into various shear mode processes, the most common of which is that of microvoid coalescence commonly found in polycrystalline metals.[4] An electron-photomicrograph of a typical microvoid coalescence fracture surface is shown in Fig.1-1. This can be compared with that of a cleavage fracture surface, as shown in Fig.1-2. A full discussion of the interpretation and characteristics of these fractures has been given elsewhere.[4]

1.3 The Problem of Brittle Fracture:

Engineering structures and components are conventionally designed in such a way that the yield strength of the steel is not exceeded. Thus the nominal working stress in

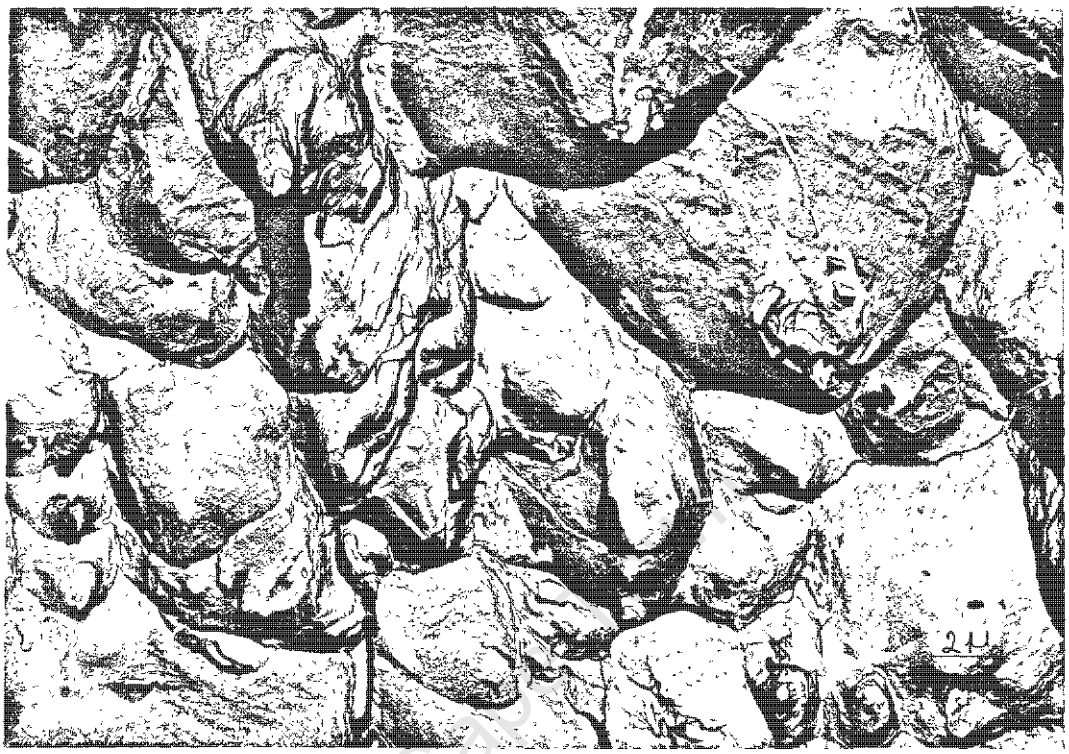

Fig.1-1 Ductile type fracture by microvoid coalescence in aluminium.

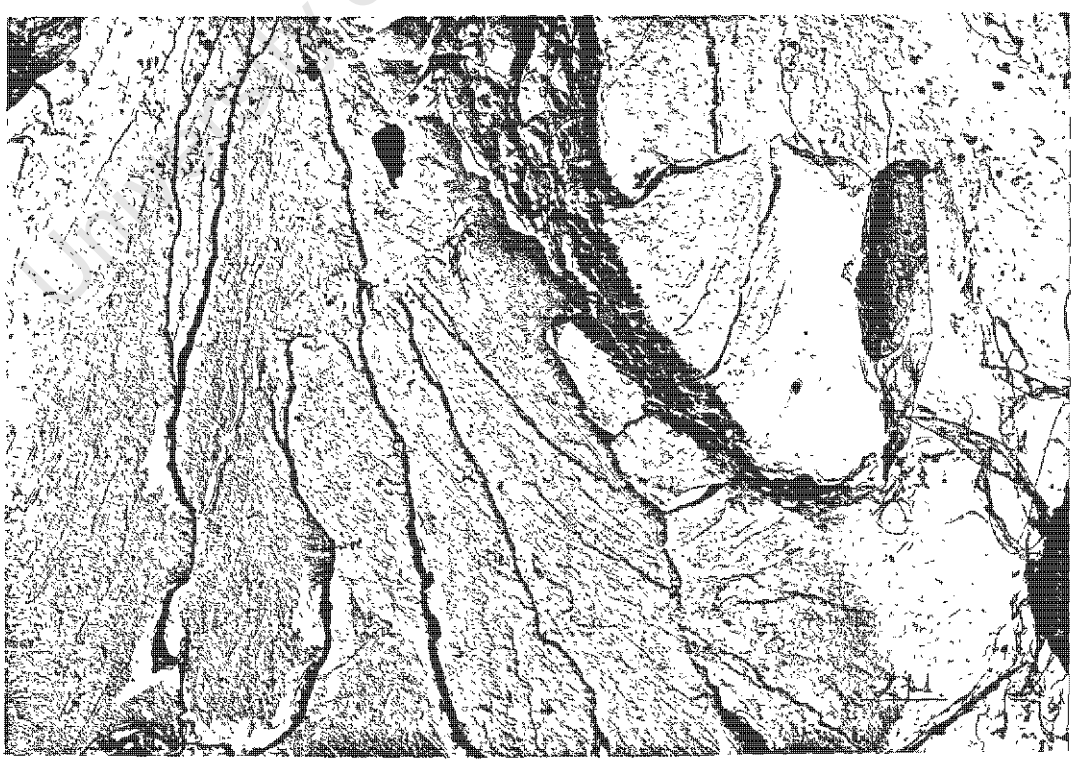

Figs.1-2 Cleavage fracture in low carbon steel showing area of dimple rupture (microvoid coalescence) near

any member is below the yield strength and the structure should be safe, this concept usually allowing for the inevitability of local yielding and plastic deformation around discontinuities, but relying on elastic or tri-axial constraint to preserve the structural integrity of a member or framework as a whole. This design approach assumes that the fracture strength is greater than the yield strength and does not concern itself with fracture, and although generally reliable accidental failures do occur, sometimes with catastrophic results.(5)

Accidental fractures will continue to occur as long as structures are built, but it is most desirable that the structure should give some warning of impending failure and if possible that the fracture should take place slowly, since with rapid fractures considerable strain energy is suddenly released. This can cause the structure to shatter and this shattering action is in many cases the cause of the most serious damage. For this reason brittle fractures which occur without warning and are characterised by a rapid rate of crack propagation are to be avoided. These fractures are usually of the transgranular cleavage type and occur in the bcc and cph metals by direct separation of the atomic lattice along the low index crystallographic planes in each grain of the polycrystalline matrix.

During the Second World War brittle fractures of this type were experienced in approximately 25% of the "all welded" Liberty ships constructed in the U.S.A.[5] Of 4,694 ships of this type, 1,289 structural failures were reported, 233 being catastrophic and the vessels were either lost or considered unsafe. These failures led to considerable research effort being concentrated on the problem of brittle fracture in low carbon steel plate, so that this phenomena has probably been more extensively studied than any other fracture mode.[6]

1.4 Fracture by Cleavage:

Cleavage fracture can be described as the transgranular splitting of a metal along certain low index crystallographic planes, called cleavage planes. The $\{100\}$ planes have been shown to be the common cleavage planes in the bcc metals, e.g., V, Cr, Mo, W, Fe and most steels, and the $\{0001\}$ planes in the cph metals, e.g., Mg, Zn, Sn, etc. Cleavage fracture does not normally occur in the fcc metals. In a polycrystalline metal such as low carbon steel, the cleavage fracture surface appears bright, or granular, owing to light being reflected from the flat "cleaved" surface of each grain. Since cleavage is the pulling apart of atomic planes as opposed to the shearing of these planes across each other as in shear fractures, fracture is governed by the tensile stress normal to the fracture plane. Cleavage fracture is therefore

more likely in components or structures where the ratio of tensile stress σ to shear stress τ is high. That is triaxially stressed structures are more likely to fail by cleavage than uniaxially stressed structures, which in turn are more susceptible than torsionally stressed structures, see Fig.1-3. The cohesive strength of the crystal structure can therefore be expected to have a controlling influence on cleavage fracture.

1.5 Theoretical Cohesive Strength:

On an atomic scale the cleavage strength of a metal will depend on the strength of its atomic bonds. Reference to Fig.1-4 shows that the resultant tensile force between atoms increases as they are pulled apart, so that the attractive force between atoms increases to a maximum σ_{max} which is the theoretical cohesive strength.

A good approximation of cohesive strength can be obtained by assuming the cohesive force to be represented by a sine curve as in Fig.1-4, and assuming x to be measured from the atom's equilibrium distance apart a_o, then

$$\sigma = \sigma_{max} \sin\left(\frac{2\pi x}{\lambda}\right) \qquad \text{.....Eqn.1.1}$$

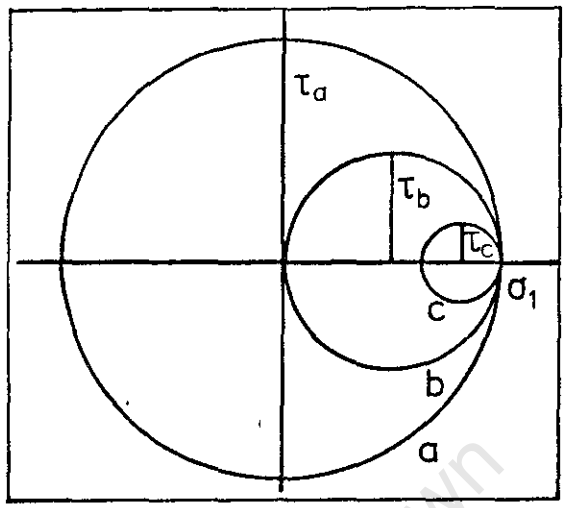

Fig. 1·3 Mohr's stress circle for components:-
(a) in torsion, $\frac{\sigma}{\tau} = 1{\cdot}0$
(b) in uniaxial tension, $\frac{\sigma}{\tau} = 2{\cdot}0$
(c) with triaxial stress, eg. a sharp notch, $\frac{\sigma}{\tau} \approx 6{\cdot}0$

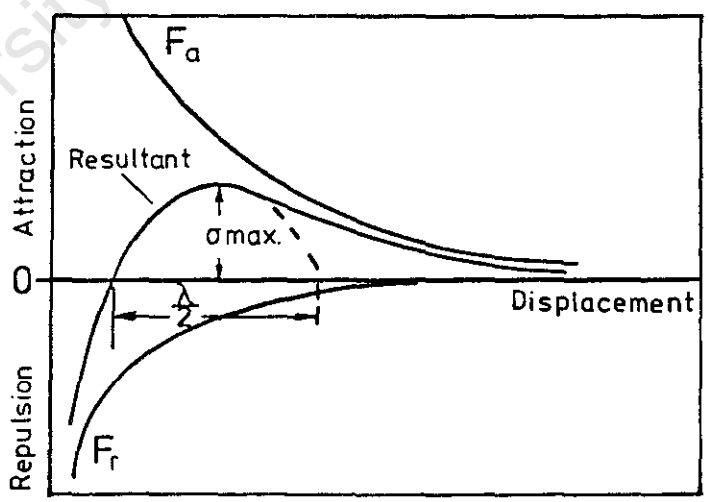

Fig. 1·4 Variation of force with distance between two atoms.

$$\therefore \quad \lambda = \sigma_{max} \left(\frac{2 \pi a_o}{E} \right)$$

and substituting in equation 1.2

$$\sigma_{max} = \left(\frac{E \gamma}{a_o} \right)^{\frac{1}{2}} \qquad \text{.....Eqn.1.3}$$

The substitution of reasonable values for the quantities involved in equation 1.3 results in the prediction of cohesive strengths between 1×10^6 lbs/in^2 and 3×10^6 lbs/in^2 (6,900 N/mm^2 to 20,700 N/mm^2). This is 10 to 100 times greater than the observed fracture strengths of commercial metals.(7)

This wide discrepancy between the calculated and observed fracture strengths implies that there is some mechanism in ordinary metals that concentrates the applied stress, so that over some small region the theoretical values of cleavage fracture stress is reached.

1.6 The Concentration of Stress Around an Elastic Crack:

If a tensile stress σ is applied across a thin plate of an elastically isotropic material containing a small elliptical hole, where the major axis of length $2c$ is perpendicular to the applied stress, the maximum tensile stress, σ_{max}, at the end of this hole can be shown to be(8)

$$\sigma_{max} = \sigma \left(1 + \frac{2c}{h} \right) \qquad \text{.....Eqn.1.4}$$

where $2c$ is the length of the elliptical hole and $2h$ its height.

For an ellipse the minimum radius of curvature at the major axis is

$$r = \frac{h^2}{c} \qquad \text{.....Eqn.1.5}$$

$$\therefore \quad \sigma_{max} = \sigma \left[1 + 2 \left(\frac{c}{r} \right)^{\frac{1}{2}} \right]$$

and for $c \gg r$

$$\sigma_{max} \cong 2 \sigma \left(\frac{c}{r} \right)^{\frac{1}{2}} \qquad \text{.....Eqn.1.6}$$

If $c \gg h$ the elliptical hole can be considered to be a crack of length $2c$ and tip radius r. For the propagation of this elastic crack the maximum tensile stress at its tip must exceed or equal the theoretical cohesive stress.

Therefore from equation 1.3

$$2\sigma \left(\frac{c}{r} \right)^{\frac{1}{2}} = \left(\frac{E\gamma}{a_o} \right)^{\frac{1}{2}}$$

$$\therefore \quad \sigma_c = \left[\frac{2E\gamma}{\pi c} \left(\frac{\pi r}{8 a_o} \right) \right]^{\frac{1}{2}}$$

$$\text{or} \quad \sigma_c \cong \left[\frac{2E\gamma}{\pi c} \left(\frac{r}{3 a_o} \right) \right]^{\frac{1}{2}} \qquad \text{.....Eqn.1.7}$$

where σ_c is the critical stress required to produce fracture.

This relation applies only for completely elastic-brittle materials under plane stress conditions and where no micro-plastic strain occurs at the crack tip.

An expression of this form was originally derived by A.A. Griffith[9] on the basis of thermodynamic considerations. He argued that the work done to extend an existing crack, that is to create two new surfaces, must be provided either from external sources or from the elastic energy stored in the body of the material. If the material is tough and ductile, a great deal of work has to be expended in increasing the fracture area, and the rate of crack propagation is correspondingly slow. However, if enough energy is stored in the loading device and in the specimen itself to complete the fracture, since this is supplied by relaxation of the stress as the crack increases in length, then the crack will propagate at high speed, deriving its energy from these sources.

Griffith assumed that the brittle amorphous materials with which he worked (glass and fused silica) contained many small invisible cracks of flat elliptical profiles and length 2c. Assuming these cracks to be perpendicular to the applied stress in an infinitely wide plate, he used Inglis[8] calculated stress distribution near the end of the major axis to determine the strain energy released as the initially present crack grew. For plane stress conditions he found that

$$\sigma_c = \left(\frac{2E\gamma}{\pi c}\right)^{\frac{1}{2}} \qquad \text{.....Eqn.1.8}$$

This can be seen to be identical to equation 1.7 where $r \cong 3a_o$. Both equations 1.7 and 1.8 must be satisfied for unstable fracture to occur, so that when $r < 3a_o$ the stress for unstable crack propagation is given by equation 1.8 and when $r > 3a_o$ the fracture stress is given by equation 1.7.

If appropriate values of modulus of elasticity, E, and the surface energy for the cleavage plane, γ, are used in the Griffith equation, critical crack lengths of the order of $1 - 10\mu$ are obtained for low carbon steels. Since cracks of this size are less than a grain diameter in length, it could be argued that they could well go undetected.

On the other hand considerable experimental evidence has been accumulated indicating that cleavage fracture is always preceded by intense localised plastic deformation.(10) Cleavage cracks produced in the edge of a low carbon steel plate at the temperature of liquid nitrogen failed to propagate directly by cleavage when the plate was later fractured in tension at room temperature. Intense plastic deformation always developed around the crack root before a new cleavage crack formed and propagated.

In addition to this, plastic work is also expended by the propagating crack in forming the characteristic river pattern[4] shown in Fig.1-2. Further plastic deformation also occurs at the grain boundaries in polycrystalline metals, where the crack is required to change its direction of propagation across the boundary to follow the change in crystal orientation. There is also considerable evidence to suggest that cleavage fracture in polycrystalline metals requires the nucleation of new cracks in each grain as the crack propagates across the grain boundary.[11]

This led to a modification of the Griffith equation as suggested by Irwin[12] and Orowan.[10] These workers recognised that when plastic deformation occurs near the tip of the crack a certain amount of plastic work, γ_p, is expended during crack propagation, in addition to the elastic work, γ, required to create the two new fracture surfaces.

The Griffith theory in its original form, should not therefore be expected to apply to cleavage fracture in metals. The modified version of the Griffith equation as suggested by the above authors includes the term γ_p expressing the plastic work required to extend the crack:-

$$\sigma_c = \left[\frac{2E(\gamma + \gamma_p)}{\pi c}\right]^{\frac{1}{2}} \qquad \ldots\ldots\text{Eqn.1.9}$$

$$\text{or} \quad \sigma_c = \left[\frac{2E\gamma}{\pi c}\left(1 + \frac{\gamma_p}{\gamma}\right)\right]^{\frac{1}{2}} \qquad \text{.....Eqn.1.10}$$

When the crack velocity is high, the temperature low, and the material intrinsically brittle, γ_p is relatively low, i.e., $\gamma_p < 10\,\gamma_s$

When $\gamma_p \gg \gamma$

$$\sigma_c \cong \left[\frac{2E\gamma}{\pi c}\left(\frac{\gamma_p}{\gamma}\right)\right]^{\frac{1}{2}} \qquad \text{.....Eqn.1.11}$$

When plastic deformation occurs near the crack tip it blunts the crack and thereby relaxes some of its concentrated stresses by increasing the tip radius, r. This is apparent when comparing equations 1.7 and 1.11, since

$$\left[\frac{2E\gamma}{\pi c}\left(\frac{r}{3a_o}\right)\right]^{\frac{1}{2}} = \left[\frac{2E\gamma}{\pi c}\left(\frac{\gamma_p}{\gamma}\right)\right]^{\frac{1}{2}}$$

so that $\frac{r}{3a_o} = \frac{\gamma_p}{\gamma}$

Hence local plastic flow at the crack tip can increase the toughness of the material.

Parker[5] estimated that cracks would have to be of the order of 2 mm long in low carbon steels, where $\gamma_p \cong 10^3\,\gamma$, for unstable fracture. Although defects of this size may occasionally exist in fabricated structures, in most instances these would not go undetected.

Even if cracks of this size existed in the steel, it is likely that plastic flow would occur during loading at the crack tip to blunt the crack. In fact it is now recognised that it is this localised plastic strain at the root of the notch or crack in metals which causes the crack to grow, so that cleavage fracture in metals is plastically induced. It follows therefore that a crack-free metal should not fracture at a stress below its yield strength. This is supported by Low's[13] experiments which showed that a steel broke by cleavage in tension, or flowed plastically in compression, at identical stresses irrespective of grain size. In the presence of notches or cracks the stress required to produce localised yielding at the root of the notch becomes equal to the cleavage fracture stress. Cleavage fracture can therefore be considered as a two-step process consisting first of the initiation stage, and secondly that of unstable crack propagation.

1.7 The Initiation of Cleavage Cracks:

A number of mechanisms of crack initiation by plastic deformation have been postulated and some of these observed. These are summarised below, and have been described in detail elsewhere.[14]

Four major methods of crack initiation have been suggested:-

a) The intersection of a deformation twin with a grain boundary, a hard second phase particle or a second twin could form a cleavage crack. At high strain rates or at low temperatures, twinning is the preferred mode of deformation in bcc metals. Because deformation twins spread more rapidly than slip bands, little relaxation of stress is able to occur when a twin is blocked by some obstacle, and consequently the twin has sufficient energy to nucleate a cleavage crack.

b) Dislocations piling up at a strong obstacle such as a grain boundary during plastic deformation could coalesce and thus form a crack. This can be most simply visualised by considering the coalescence of a series of edge dislocations fusing together against some such obstacle. Other slip bands and twin interfaces are also thought to act as dislocation obstacles causing cleavage cracks.

c) If a low angle tilt boundary is sheared through by slip approximately perpendicular to the boundary, the local normal stress can equal the cleavage strength and a crack can be nucleated. This mode of crack initiation is common in the cph crystal structure metals

where the {0001} planes are both the primary slip planes and also the cleavage planes.

d) Dislocations on intercepting slip planes may glide together to coalesce along the line of interception, thereby changing to a cavity dislocation. If a tensile stress, σ, is applied to a single grain in a polycrystalline matrix, slip would occur along the planes of maximum shear stress at 45° to the applied stress. These intercepting planes would then form a cavity dislocation on a plane of maximum normal stress. This is significant since after the crack attains a critical size it would propagate as a Griffith crack under the influence of the normal stress σ.

e) Cracking of 2nd phase particles eg. Fe$_3$C in pearlite.

1.8 Summary:

Although the above mechanisms and equations do much to explain how cleavage cracks, once formed, can become unstable and propagate at a low fracture stress, many of the characteristics of fracturing metals are not explained by these equations. For example, cleavage occurs readily in the bcc and cph metals, but not in the fcc metals. Furthermore, the ductility of the bcc and cph metals is very sensitive to the temperature of deformation, the propensity to fracture by cleavage increasing as the temperature is lowered. It is necessary therefore to examine in greater detail the process of cleavage crack initiation and propagation.

CHAPTER 2.

THE BRITTLE-DUCTILE TRANSITION

2.1 The Transition Temperature:

Many crystalline materials whose flow stress rises rapidly with decreasing temperature and with increasing strain rate exhibit a fracture mode transition when the temperature is lowered. Above the transition temperature the fracture is predominantly ductile and occurs by micro-void coalescence or one of the shear mode processes. Below this temperature fracture is by cleavage with its characteristic brittle appearance. Ionic salts such as NaCl, AgCl, MgO, the bcc and cph metals and particularly low carbon steels show this transition in fracture mode. This transition temperature is a function of stress state and strain rate, and in the low carbon steels occurs relatively sharply.

The variation of yield stress, fracture stress, ductility and microcrack formation with temperature for low carbon steel has been determined by Hahn et al[15] and is shown in Fig.2-1. In the region A a tensile specimen failed with a ductile cup and cone-type fracture. The reduction of area at fracture was of the order of 50-60%. In region B the fracture was still predominantly ductile, but areas of cleavage were found in the outer rim where the crack propagation rate had been high enough to nucleate cleavage cracks. A sharp transition

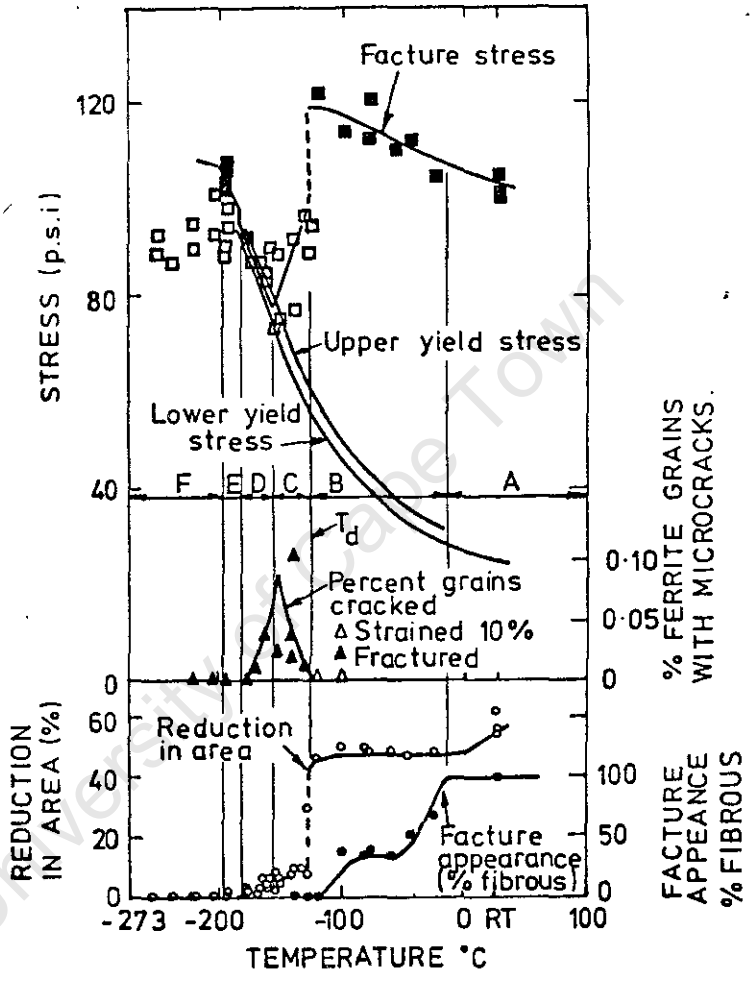

Fig. 2·1 Temperature dependence of fracture stress, yield stress, ductility & microcrack frequency in low carbon steel. (Ref. 15)

from ductile to brittle fracture occurred at the transition temperature T_d, and was indicated by a drop in the reduction of area at fracture to practically a zero value. Below this transition temperature fracture was by cleavage, although some areas of mixed microvoid coalescence-cleavage fracture were still observed at the transition temperature T_d. Accompanying this ductility transition was a large decrease in the fracture stress. The percentage of grains containing microcracks increased rapidly in region C at temperatures just below T_d. However, some microcracks were found above T_d, indicating that the ductility transition occurred when the conditions were suitable for the growth of microcracks into propagating fractures. Apparently the initiation of microcracks was not therefore a sufficient criterion for fracture. Microcracks were observed only in the regions of the specimen which had undergone discontinuous yielding. As the temperature was lowered further in the region C, the fracture stress dropped to the extrapolated lower yield stress, so that in region D the fracture stress and the lower yield stress coincided. In the region E cleavage fracture occurred abruptly at the extrapolated upper yield stress, presumably at the first area to undergo discontinuous yielding, and plastic deformation and the fracture propagated from the first microcrack to form. Finally at very low temperatures, in region F, fracture was initiated by deformation twins. The fact that cleavage fracture was

shown in this work to occur at the yield stress can be considered as further evidence that plastic deformation is necessary for the nucleation of cleavage cracks.

Cottrell and Petch[16] have both suggested fracturing laws to explain the transition temperature on a basis of dislocation pile-ups. This development requires that the Griffith equation be written so that the energy of a dislocation pile-up can be equated to the surface energy of a crack. The energy of the pile-up is given by the product of the applied stress and the displacement between the crack faces. Hence

$$\sigma n a = 2\gamma \qquad \text{.....Eqn.2.1}$$

where n = number of dislocations

a = interatomic spacing

σ = applied stress

The magnitude of the total displacement can also be expressed as

$$n a = \left(\frac{\tau - \tau_o}{G} \right) d \qquad \text{.....Eqn.2.2}$$

where $\tau - \tau_o$ = effective shear stress

τ = applied shear stress

τ_o = friction stress

d = length of slip band containing dislocations and taken as half the grain diameter in polycrystalline metals.

G = shear modulus

By analogy with the Petch[17] equation

$$\tau_y = \tau_o + k_y^* d^{-\frac{1}{2}} \qquad \text{.....Eqn.2.3}$$

where τ_y = shear stress at yield

k_y^* = a measure of the contribution of grain boundaries to the shear strength of polycrystalline metals

and when the fracture and yield stress are approximately equal, by substitution in equation 2.2

$$n\,a \cong \frac{k_y^* d^{\frac{1}{2}}}{G} \qquad \text{.....Eqn.2.4}$$

If crack propagation is more difficult than crack initiation, the competitive processes on the application of a load are yielding and crack propagation. Now since cleavage cracks propagate under normal stress, σ , rather than shear stress, a factor β which equals $\frac{2\tau}{\sigma}$ can be introduced, where β = 2 for torsion

= 1 for tension

$\cong \frac{1}{3}$ for notches in tension (see Fig.1-3).

Therefore at the yield point, equating equations 2.1 and 2.4

$$\sigma_y k_y d^{\frac{1}{2}} = \beta G \gamma \qquad \text{.....Eqn.2.5}$$

where k_y = contribution of grain boundaries to the strength of polycrystalline metals in tension. If in equation 2.5, the LHS is smaller than the RHS, ductile yielding results. If the LHS is greater than the RHS, cleavage fracture results.

This equation makes fracturing a function of grain size d and stress state β. Cottrell[16] originally assumed that the temperature dependence of this equation came about through the temperature sensitivity of k_y. This factor k_y has since been shown to be constant for steels in the normalised condition.[18] Petch[16] on the other hand stated that temperature influenced fracture by affecting the friction stress σ_o, and suggested that σ_o was made up of two parts, a temperature independent friction σ_o^* and a temperature dependent σ_o^+. The former, thought to arise from the resistance of random solute atoms, fine precipitates and lattice defects to dislocation movement, and that σ_o^+ represented an appreciable Peierls-Nabarro stress. The temperature dependence of σ_o^+ can be given by an expression of the form[16]

$$\sigma_o^+ = K e^{-CT} \qquad \text{.....Eqn.2.6}$$

where K and C are constants and T the temperature. Provided σ_o^* is not too large, the whole σ_o approximates to a similar relationship.

Now since[17] $\sigma_y = \sigma_o + k_y d^{-\frac{1}{2}}$ equation 2.5 can be rewritten:-

$$\sigma_o k_y d^{\frac{1}{2}} + k_y^2 = \beta G \gamma \qquad \text{.....Eqn.2.7}$$

and if $\sigma_o = K e^{-CT}$

then $-C.T + \log_n \left[K.k_y.d^{\frac{1}{2}} \right] = \log_n \left[\beta G \gamma - k_y^2 \right]$

or at the transition temperature, T_c

$$-C.T_c = \log_n \left[\frac{\beta_G \gamma - k_y^2}{K.k_y.d^{\frac{1}{2}}} \right]$$

$$\therefore C.T_c = \log_n K - \log_n \left[\frac{\beta_G \gamma}{k_y} - k_y \right] - \log_n d^{-\frac{1}{2}}$$

.....Eqn.2.8

Less accurately, where the temperature range is not too wide, the temperature dependence of σ_o^+ can be taken as linear

i.e. $\sigma_o^+ = C - \Sigma T$

where C and Σ are constants

$$\therefore \sigma_o = \sigma_o^* + C - \Sigma T$$ Eqn.2.9

By substitution in equation 2.7

$$\Sigma T_c = \sigma_o^* + C - \left(\frac{\beta_G \gamma}{k_y} - k_y \right) d^{-\frac{1}{2}}$$

.....Eqn.2.10

The similarity between equations 2.8 and 2.10 and Petch's original equations[16] can be readily seen, and the relationship can be reduced to

$$T_c \propto M \log_n d^{-\frac{1}{2}}$$

or less accurately

$$T_c \propto M' d^{-\frac{1}{2}}$$

and $T_c \propto N \sigma^*$

where M, M' and N are constants

The development of the above equations does not account for the occurrence of transition temperatures in bcc and cph metals and its absence in fcc metals. However, Johnson et al[19] have recently suggested that cph metals, which exhibit few slip systems, as well as bcc metals which slip on several systems but in which cross-slip is difficult, will tend to have high values of k_y, and will therefore be more susceptible to cleavage fracture than the fcc metals with many degrees of freedom to slip. The effect of discontinuous yielding, as occurs in low carbon steels, must also be effective here, since when one dislocation breaks away from its precipitate, an entire avalanche of dislocations can glide behind it on the slip plane. When these encounter an obstacle their high velocity does not allow the initiation of new dislocation sources which would relax the stress by plastic flow, and a crack is formed instead.

2.2 Tests for Cleavage Fracture:

During the past 50 years numerous tests have been developed for the purpose of assessing the susceptibility of metals, and steels in particular, to cleavage fracture. These tests have been summarised in detail elsewhere,[4,5,& 20] and some of these are detailed in I.S.O. and other standard specifications. Since the temperature at which the transition from ductile to cleavage fracture occurs is dependent on the stress state and applied strain rate, it is natural that the transition

temperature, as determined by the various tests, should vary according to the specimen size, the size and shape of the notch and the loading rate, e.g., as in impact or slow bend tests. The seven most common tests used for assessing susceptibility to cleavage fracture are summarised in Table 2.1, and references to more detailed descriptions of these tests are also given in the table. Basically these tests can be divided into tests that are comparative, e.g. tests 1 - 3 in Table 2.1, and tests that are specific, e.g., tests 4 - 7 in Table 2.1. Comparative tests should be reproducible, simple to operate and as far as possible, inexpensive. Specific tests on the other hand are used to obtain information that may be directly incorporated in structural design, and tend to be expensive.

In research projects in the nature of those reported here, simplicity, reproducibility and low unit cost are essential requirements, due to the large number of test specimens involved. Since the experimental steel was also to be produced in small ingots, it was considered necessary to select a test where the specimens were small enough to allow sufficient hot working from ingot form for the steel to be representative of a fully wrought material. For this reason the standard Charpy test was chosen for this investigation. This choice had an additional advantage in that it allowed comparisons to be made with published data, which

Table 2.1

Some of the most widely used transition temperature tests.

Test Designation	Test Procedure	Criteria for Assessing Transition Temperature
1. Charpy V-Notch (21)	A square, notched bar is broken as a simple beam in impact bending at various temperatures.	i) Temperature which corresponds to a certain fibrous fracture appearance, e.g. 50%. ii) Temperature which corresponds to a certain energy level, e.g. 20 ft.lbs. (27 Joule) iii) Temperature which corresponds to a certain lateral contraction or expansion at the notch.
2. Van Der Veen (slow bend test) (20, 22)	A notched bar with a shallow, cold pressed notch is broken in static bending at various temperatures.	i) Nominal bend strength. ii) Temperature which corresponds to a certain amount of shear fracture, e.g. 50%

Test Designation	Test Procedure	Criteria for Assessing Transition Temperature
2.(Cont'd)		iii) Temperature which corresponds to a certain lateral contraction at root of notch.
3.Pellini Drop Weight (Drop Weight Test) (22)	A rectangular plate containing a weld crack is deformed, by a dropped weight, in bending to a strain corresponding to incipient yielding. A notch is ground in a short longitudinal bead of brittle weld deposited on the tension surface to initiate fracture.	i) The temperature above which fracture will not propagate easily across an elastically loaded specimen. Nil ductility-transition (N.D.T.)
4.Robertson Test (Brittle crack-arrest test) (20, 22)	A wide plate with a temperature gradient across the width is loaded in tension to a given stress level. A cleavage crack is initiated by impact at the	i) Temperature above which a crack will not propagate at a given stress level i.e. the crack arrest temperature (C.A.T.)
		ii) The critical stress for a cleavage

Test Designation	Test Procedure	Criteria for Assessing Transition Temperature
4.(Cont'd)	cold end and travels across the specimen until it reaches a temperature zone where plastic flow is high enough to arrest the crack.	fracture at a given temperature.
5.Esso(SOD)Test (Standard Oil Development) (22)	A plate specimen at uniform temperature is loaded in tension to a given stress level. A cleavage crack is initiated at one edge by means of an impact loaded wedge.	i) The critical stress for cleavage fracture propagation at a given temperature.
6.Explosive Bulge Tests (20, 22)	A square plate, with a brittle weld bead on the underside is placed on an open die and an explosive charge is detonated over the plate.	i) The fracture transition temperature for elastic loading (F.T.E.) Below this temperature the fracture will propagate only through elastically loaded regions.

Test Designation	Test Procedure	Criteria for Assessing Transition Temperature
6.(Cont'd)		ii) The fracture transition temperature for plastic loading (F.T.P.) Above this temperature cleavage fractures cannot propagate, i.e. there is extensive deformation without brittle cracking.
7.C.O.D. Test (Crack opening displacement) (23)	Full plate thickness notched specimens are broken in static bending or tension and the crack opening measured.	i) Temperature which corresponds to an arbitrary C.O.D. at fracture.

in most cases also used the Charpy test for the evaluation of the effect of alloying additions on the transition temperature of steel.

2.3 Interpretation of Charpy Test Results:

Full details of the Charpy V-notch impact test are given in British Standard 131, Part 2, (1959). Briefly the standard Charpy specimen consists of a 10 mm square beam, 55 mm long, containing a 2 mm deep V-notch with a root radius of 0.25 mm at its mid length, and is supported at its ends in a horizontal position. The test specimen, after being cooled or heated to the desired test temperature, is placed on the machine supports and an impact load is applied via a striker on a swinging pendulum at specimen midspan opposite the notch. The results can be expressed as the energy absorbed in fracturing the test specimen or by assessing the proportion of the fracture surface showing a granular (cleavage fracture) or fibrous (microvoid coalescence) appearance. Occasionally the lateral contraction at the root of the notch is also used as an assessment of ductility. These results become most meaningful when the tests are conducted over a range of temperatures to show the impact transition temperature, see Fig.2-2. It will be seen from this figure that a similar type of curve is obtained for each of the above criteria with change in temperature. The impact transition can be assessed in various ways using the above criteria, e.g.,

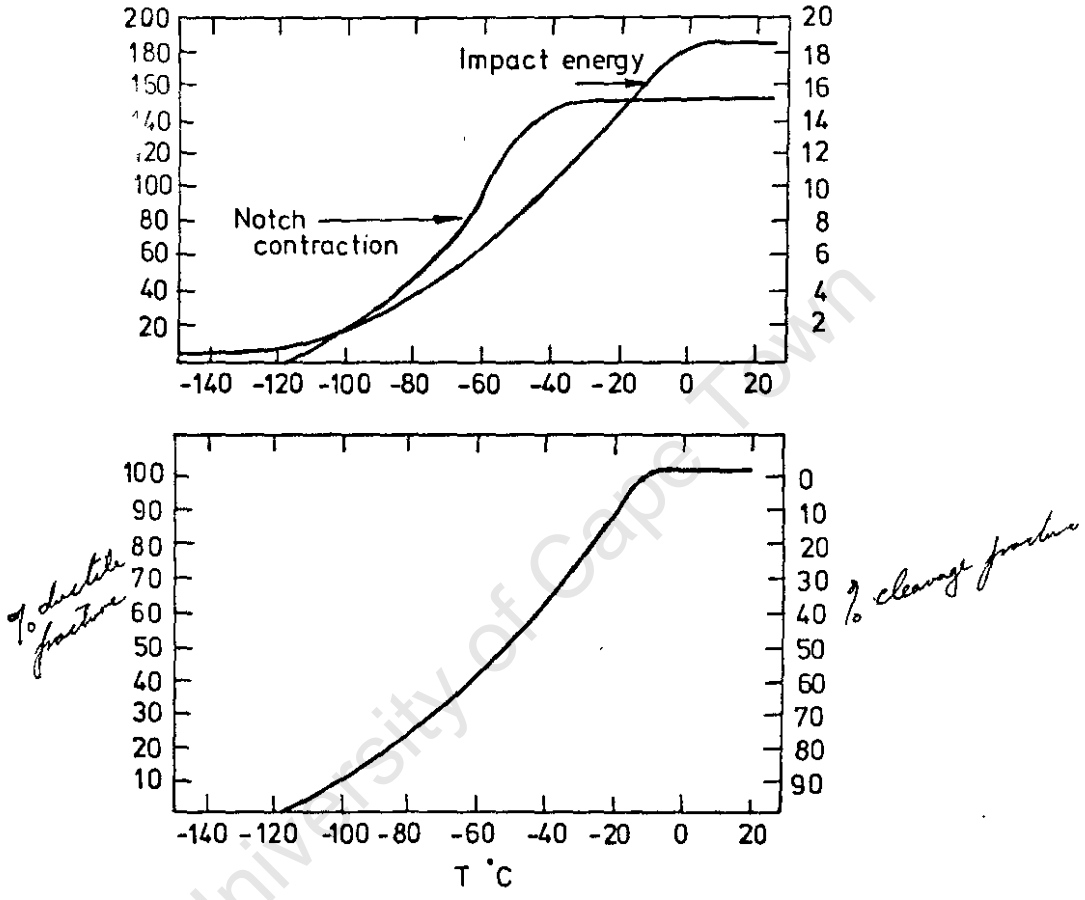

Fig. 2·2 Effect of temperature on the impact energy, percentage fibrous fracture & notch root contraction for Charpy V notch specimens of $3\frac{1}{2}$% Ni low carbon steel. (Ref. 7)

i) the temperature corresponding to some arbitrary value of impact energy such as 20 ft.lbs (27 Joule);

ii) the 70% or 50% granular fracture temperature; or

iii) the temperature corresponding to some arbitrary value, say 2%, lateral contraction.

Before selecting some such arbitrary criteria for the transition temperature, it would seem beneficial to examine in detail the deformation and fracture mechanisms which occur in the Charpy test, so that the exact fundamental material properties which are being compared are known. The instrumented Charpy test[24] has been of great importance here, and successful dynamic measurements of the load-time relationships during fracture has provided information on the deformation process and the fracture mechanisms. A typical series of results measured over a range of temperatures is shown in Fig. 2-3. The close similarity between this figure and that of the tensile test, shown in Fig.2-1, is immediately obvious. Noticeable deviations occur in the region CDE of Fig. 2-3 where the section CD corresponds more closely with the upper yield stress than with the lower yield stress as found with tensile tests. There is, however, some difficulty in distinguishing clearly both the upper and lower yield points due to the stress variation across the specimen section below the notch in bending. The lower yield stress is consequently

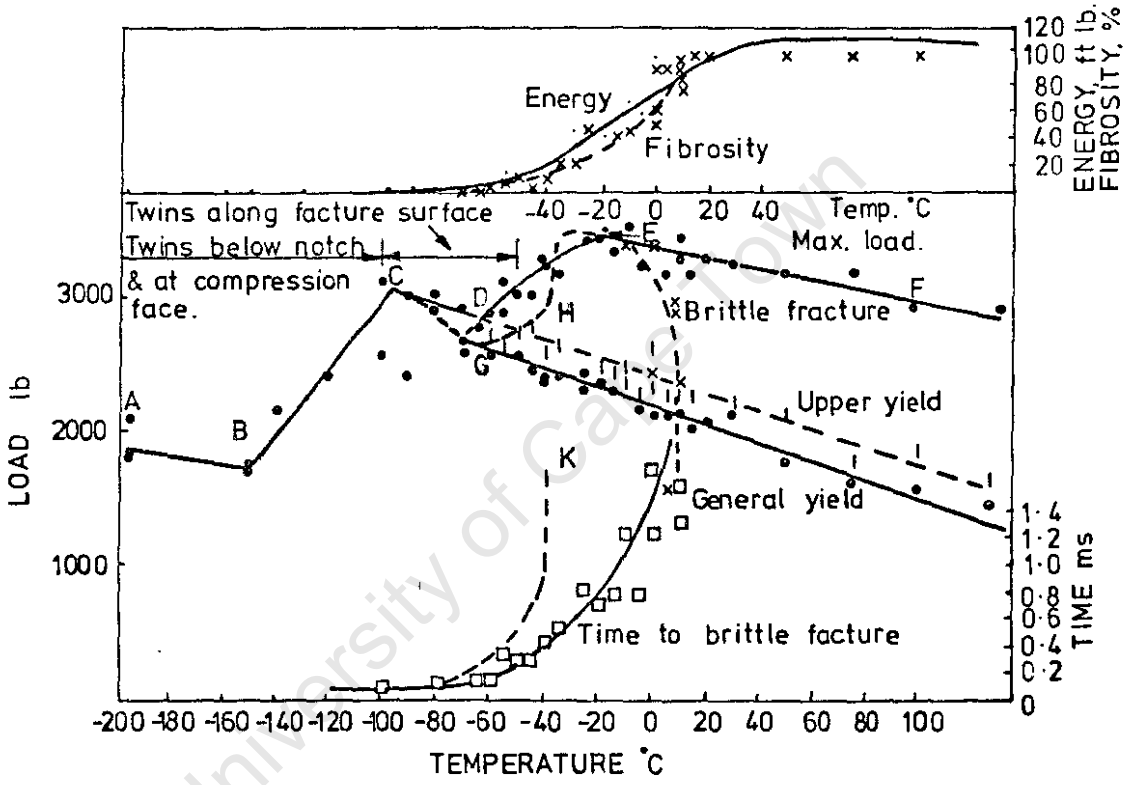

Fig. 2·3 A typical curve from the instrumented Charpy test on low carbon steel. (Ref. 24)

replaced by a "general yield" line, and experimental scatter indicates that some of the line CD could coincide with the extrapolated general yield line.[24] The ductility transition temperature (T_d in Fig. 2-1) is also less clearly defined, the line DE dropping more slowly with decrease in temperature than that for the uniaxial tensile test. On the other hand, tests conducted on Charpy V-notch specimens in slow three point bending[25] indicate a well defined ductility transition temperature, as shown in Fig. 2-4. This transition is clearly defined on both the load-temperature and the bend angle-temperature curves, these curves now being almost identical to those for the uniaxial tensile test. If the striker velocity is assumed constant during the dynamic Charpy test, then the curve for "time to brittle fracture-temperature" in Fig. 2-3 should be identical to that for "angle of bend to brittle fracture-temperature" curve shown in Fig. 2-4. The observed difference in these curves can be attributed to the following causes:-

i) differences in the behaviour of the steels due to chemical composition differences;

ii) errors in assuming constant pendulum velocity in the dynamic test;

iii) errors in the dynamic recording system.

Since a wide range of steels were tested[24] with the

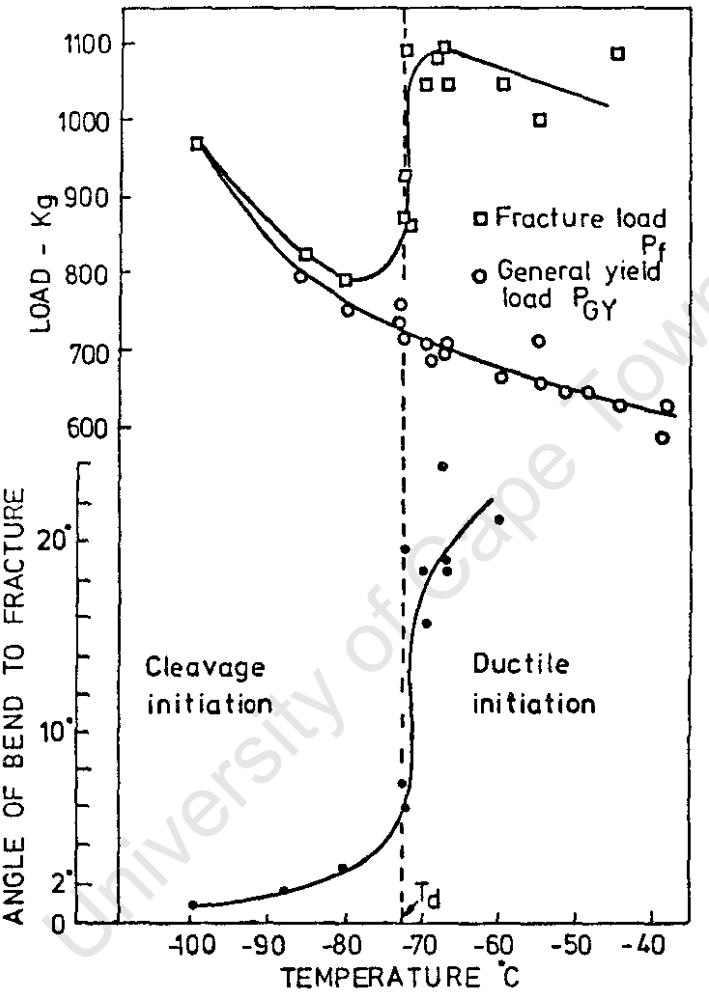

Fig. 2·4 Facture loads, general yield loads & bend angles at various temperatures for Charpy V notch specimens in slow three point bending. (Ref .25)

instrumented dynamic test, and all showed similar curve forms to that shown in Fig. 2-3, it seems likely that the section C D E of this curve is in error due to errors (ii) and (iii) above, and that the actual curve form should be along the dotted lines C G H E and J K in this figure.

Based on this assumption the ductility transition temperature would appear to coincide with a low value of lateral notch strain, Fig. 2-2 (assuming that this is proportional to the bend angle at brittle fracture) or alternatively, within the lower portion of the energy transition curve, Fig. 2-2. From published results[24] of instrumented tests on steels of similar composition to those being tested in this investigation, the arbitrary low level of 20 ft.lbs (27 Joule) of energy absorbed in fracture would appear to coincide with reasonable limits with the ductility transition temperature. That is, the temperature corresponding to a value of 20 ft.lbs (27 Joule) of energy absorbed in fracturing the specimen corresponds to that where conditions are suitable for the microcracks, initiated during discontinuous yielding, to grow into propagating fractures. Above this temperature fracture is by microvoid coalescence, although cleavage is still possible when the ductile crack propagation rate is high enough to initiate cleavage. Below this transition temperature cleavage fracture is initiated from the first area below the notch to undergo discontinuous yielding, and at lower

temperatures still cleavage fracture is also initiated by deformation twins.

It must be emphasised that the 20 ft.lbs(27 Joule) transition temperature is an arbitrary value which appears to coincide with the ductility transition temperature of similar steels tested using the instrumented Charpy test. It is, however, more readily determined than some arbitrary low value of lateral contraction at the root of the notch. Transition temperatures based on an assessment of macroscopic or visual fracture appearance are not favoured, since considerable areas of microvoid coalescence can be found on fractures considered to be fully granular, e.g., see Fig.1-2.

2.4 Correlation of the Charpy Energy Transition Temperature With Other Fracture Tests:

Various types of test give different transition temperatures because they are made under different conditions of stress and strain rate, and are evaluated by different criteria. In general, however, laboratory tests evaluate the tendency for steels to fail by cleavage and classify these materials in the same order of susceptibility.

Boulger[26] has shown that for carbon-manganese steels in the as-rolled and heat treated conditions, the relationship between the N D T temperature and the Charpy V-notch transition temperature can be given by

$$NDT = 0.46\ (V_{15}) - 4^{\circ}C. \quad R^2 = 56.3\%$$

and $$NDT = 0.48\ (V_{25}) - 10^{\circ}C. \quad R^2 = 76.4\%$$

where V_{15} and V_{25} correspond to the Charpy V-notch transition temperatures at 15 and 25 ft.lbs (20 and 34 Joule) and R^2 is the fraction of variance removed by the correlation.

Similarly it has been shown[27] that for low carbon pressure vessel steels, the Robertson crack arrest temperature (CAT) is approximately 33°C. above the NDT.

The following relationships can therefore be assumed to be reasonable approximations

$$NDT = 0.47\ (V_{20}) - 7^{\circ}C.$$

$$CAT = 0.47\ (V_{20}) + 26^{\circ}C.$$

where V_{20} = Charpy V-notch 20 ft.lb transition temperature. Empirical relationships of this type are often useful in interpreting results, but too much importance should not be attached to them.

CHAPTER 3

THE EFFECT OF METALLURGICAL FACTORS ON THE DUCTILITY TRANSITION TEMPERATURE.

3.1 The Low Carbon, Low Alloy Steels:

Ferritic-pearlitic steels account for most of the steel tonnage produced today. These are iron-carbon alloys containing from 0.05% to 0.25% carbon and a small percent of other alloying elements added to increase the yield strength and toughness. They are generally used in the "hot rolled" or normalised conditions, where the structure consists of bcc iron (ferrite) containing about 0.01% carbon and soluble alloying elements, and Fe_3C (cementite). The Fe_3C exists as carbide particles along the ferrite grain boundaries in steels of very low carbon content, and in the form of grains of a lamellar structure consisting of alternating layers of Fe_3C and ferrite (pearlite) when the carbon content is above approximately 0.08%.

In these steels the size and strength of the ferrite grains, and the volume and spacing of the carbide particles, would appear to be the most important variables determining fracture toughness. Although the pearlite grains account for up to 30% of the microstructure in steels of 0.25% carbon, the yield strength σ_y has been shown to be independent of the amount of pearlite in steels of the same ferrite grain size.[28]

It would seem therefore that despite their high hardness pearlite grains in steels of less than 0.25% carbon are so widely dispersed that the ferrite matrix can deform around them with little difficulty. However, since cleavage cracks are initiated relatively easily in carbide particles[14] and within pearlite grains,[29] the volume fraction of pearlite in the microstructure should influence the ductility transition temperature. Since the volume fraction pearlite can be assumed to be directly proportional to the carbon content of low alloy steels in the "hot rolled" or normalised conditions, it is likely that its influence on the ductility transition temperature will be seen as a function of the carbon content.

In addition to the effect of ferrite grain size $(d^{-\frac{1}{2}})$ on the ductility transition temperature, alloy additions to low carbon steels which alter the friction stress σ_o, or the grain boundary strengthening constant k_y of the ferrite would be expected from equation 2.10 to alter the transition temperature. These factors are often governed by the alloy content of the steel.

3.2 Summary of the Effect of Various Alloys in Low Carbon Structural Steels:

All structural steels contain sulphur and phosphorus as residual elements, although most specifications limit these

elements to 0.05% maximum. With most modern steelmaking processes it is possible to consistantly achieve sulphur and phosphorus contents of 0.02% or less, so that although both elements raise the transition temperature,[30,31] their content in steels can be controlled to levels which do not normally cause variation in the transition temperature.

Other residual elements include nitrogen and oxygen, and when the steel is manufactured from scrap, residual levels of copper and molybdenum are also encountered. Nitrogen has been shown[32] to be an important element so far as fracture toughness is concerned, and its effect will be discussed in greater detail in later chapters. Oxygen has been shown to raise the transition temperature of ferrite in the absence of silicon or other strong deoxidisers, to promote intergranular fracture.[33] Its effect in steels containing deoxidisers such as silicon and aluminium is however largely unknown and will also be discussed in later chapters. Both copper and molybdenum have been shown to raise the transition temperature[34] ?? when added to synthetic steels in amounts greater than normally encountered as residuals in steels produced using scrap as the raw material. Little effect is however expected with upper limits of less than 0.20% Cu and less than 0.10% Mo as is normally found in steels produced by this process.

Alloying elements such as manganese, nickel, chromium, silicon and aluminium are added to these steels specifically to alter the properties. In addition to combining with sulphur and preventing the formation of grain boundary iron sulphide films, manganese also acts as a mild deoxidiser. It is however more widely used to increase the yield and tensile strength, and at the same time appears to lower the transition temperature.[34,35] Nickel is the only other alloy addition widely used to lower the transition temperature, although its effect is less marked than that of ?? manganese.[34] The role of both manganese and nickel in lowering the transition temperature is discussed in detail in later chapters. Chromium is often used in conjunction with nickel, and although it is commonly thought not to alter the transition temperature (see Table 1.1), it has been shown to increase the transition temperature of steels.[34]

Silicon is used in amounts varying up to 0.40% in structural steels, its main role being that of a deoxidant. In this role it appears to lower the transition temperature,[6] although it has been shown to increase the transition temperature when present in amounts exceeding 0.40%.[34] Although aluminium can also be used as a steel deoxidiser, its principal role is to produce a fine-grain steel. In this case it is added after the steel has been deoxidised with silicon. The aluminium then combines with the nitrogen in

the steel to form aluminium nitride, which produces a smaller ferrite grain size by preventing austenite grain coarsening during heat treatment,[36] and by the precipitate particles acting as nuclei for ferrite grains during transformation on cooling. The removal of nitrogen from solid solution to form aluminium nitride is thought to lower the transition temperature further.[37] It is not, however, generally appreciated that aluminium nitride decomposes to aluminium and nitrogen in solid solution at high temperatures,[36] and since their recombination to aluminium nitride on cooling is sluggish,[38] steels in the "as rolled" condition containing appreciable amounts of aluminium may yet contain very little aluminium nitride.[39] Under these circumstances the aluminium addition neither refines the ferrite grain size nor removes nitrogen from solid solution, and the transition temperature is consequently not lowered.

3.3 Assessing the Effect of Metallurgical Factors:

The relationship between grain size ($d^{-\frac{1}{2}}$) and the ductility transition temperature has been proved by many researchers, and the results of Petch[16] may be taken as typical. The effect of alloying elements on the transition temperature of steel has also been the subject of much investigation. Two separate, but related approaches have been established by these investigators:-

a) to study the variation in transition temperature brought about by the addition of separate alloying elements to a controlled base composition.[32 & 34]

b) To correlate the variations in transition temperature with steel analysis.[28 & 36,37]

The first method, although producing useful qualitative information, has a number of inherent difficulties. The effect of only one, or at best two, alloying additions can be examined at any one time, since variations in transition temperature brought about by more than two alloying additions can become incomprehensible. It is also often difficult to hold the base composition of these synthetic steels constant, since the planned alloy additions often alter the base composition either by contamination or by altering the solubility of other elements in the base steel.

The second method relies heavily on statistical methods of analysis. In this technique a number of alloy variations can be made at any one time, and provided all the possible variations in the steels are analysed, the regression analysis should correct for base composition variations. This is best done therefore on a series of experimental steels where the production method variations can be kept to a minimum, thus reducing the total number of variables to be examined. The linear regression analysis techniques generally used have several

major limitations. The derived mathematical equations only include variables which have been included in the analysis, and equally important, this analytical technique assumes linear relationships between dependent and independent variables. Since non-linear relationships are not indicated, the resultant analytical equation will give only a mean slope to any non-linear relationship. Some correction can however be made with prior knowledge of non-linear relationships. Realistic formulae can in these instances be obtained by using appropriate functions of variables which will give linear relationships. Appreciable uncertainty in the equation coefficients can also result from inter-related independent variables, and it is often difficult to avoid chance inter-relationships between the independent variables when examining a large number of them.

Grouping of results is also often found when important variables have not been included in the analysis, e.g., vacuum melted steels may give transition temperature results in a group at lower temperatures than similar air cast steels.

When examining the effect of alloying elements on the ductility transition temperature, grain size measurements are necessary in both of the above-mentioned approaches, since many of the alloy additions also influence the grain size of the steel. Some authors have also made use of estimations of pearlite content in these steels.[28] Both of these

variables require careful metallographic technique. The measurement of grain size in steels is further complicated by the presence of two phases in the microstructure. In the low carbon steels (C $<$ .25%) the pearlite grains are usually regarded as boundaries between ferrite grains in much the same way as the normal ferrite grain boundary. Technically it can be claimed that this method of grain size measurement is misleading, since it virtually assumes that the pearlite grain size plays no part in cleavage fracture. Metallographic measurement can be further complicated by widmanstatten structure, and is also unsatisfactory when examining quenched and tempered steels.

In the present investigation the second of the two analysis techniques was used, i.e., the linear regression analysis technique. Since it was also intended to compare the transition temperature of quenched and tempered steels with that of normalised steels, metallographic measurement was kept to a minimum, and replaced when possible by chemical analysis; i.e., all the experimental steels were analysed for aluminium nitride, since it has been shown that grain size is dependent on the aluminium nitride content.[40] Grain size measurements were however also made where possible to enable verification of this relationship. Full Charpy impact transition curves were drawn for each experimental steel, and the 20ft-lb energy level temperature was extracted

from these curves and used as the criterion of transition temperature.

3.4 Multiple Linear Regression:

This form of analysis assumes that the regression can be referred to in terms of one dependent and several independent variables. The regression formulae are not restricted to variables having a dependent-independent relationship, but merely describe in mathematical terms the nature of the relationship between the variables. However, in evaluating the degree of the relationship, all error or inaccuracy is assumed to be in the measurements of one of the variables, and the other variables are assumed to be precisely known. That is, the impression is assumed associated with the dependent variable and the independent variables are assumed to be the precise variables.

In general, a dependent variable y may be expressed in terms of the independent variables

$x_1, x_2, x_3, - - - - - - -$ as

$$y = a + b_1 x_1 + b_2 x_2 + b_3 x_3 - - - - - - -$$

.....Eqn.3.1

where $b_1, b_2, b_3, - - - - - - -$ are the respective regression coefficients. If the degree of fit of a multiple linear regression is measured by the sum of the squares of

deviation of the observed from the predicted values, then in a manner directly analogous to that for a simple linear regression, an expression for the constants in equation 3.1 can be obtained. A detailed description of linear regression techniques are given by Volk[41] and Williams[42]. Most of the analysis reported here was carried out on an I.B.M.360/44 Computer using a standard program (REGR) from a Scientific Subroutine package.[43] Some of the early multiple regression analysis was carried out using an I.B.M. program modified to suit the reduced memory storage of the smaller computer available at that time. This reduced the number of variables which could be handled to ten.

A sample of the printout from the I.B.M.360/44 is shown in Table 3.1. The significance of the multiple regression may be tested by comparing the Variance ratio (F in Table 3.1) with tables of Fisher's F.[44] In the example shown in Table 3.1 comparison of the Variance ratio with Fisher's F tables shows that the multiple regression is significant at the 0.5% probability level but not significant at the 0.1% probability level. That is, we can say with 99.5% certainty, but not with 99.9% certainty, that there is a correlation. The right-hand column of Table 3.1 can also be used to determine the significance of any particular regression coefficient. In this example there are 29 sets of data and the computed T values can be compared with t test tables for the analysis

TABLE 3.1 - I.B.M. 360/44 PRINTOUT

Multiple linear regression analysis of form $y = a + b_1 x_1 + b_2 x_2 + b_3 x_3 + \cdots$

Variable No.6 = $d^{-\frac{1}{2}}$ ($mm^{-\frac{1}{2}}$) (dependent variable)

Variable No.2 = % C

Variable No.3 = % Mn

Variable No.4 = % Ni

Variable No.7 = % N_{AlN}

VARIABLE (x)	MEAN	STANDARD DEVIATION	CORRELATION x vs y	REGRESSION COEFFICIENT(b)	STD.ERROR OF REG.COEF.	COMPUTED T VALUE
2	0.17483	0.04845	-0.23658	1.83335	3.88608	0.47177
3	0.66448	0.24797	0.16895	0.98178	0.72740	1.34972
4	0.05517	0.20299	0.14609	0.99694	0.77431	1.28753
7	0.00568	0.00405	0.62704	167.59799	40.85349	4.10242
DEPENDENT(y)						
6	8.67793	1.03043				

Intercept (a)	6.69819
Multiple Correlation, R	0.67911
Std.Error of Estimate(s)	0.81698

Analysis of Variance for the Regression

SOURCE OF VARIATION	DEGREES OF FREEDOM	SUM OF SQUARES	MEAN SQUARES	F VALUE
Attributable to Regression (k)	4	13.71121	3.42780	5.13564
Deviation from Regression(N-k-1)	24	16.01889	0.66745	
TOTAL	28	29.73010		

From Fisher's Tables, $F_{0.01,4,24} = 4.22$

$F_{0.005,4,24} = 4.89$

$F_{0.001,4,24} = 6.59$

∴ The regression is significant at 0.5% but not at 0.1%

of variance using (N-k-1) degrees of freedom. From such tables[44] for 24 degrees of freedom

Significance	t test value
50%	0.685
20%	1.318
10%	1.711
5%	2.064
2%	2.493
1%	2.797
0.1%	3.745

Reference to Table 3.1 shows that carbon content has no significant effect on grain size ($d^{-\frac{1}{2}}$). The correlation of Mn with $d^{-\frac{1}{2}}$ is significant at the 10% level, but not the 5% level, and that N_{AlN} has the best correlation with $d^{-\frac{1}{2}}$ being significant at the 0.1% probability level. Carbon could therefore be removed from the multiple regression without much effect on the overall significance of the regression equation.

The multiple correlation coefficient, R, and the Variance ratio, F, are related by the following equation[41]

$$F = \frac{R^2 (N-k-1)}{(1-R^2)k} \qquad \text{.....Eqn.3.2}$$

where N = number of data sets

k = number of independant variables.

The confidence limits for the regression line may be determined about $\bar{y}$ (mean) as $\pm t.s$ where t is selected at the proper degrees of freedom and the desired probability level and s is the standard error of estimate.

In the example shown in Table 3.1, the 95% confidence limits for 24 degrees of freedom is found from the t test tables $t_{.05,24} = 2.064$

From Table 3.1 $\bar{y} = 8.678$ $s = 0.817$

$\therefore$ 95% confidence limits $= 8.678 \pm (0.817 \times 2.064)$

$= 8.678 \pm 1.688$

i.e., we can say with 95% confidence that all value of y will be within $\pm$ 1.688 of the regression line.

One further factor needs brief mention here, that of the "fraction of variance". This usually means the fraction of variance accounted for by the correlation and is equal to R^2. This function is also sometimes referred to as the "percentage of total variation in the dependent variable explained by the regression equation."

CHAPTER 4

EXPERIMENTAL PROCEDURE AND RESULTS.

4.1 Experimental Steels:

Initially 42 separate 1-cwt casts of steel were produced in small high frequency induction furnaces. Sixteen of these casts were produced by vacuum melting, and the remaining 26 ingots as normal air casts. The ingots, initially 3-inches square, were forged to $\frac{7}{8}$-inch diameter bar before heat treatment. Sixteen standard 2mm Vee notch Charpy specimens were produced from the heat treated bars and a full impact transition curve determined for each condition. Broken Charpy specimens from each cast were used for the chemical analysis and for metallographic measurement of grain size, pearlite grains being considered as grain boundaries for this measurement. Since it was not practical to determine grain size on the quenched and tempered steels, metallographic measurement was only made on the normalised and slow cooled test specimens. The chemical analysis, the reciprocal of the root mean ferrite grain diameter ($mm^{-\frac{1}{2}}$), and the Charpy 20ft-lb energy level transition temperatures are given in Appendix 'A', Table A1, for the vacuum melted steels and in Table A2 for the air cast steels. Some of the high manganese steel bars and a series of bars from the nickel steel group were also furnace cooled. These results are shown in Table A3. A further group of bars

from the carbon-manganese and nickel steel casts were oil quenched from 890°C. and tempered at 680°C. These results are shown in Table A4, together with the nickel-chromium steel series which was oil quenched from 850°C. and tempered at 680°C. All normalising and furnace cooling was carried out from 890°C. or 900°C.

4.2 Statistical Analysis of Data:

The above tests yielded 52 complete sets of data for examination by computer using linear multiple regression analysis techniques. In order to obtain realistic formula from the regression equations, the variables were reduced to functions which, it was hoped, would give linear relationships. The functions initially examined as variables are shown in Table 4.1. This table also shows the range of variation in each of the examined functions. The following definitions apply to the terms shown in this and other tables:-

N_{AlN} = Nitrogen combined as aluminium nitride determined by the Beegley[45] process.

N_{sol} = Acid soluble nitrogen,[46] which includes nitrogen as aluminium nitride, in solid solution or as iron nitride.

N_{insol} = Acid insoluble nitrogen,[46] and includes the more stable nitrides such as titanium nitride, vanadium nitride and possibly silicon nitride.

N_R = Residual nitrogen in solid solution or combined as iron nitride = $N_{sol} - N_{AlN}$

Al_{sol} = Acid soluble aluminium[46] and includes the aluminium in solid solution and combined as aluminium nitride.

Al_{insol} = Acid insoluble aluminium[46] and considered to be Al_2O_3.

Al_R = Residual aluminium in solid solution = $Al_{sol} - Al_{AlN}$

O_T = Total oxygen content.

O_{SiO_2} = Oxygen assumed combined with Si as $SiO_2 = O_T - O_{Al_2O_3}$ where the $O_{Al_2O_3}$ is calculated from the Al_{insol} content.

Si_T = Total silicon content.

Si_R = Residual Si content = $Si_T - Si_{SiO_2}$ where Si_{SiO_2} is the silicon assumed in combination with oxygen and calculated from the O_{SiO_2} content.

$d^{-\frac{1}{2}}$ = Reciprocal of the root mean ferrite grain size, $(mm^{-\frac{1}{2}})$.

T_{20} = The temperature in °C at which a minimum of 20ft-lbs of energy are absorbed by the 2mm Vee notch Charpy specimens.

TABLE 4.1

Summary of the variables in the initial 52 sets of data examined by regression analysis

		Minimum	Mean	Maximum
Carbon	%	0.09	0.1688	0.26
Silicon	%	0.07	0.2124	0.38
Manganese	%	0.32	0.6254	1.39
Nickel	%	0.01	1.0623	3.93
Chromium	%	0.01	0.4413	0.99
Oxygen	%	0.0010	0.0066	0.0285
N_{AlN}	%	0.0000	0.0049	0.0140
N_R	%	0.0000	0.0032	0.0095
Al_R	%	0.000	0.0292	0.195
N_{insol}	%	0.0000	0.0008	0.0034
Al_{insol}	%	0.000	0.0048	0.014
T_{20} (°C)		-143	-57.10	5

The regression analysis of the 52 sets of data yielded the following equation:-

$$T_{20} = 322(\%C) - 59(\%Mn) - 18(\%Ni) + 29(\%Cr) - 1753(\%N_{AlN}) + 196(\%N_R) + 127(\%Al_R) + K_1$$

.....Eqn.4.1

The constant K_1 has the value -63 for steel normalised from 890°C., -15 for steel slow cooled from 890°C. and -90 for steel oil quenched and tempered at 680°C.

Equestion 4.1 is significant at the 0.1% level, i.e., such a high degree of correlation will only occur by chance once in one-thousand times. All the regression coefficients except N_R and Al_R were significant at the 0.1% level and these two factors at the 1.0% significance level. The correlation coefficient is such that 95% of the total variation in transition temperature is explained by the equation; i.e., only 5% of the total variation in transition temperature has to be accounted for by unconsidered factors and experimental error. The 20ft-lb ductility transition temperature, calculated from equation 4.1 is plotted against the actual transition temperature of the 52 experimental steels in Fig.4-1. Also shown on this figure are lines representing the 95% confidence limits of $\pm$ 16.8°C.

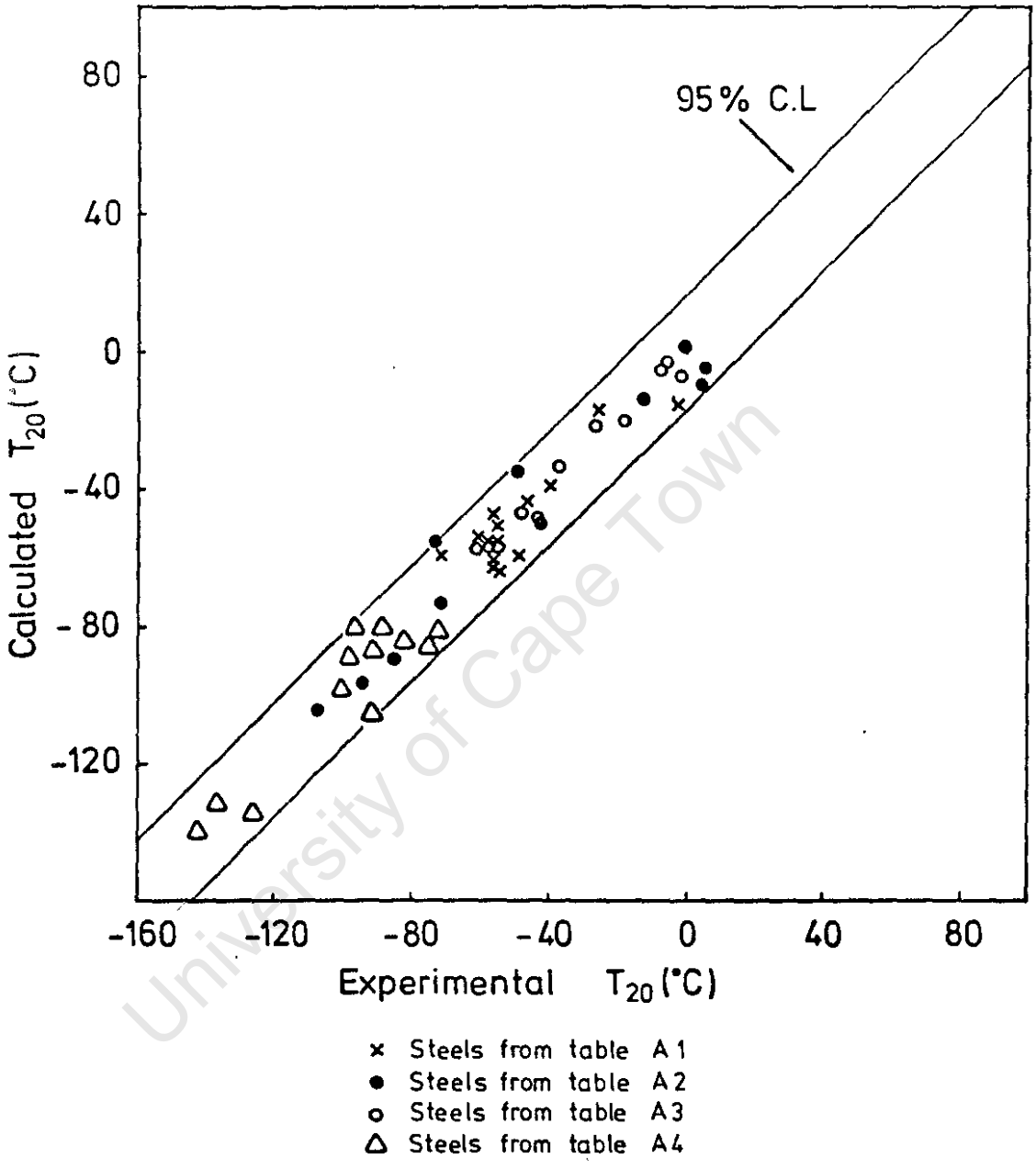

Fig. 4·1 Calculated and observed transition temperatures for experimental steels using equation 4.1.

The inclusion of other factors such as total oxygen content, total silicon content, N_{insol} and Al_{insol} only raised the percentage of the total variation in transition temperature explained by equation 4.1 to 96% and since these individual factors were all of low significance they were dropped from the equation. An attempt was made to improve the significance level of these functions by subdivision of total oxygen into oxygen combined as SiO_2 and Al_2O_3 and total silicon into silicon combined as SiO_2 and silicon in solid solution. These new functions did not, however, give any improvement in the significance of these terms.

On examination of Fig.4-1 a minor degree of grouping of results on the quenched and tempered steels can be seen, i.e., although these results overlap those of the normalised steels to some degree, they could influence the general form of equation 4.1 since all these steels have transition temperatures at the lower end of the range. When these results are replotted using equation 4.1 with $K_1 = -63$, but without altering the constant term to compensate for the various heat treatments, see Fig.4-2, three parallel lines are produced corresponding to the various heat treatments. It can therefore be concluded from Fig.4-2 that the grouping of the quenched and tempered specimen results in Fig.4-1 has had an insignificant effect on the coefficients of equation 4.1

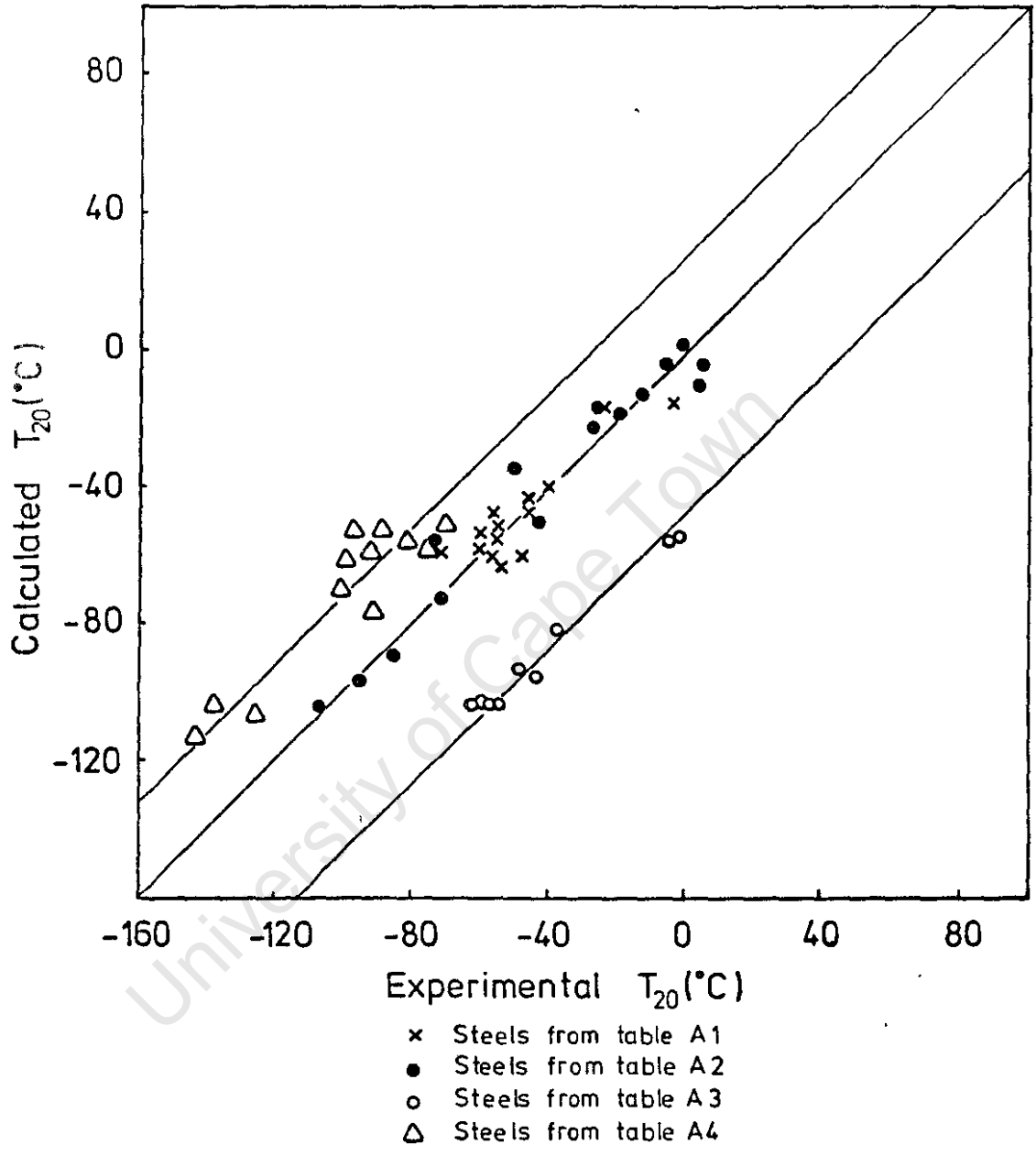

Fig. 4·2 Calculated and observed transition temperatures for experimental steels using equation 4.1 with $K_1 = -63$.

The grain size term $d^{-\frac{1}{2}}$ was not included in the above regression analysis since grain size measurements were not possible on the quenched and tempered steels (Table A4). For this analysis it was assumed that there would be a correlation between $d^{-\frac{1}{2}}$ and the N_{AlN} content so that any effect of $d^{-\frac{1}{2}}$ would be shown in the N_{AlN} coefficient. However this correlation between $d^{-\frac{1}{2}}$ and N_{AlN} would not necessarily exist in those steels with very low N_{AlN} contents. The analysis was therefore repeated using only that data with N_{AlN} contents in excess of 0.0010%. The 45 sets of data which satisfied this criteria gave the following regression equation:-

$$T_{20} = 212(\%C) - 65(\%Mn) - 18(\%Ni) + 31(\%Cr) - 1941(\%N_{AlN}) + 1239(\%N_R) + 135(\%Al_R) + K_2$$

.....Eqn.4.2

The constant K_2 has the value -39 for the normalised material, 9 for the slow cooled material and -66 for the oil quenched and tempered material.

The above equation can be seen to be very similar to equation 4.1 with only minor alterations in some of the regression coefficients. Equation 4.2 is significant at the 0.1% significance level and all the coefficients with the exception of N_R and Al_R are significant at the 0.1% level. The coefficient for N_R was only significant at the 10%

level and Al_R at the 1.0% level. The correlation coefficient of equation 4.2 is such that only 93% of the total variation in transition temperature is explained by this equation. Since this is slightly less than the percentage variation explained by equation 4.1, equation 4.1 is preferred. The exclusion from equation 4.1 of terms relating to grain size or volume fraction pearlite makes this equation suitable for the comparison of transition temperatures between steels in the quenched and tempered condition as well as the normalised condition.

To determine the effect of the reciprocal square root grain size, $d^{-\frac{1}{2}}$, on the ductility transition temperature, a further subdivision of the above data was made. For this data on the quenched and tempered steels (Table A4) was excluded from the regression analysis. The remaining 40 sets of data all contain measurements of $d^{-\frac{1}{2}}$, and gave the following equation:-

$$T_{20} = 315(\%C) - 32(\%Mn) - 9.65(d^{-\frac{1}{2}}) + 4.5$$

.....Eqn.4.3

This equation is significant at the 0.1% significance level but with the coefficient for Mn only significant at the 1.0% level. The coefficients for Ni, N_R and Al_R proved to be of low significance and were consequently excluded from the equation. When this analysis was repeated including N_{AlN}

as an independent variable, the significance of the carbon coefficient was reduced to the 1.0% significance level and the coefficient for $d^{-\frac{1}{2}}$ reduced to the 2.0% level without any appreciable alteration to the coefficients. The coefficient for N_{AlN} also had a very low significance level. This suggests a definite correlation between $d^{-\frac{1}{2}}$ and the N_{AlN} and carbon contents. Regression analysis of the data sets from Tables A1 and A2 (normalised steels only) using $d^{-\frac{1}{2}}$ as the dependent variable and C, Mn, Ni and N_{AlN} as independent variables gave the following regression equation

$$d^{-\frac{1}{2}} = 1.83(\%C) + 0.98(\%Mn) + 1.00(\%Ni) + 167.60(\%N_{AlN}) + 6.70 \quad \ldots\ldots\text{Eqn.4.4}$$

This equation is significant at the 0.5% significance level and the significance of the various coefficients are - N_{AlN}, 0.1%; Mn, 20%; Ni, 30%. Although equation 4.4 confirms the correlation suggested above, the significance of the coefficient for carbon is very low and this coefficient could therefore be excluded from equation 4.4.

The 20ft-lb transition temperature, calculated from equation 4.3, is plotted against the experimental transition temperature in Fig.4-3 for the 40 sets of data used in the regression analysis. Also shown is the 95% confidence limits of $\pm$ 30.3°C.

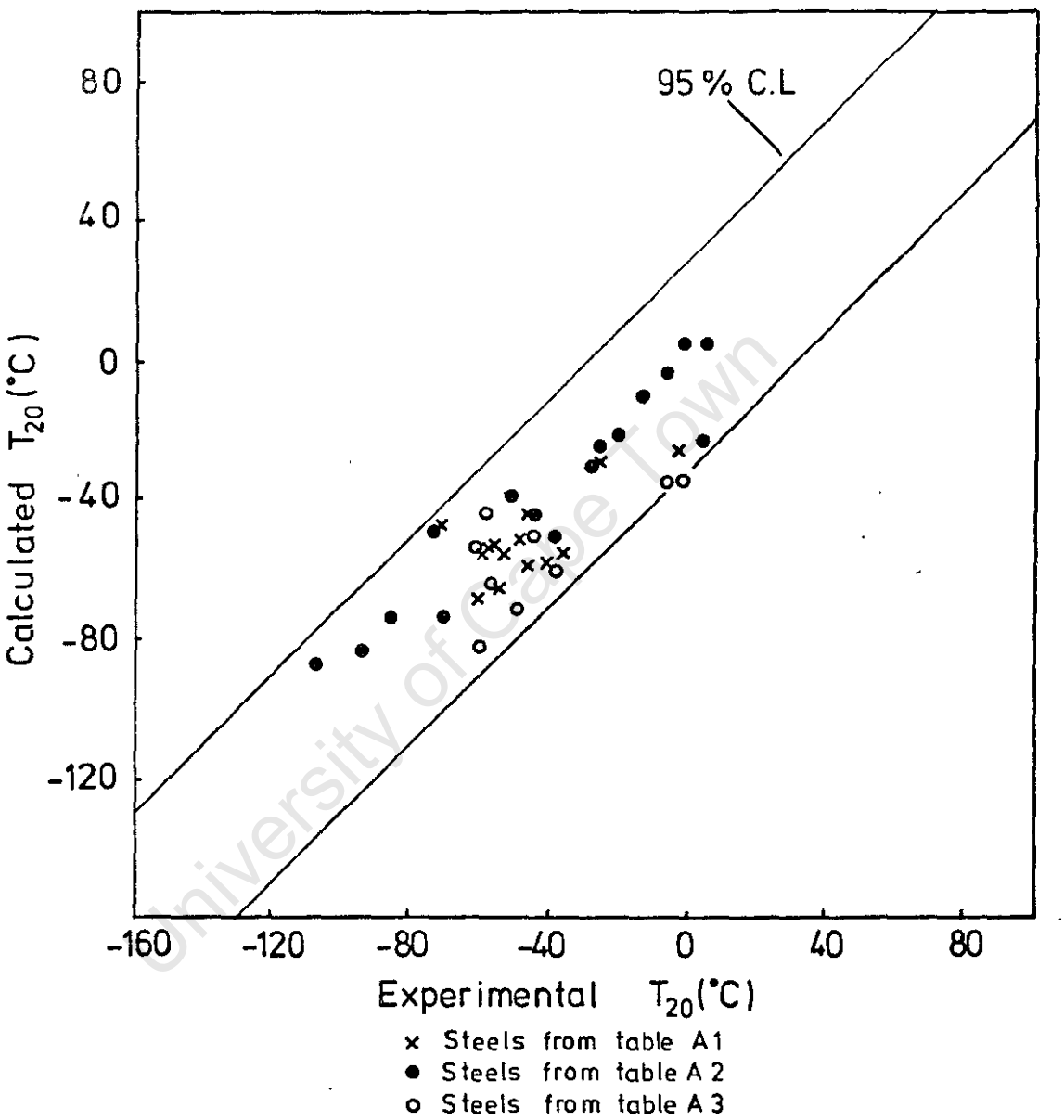

Fig. 4·3 Calculated and observed transition temperatures for experimental steels using equation 4.3.

This data was again modified to include only that data with N_{AlN} contents in excess of 0.0020% thus dividing the data into a high N_{AlN} series and a low N_{AlN} series. In an endeavour to improve the regression analysis further data was accumulated at this stage. This is shown in Table A6 of Appendix 'A' which provided a further eight sets of data for the low N_{AlN} series and two sets for the high N_{AlN} data series. All of these steels were produced in the manner described in paragraph 4.1, the low N_{AlN} series being produced by vacuum melting.

The following regression equation was obtained from the 33 sets of data with N_{AlN} contents in excess of 0.0020%

$$T_{20} = 292(\%C) - 30(\%Mn) - 15.5(d^{-\frac{1}{2}}) + 1577(\%N_R) - 66(\%Si_T) + 72.4 \quad \ldots\ldots\text{Eqn.4.5}$$

This equation is again significant at the 0.1% significance level, although only the $d^{-\frac{1}{2}}$ coefficient proved to have a significance level of better than 0.1%. The coefficient for carbon was better than 1.0%, that for manganese better than 2.0%, and that for silicon better than 5.0%. The coefficient for N_R was only significant at the 30% level and could be neglected. Fig.4-4 shows the 20ft-lb transition temperature calculated from equation 4.5 plotted against the experimental transition temperature, with the 95%

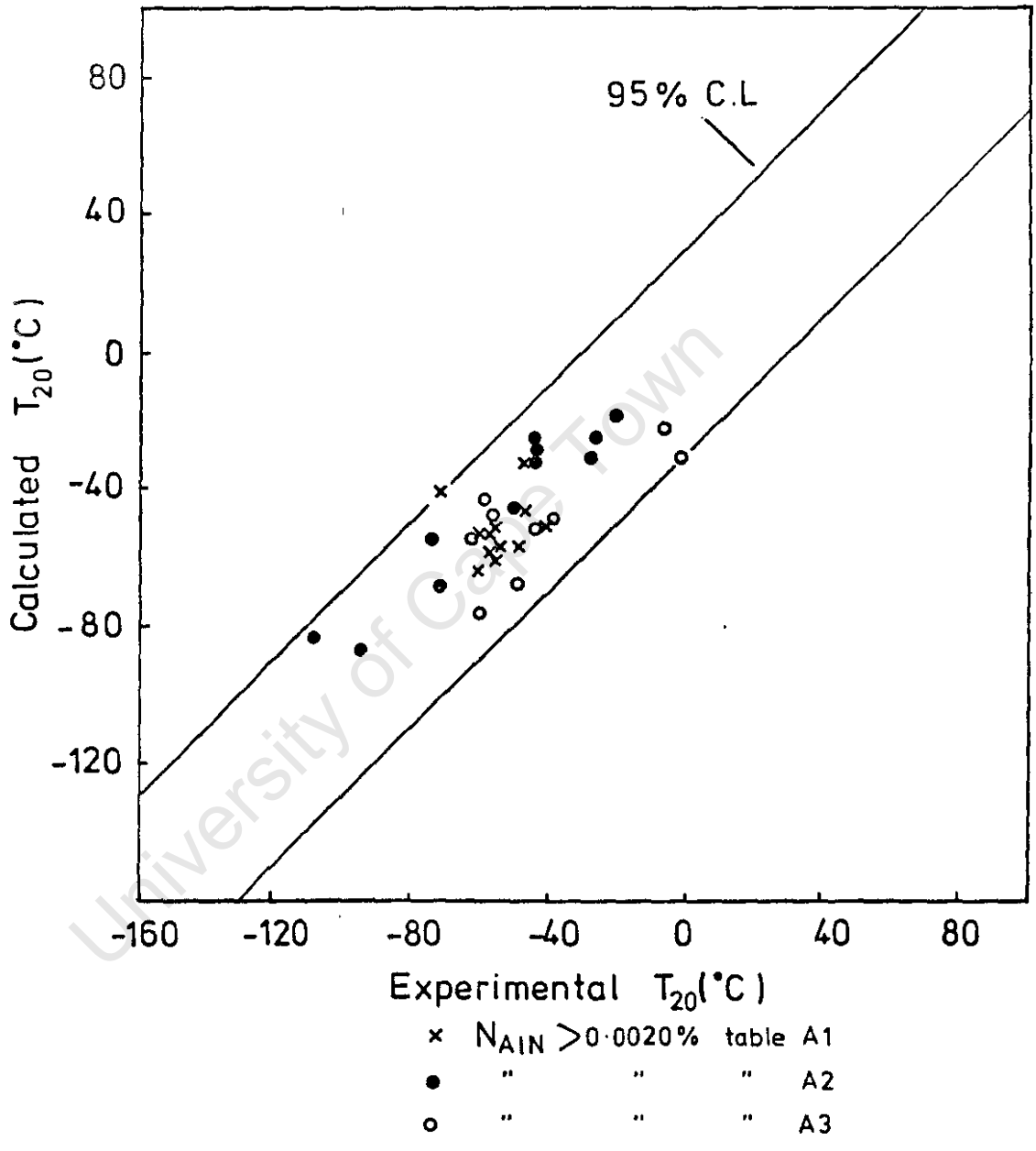

Fig. 4·4 Calculated and observed transition temperatures for experimental steels using equation 4.5 .

confidence limits of $\pm$ 29.4°C.

Multiple regression analysis of the 17 sets of data with N_{AlN} contents of less than 0.0020% was not successful, the regression coefficients contrasting with those of equations 4.1, 4.2, 4.3, and 4.5, and in general having very low significance levels. In every case the Variance ratio, F, showed the resulting regression equation to have significance levels of 10% or less. When this data is used in equations 4.1, 4.3 and 4.5, the resultant graphs, given in Figs.4-5, 4-6 and 4-7 respectively, show considerable variation beyond the 95% confidence limits. This error is to be expected when using equation 4.1 on these steels of low N_{AlN} content, see Fig.4-5, since the grain size of these steels will be independent of the N_{AlN} content, and equation 4.1 contains no term for $d^{-\frac{1}{2}}$. Equations 4.3 and 4.5 do however contain coefficients for $d^{-\frac{1}{2}}$ instead of N_{AlN}, and the resultant regression equations should consequently be applicable to the steels of low N_{AlN} content. The variation in calculated transition temperature beyond the confines of the 95% confidence limits in Fig.4-7 is, however, appreciable despite equation 4.5 containing a coefficient for $d^{-\frac{1}{2}}$. This variation is less obvious in Fig.4-6, principally because some of the steels with low N_{AlN} contents were included in the original regression analysis which resulted in equation 4.3.

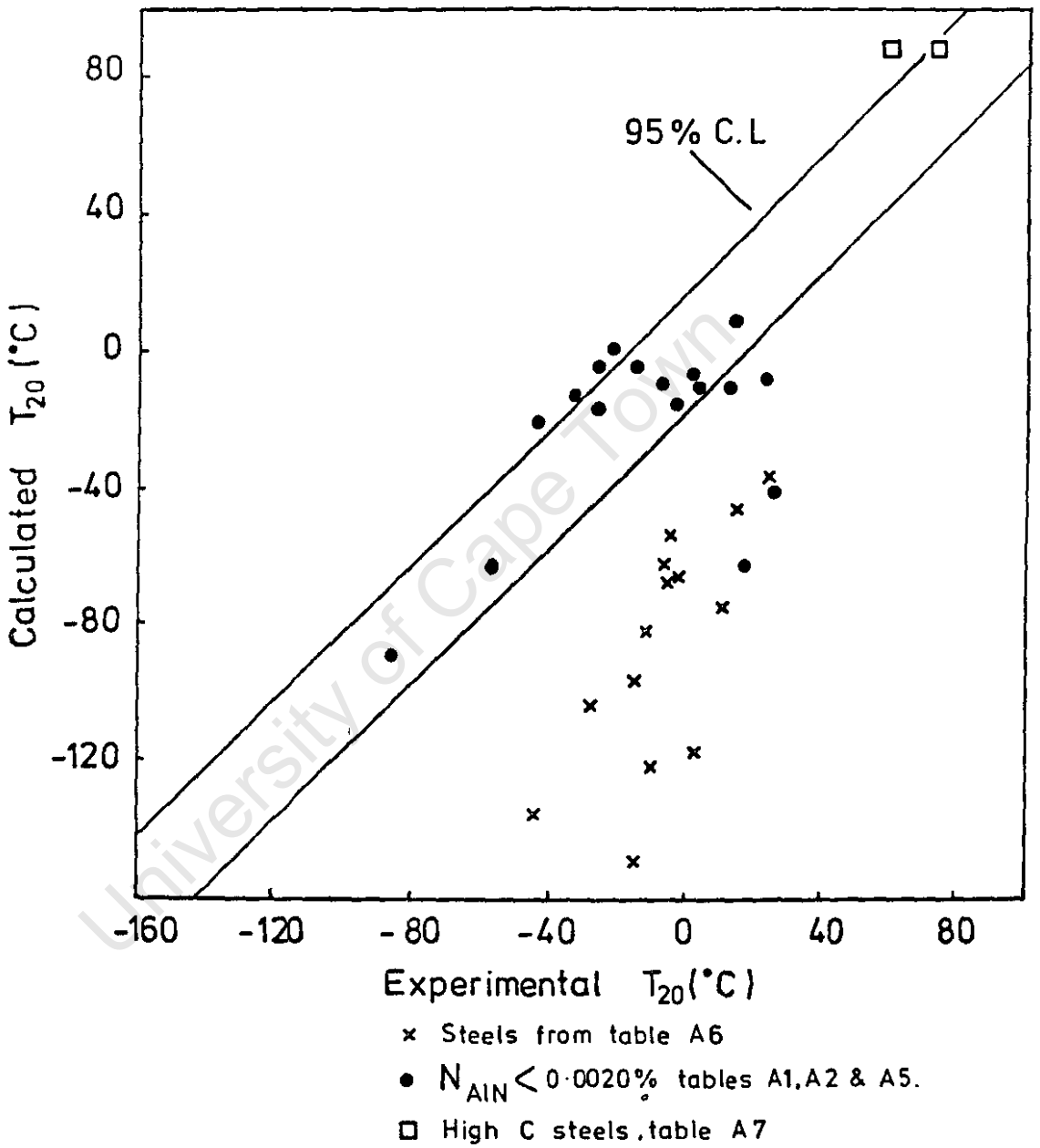

Fig. 4·5 Calculated and observed transition temperatures for experimental steels using equation 4.1 .

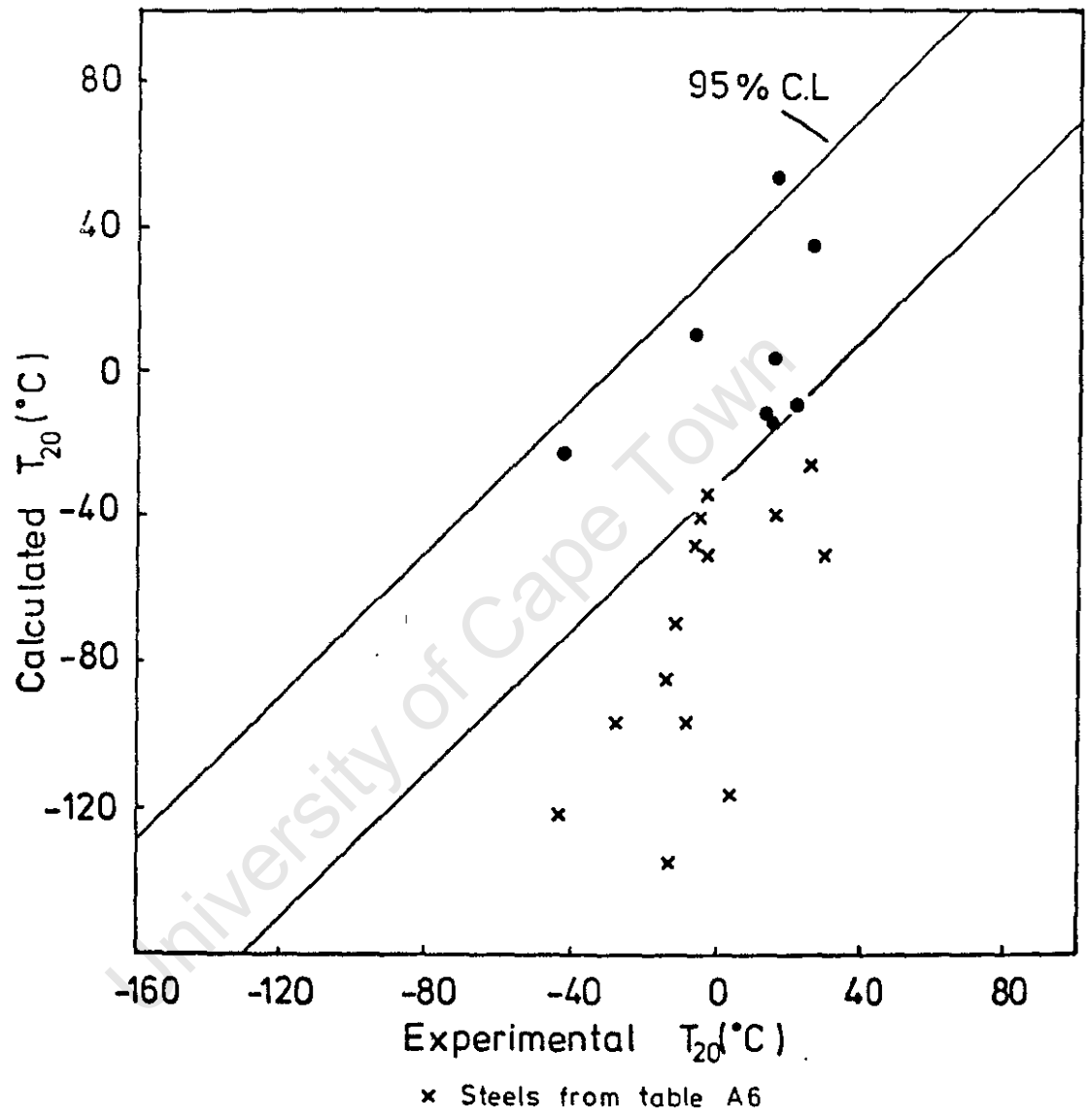

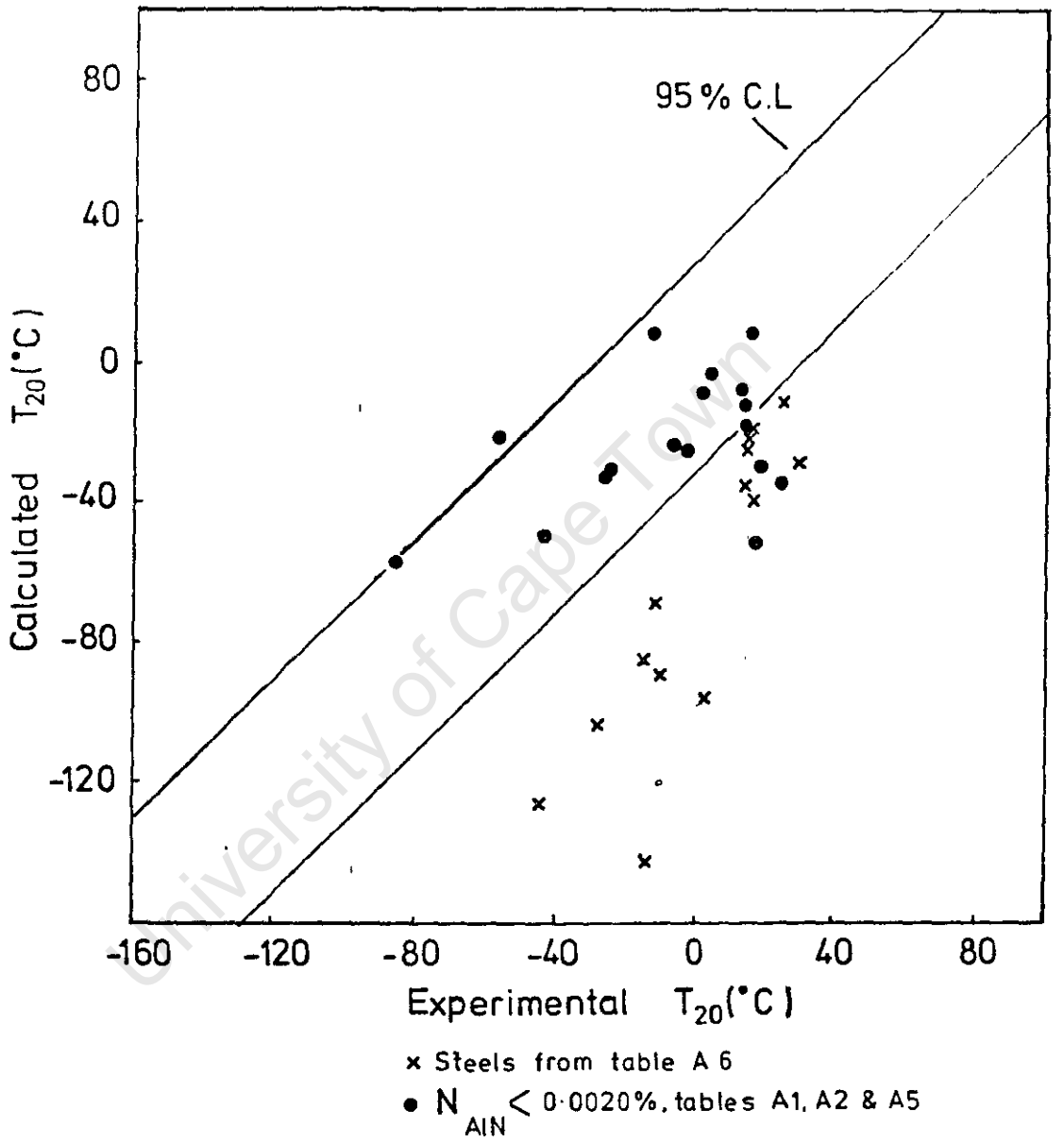

Fig. 4·7 Calculated and observed transition temperatures for experimental steels using equation 4.5 .

It would appear from the above that the steels of low N_{AlN} content have transition temperatures controlled by factors other than those expressed by equations 4.1, 4.3 and 4.5 for steels of high N_{AlN} content. One noticable feature of the steels of low N_{AlN} content is that many of them have been produced by vacuum melting and have consequently low nitrogen (N_{sol}) contents. Although it is generally recognised that manganese lowers the ductility transition temperature, see Table 1.1, manganese has also been shown to raise the lower yield stress by 2.1 tons per inch^2 per 1% weight after compensating for changes in grain size and volume fraction pearlite.(28) Since alloying elements in solid solution in ferrite usually increase the yield stress by raising the temperature independent friction stress, σ_o^*, it would be natural to expect manganese to raise the transition temperature in low carbon steels. Petch(47) has explained the lowering of the transition temperature by manganese as a two-fold effect, brought about partly by a refinement of grain size and partly due to a weakening of dislocation locking. If, as Petch suggests, dislocation locking in steels is mainly by nitrogen, and dislocation locking raises the transition temperature very markedly, the overall effect of manganese would be to lower the transition temperature. Nitrogen-free steels would however be expected to show an increase in transition temperature with increasing manganese content due to its effect

on the friction stress alone.

4.3 The Low Nitrogen Steels:

To determine the expected increase in the ductility transition temperature brought about by manganese in the absence of nitrogen, a further series of vacuum melted steels was produced with the manganese content varying from 0.2% to 2.0%. Eighteen 50-lb ingots were produced and rolled to $\frac{13}{16}$ inch($\cong$ 20mm) diameter bar for heat treatment. Twelve standard 2mm Vee notch Charpy specimens were produced from the heat treated bars and the lower end of the impact transition curve determined for each condition. Sections of the heat treated bars were used for chemical analysis and broken Charpy specimens were used for metallographic measurement of grain size. In this instance the pearlite grains were also counted as individual grains, since the pearlite grain size was approximately equal to the ferrite grain size in many of the steels in this series. Four of these cast were rejected from the initial analysis because of a banded ferrite-pearlite microstructure, thought to have resulted from a low rolling temperature. The chemical analysis, the reciprocal of the root mean ferrite grain diameter ($mm^{-\frac{1}{2}}$) and the Charpy 20ft-lb energy level transition temperatures are given in Table A6 (Appendix 'A') for the fourteen satisfactory steels and the above data for the four rejected casts is included in Table A7.

Linear multiple regression analysis of the data from Table A6 showed that there was no linear increase in transition temperature with increasing manganese content. When the transition temperature was corrected for variation in carbon content and $d^{-\frac{1}{2}}$ by using coefficients from equation 4.3, examination of the data indicated that the transition temperature decreased with increasing manganese content up to approximately 1% Mn, and that further increases in manganese content increased the transition temperature. This increase in transition temperature was most noticable on the data with high manganese contents and very low nitrogen contents, e.g., N_R = 0.0002%. It seemed therefore that the nitrogen content of this series was not low enough to determine the sole effect of manganese.

It was assumed therefore that some factor combining the manganese and nitrogen contents should be included in the regression analysis to account for any interaction between these two elements. After a number of attempts using different combined factors and fitting the curves to the experimental results, the following combined equation was selected for determining the coefficients for manganese and nitrogen:-

$$\Delta T_{20} = K_3(\%Mn) + K_4(F') + K_5(\%N_R) + K_c$$

.....Eqn.4.6

where $F' = \frac{(\%Mn)\ (\%N_R)}{(\%Mn)+K_n(\%N_R)}$

K_3, K_4 and K_5 are regression coefficients and K_n a constant.

This equation satisfies the expected limiting conditions of $\Delta T_{20} = K_3(\%Mn)$ where $N_R \longrightarrow 0$ and $\Delta T_{20} = K_5(\%N_R)$ where $Mn \longrightarrow 0$.

If the regression coefficient K_4 is negative and large enough, intermediate values of Mn and N_R will show the overall effect of Mn as a negative coefficient.

The constant K_n was found by trial and error to give the best variance ratio values when it had values in the range 1200 to 1500.

Using $K_n = 1500$, regression analysis of the 14 sets of data shown in Table A6 gave the following equation:-

$$T_{20} = 116(\%C) - 13.3(d^{-\frac{1}{2}}) + 33(\%Mn) - 158,856(F') + 22376(\%N_R) + 489(\%Si_T) - 32$$

.....Eqn.4.7

This equation is significant at the 1.0% significance level, but most of the individual coefficients, except $d^{-\frac{1}{2}}$ (30% significance) and the factor F' (5% significance), had low significance levels.

4.4 Final Regression Analysis:

For the final regression analysis of all the accumulated data, the data was sectionalised into groups, each data group consisting of data of similar independent variables. These regression subgroups are shown on the tables in Appendix 'A' and their classification is as follows:-

Regression Group	Data	No.Sets
1	Low N_R, $Al_R = 0$	14
2	High N_R, $N_{AlN} < 0.0020\%$	7
3	Low N_R, $Al_R > 0$	8
4	$N_{AlN} > 0.0020\%$	30
5	$Si_T > 0.35\%$	4
9	Commercial and others	14
11	Quenched and Tempered	12

The above regression groups were analysed separately and in combination, but in general regression analysis was not completely successful because of inter-correlations between independent variables and in some cases due to limited variation ranges in certain independent variables.

These regression equations are summarised in Table 4.2 which also shows the significance level of each coefficient and the equation as a whole. It can be seen from this table that the addition of data from regression group 1 to data

TABLE 4.2

Regression Equations.

Regression Group	Regression Coefficients and Significance Levels: C	$d^{-\frac{1}{2}}$	Mn	F	N_R	Al_R	Si_T	Constant	Equation No.
1 + 2	311	-11.9	27	-130,614	-2588		359	-21	4.8
	(0.1%)	(20%)	(<20%)	(0.1%)	(20%)		(2.0%)		
4	264	-14.3	-30	-9,360	1835	-20	-11	52	4.9
	(0.5%)	(10%)	(2.0%)	(<20%)	(<<20%)	(<20%)	(<<20%)		
1+2+4	112	-11.8	26	-141,826	960	-475		81	4.10
	(0.1%)	(10%)	(0.1%)	(2.0%)	(0.1%)	(<20%)	(1.0%)		
1+2+3+4	146	-12.9	27	-144.317	328	-276		86	4.11
	(0.1%)	(2.0%)	(0.1%)	(2.0%)	(0.1%)	(<20%)	(5.0%)		
2+3+4	272	-11.0	-20	-48,320	959	54		33	4.12
	(0.1%)	(1.0%)	(0.1%)	(<20%)	(<20%)	(<<20%)			

from groups 2, 3, and 4 seriously affects the coefficients for carbon and residual aluminium, e.g., comparing equations 4.11 and 4.12 the addition of data from group 1 reduces the coefficient for carbon from 272 to 146 and the residual aluminium coefficient is changed from 54 to -276, despite the group 1 data having zero aluminium. It was consequently assumed that the different technique used for measuring grain size on the low nitrogen steels of group 1 was responsible and that data from group 1 should therefore be analysed separately. In view of the low significance levels of many of the coefficients resulting from regression analysis of data from regression group 1, the transition temperature, T_{20}, of this data was corrected for variations in carbon and $d^{-\frac{1}{2}}$, using regression coefficients from equations derived from data of groups 2, 3, and 4. Coefficients for carbon ranging from 264 to 320 were chosen for this analysis, with the coefficient for $d^{-\frac{1}{2}} = -11.8$.

The best Variance ratio for the resulting regression equation was obtained with a carbon coefficient of 264, giving the following equation:-

$$\Delta T_{20} = 28(\%Mn) - 140,000(F') + 11,452(\%N_R) + 421(\%Si_T) - 36$$

.....Eqn.4.13

This equation is significant at the 2.5% significance level and the coefficients for F' and Mn significant at the 10% and 5% levels respectively. The remaining coefficients had significance levels of less than 20%. The close similarity of the coefficients for Mn and F' with those shown in Table 4.2 led to the use of these coefficients for the correction of T_{20} for the data in regression groups 2, 3, and 4. When the coefficient for Mn was taken as 26 and that for F' as -144,000, the following regression equation was obtained using data group 2 + 3 + 4.

$$\Delta T_{20} = 280(\%C) - 11.6(d^{-\frac{1}{2}}) + 3530(\%N_R) + 38 \quad \text{.....Eqn.4.14}$$

This equation is significant at better than the 0.1% significance level, the coefficients for carbon and $d^{-\frac{1}{2}}$ having significance levels of 0.1% and N_R a significance level of 1.0%. Al_R, Si_T and O_T all have low significance levels and have consequently been excluded from equation 4.14.

Re-examination of the original 52 sets of data used to determine equation 4.1, but correcting T_{20} for C, Mn and F' by using 264, 26 and -144,000 as the respective coefficients, the following regression equation was obtained

$$\Delta T_{20} = -13(\%Ni) + 18(\%Cr) - 1090(\%N_{AlN}) + 5369(\%N_R) + 73(\%Al_R) - 73(\%Si_T) + K_6 \quad \text{.....Eqn.4.15}$$

where ΔT_{20} is the corrected ductility transition temperature and K_6 is a constant with values -60 for the normalised steels, -20 for the slow cooled steels, and -92 for the quenched and tempered steels.

The above regression equation is significant at better than the 0.1% significance level, and the significance level of the individual coefficients are, Ni and N_R, 0.1%; Cr, 5%; Si_T, 10%; N_{AlN}, 20%; and Al_R, 30%. The coefficient for O_T had a very low significance level and has consequently been excluded from equation 4.15.

For the final series of regression analyses a range of coefficients, suggested by the above equations, were used to correct the transition temperature for the various independent variables. The following regression equation gave the best Variance ratio, F, for all the coefficients examined:-

$$T_{20} = 264(\%C) - 11.8(d^{-\frac{1}{2}}) + 28(\%Mn) - 140{,}000(F') + 3850(\%N_R) + 18(\%Cr) + 68(\%Si_T) + 50(\%Al_R) + K_7$$

.....Eqn.4.16

The constant K_7 has values of 53.9 for data from regression group 1 and 17.6 for data from regression groups 2, 3, and 4. It was found that equation 4.16 could be used for data from regression group 11 (quenched and tempered steels) if a correction was made for $d^{-\frac{1}{2}}$ by using the coefficients for

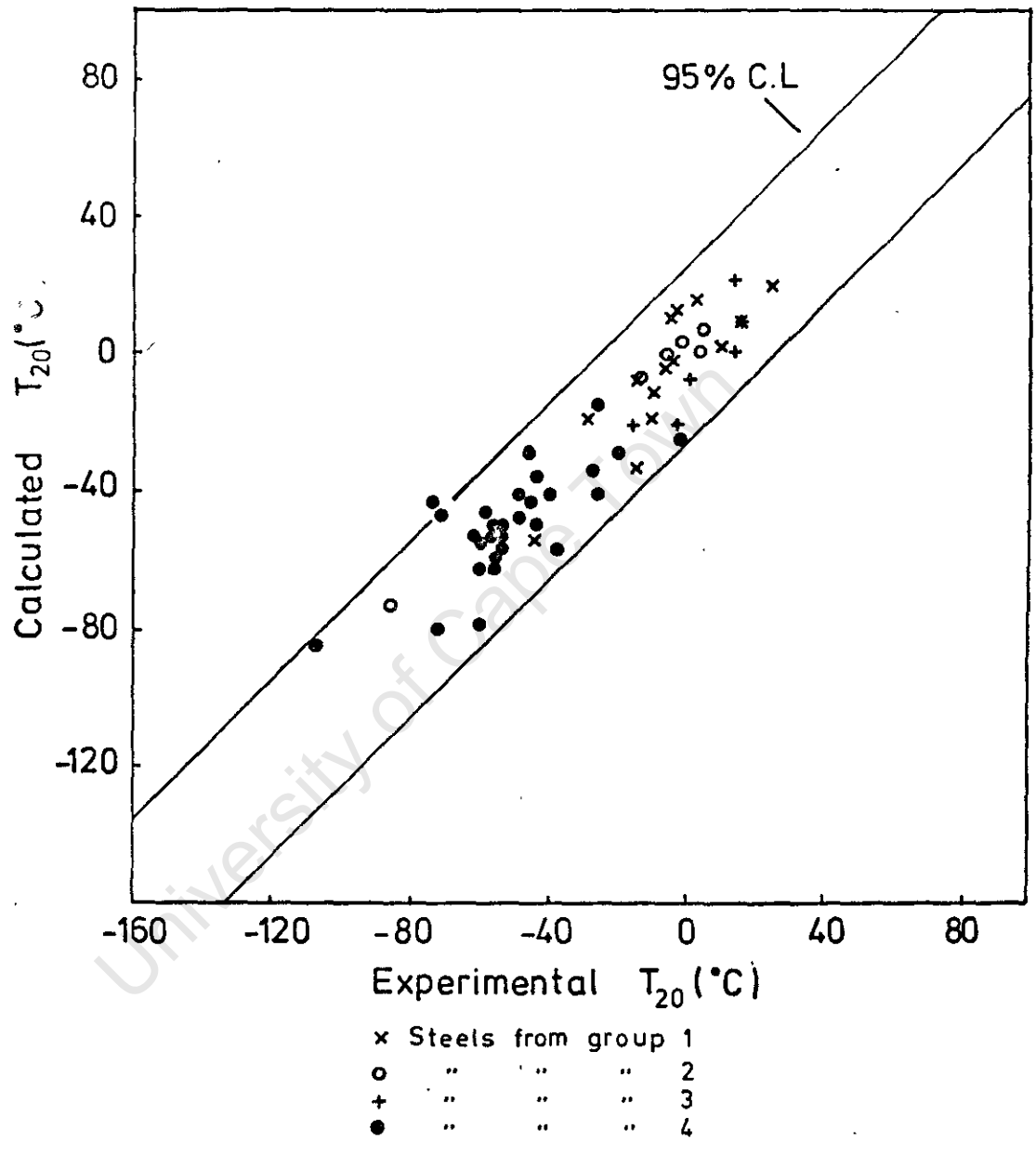

Fig. 4·8 Calculated and observed transition temperatures for experimental steels using equation 4.16 .

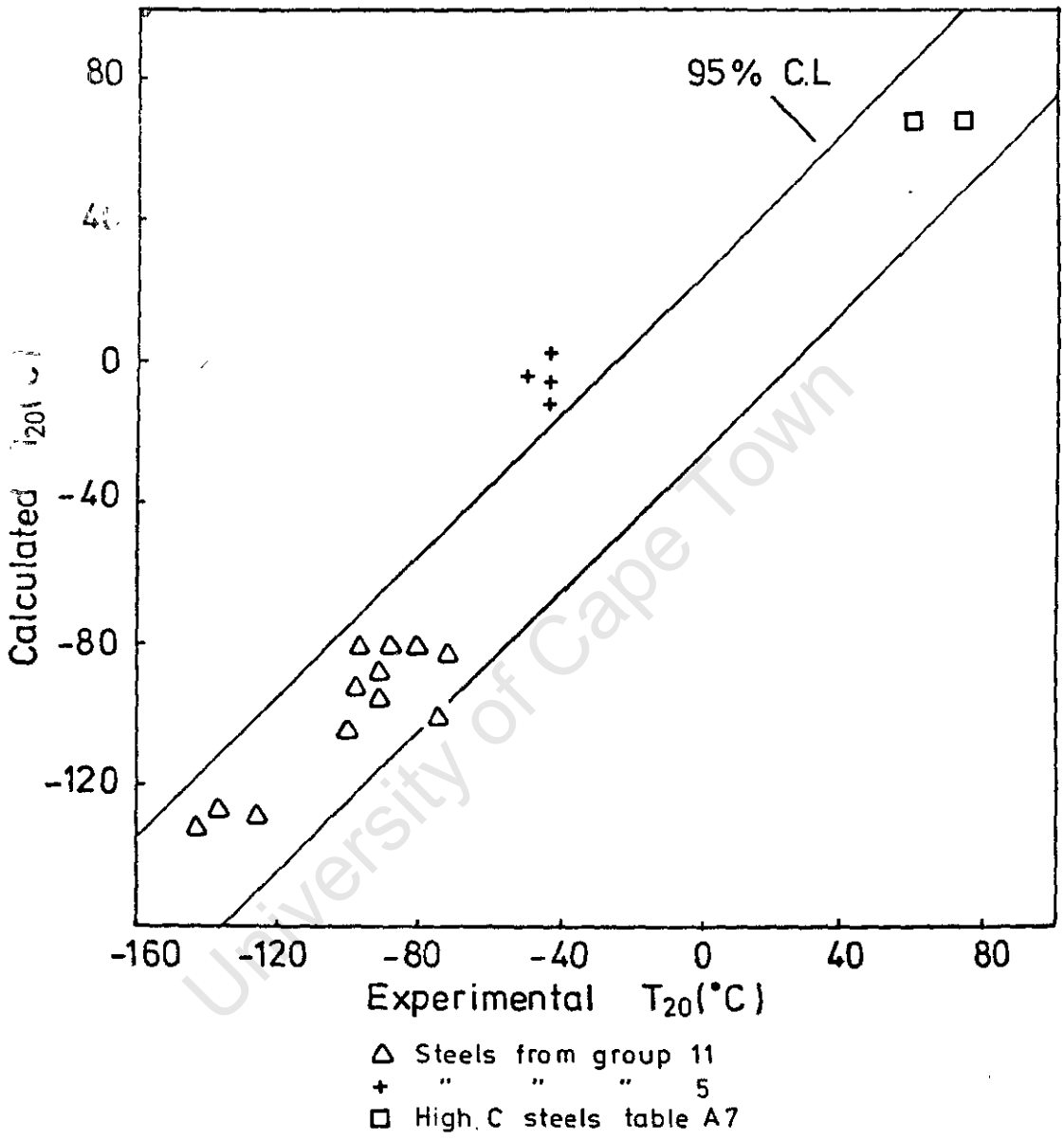

Fig. 4·9 Calculated and observed transition temperatures for experimental steels using equation 4.16.

N_{AlN}, Mn, and Ni from equation 4.4. The constant K_7 has a value of -29.7 in this instance.

The Variance ratio, F, for equation 4.16 is 33 for the 14 sets of data from group 1, 180 for the 41 sets of data analysed from group 2 + 3 + 4, 282 for the 55 sets of data analysed from group 1 + 2 + 3 + 4, and 37 for the 12 sets of data from group 11. This equation is consequently significant at better than the 0.1% level, and very much better than this for the combined sets. The data is shown in Figs.4-8 and 4-9 with the 95% confidence limits of $\pm$ 25°C. determined from regression group 1 + 2 + 3 + 4. All the coefficients in equation 4.16 except those for Al_R and Si_T were significant at the 0.1% significance level. The coefficients for Al_R and Si_T had low significance levels and the coefficient for Si_T could be excluded without much alteration to the Variance ratio for the equation. When equation 4.16 is used in conjunction with data from regression group 5, the constant K_7 is found to equal -22.6. Since the steels in this regression group have silicon contents in excess of 0.35% and in one case up to 0.648%, it would appear that silicon contents of this magnitude lower the transition temperature. However, when the data from group 5 was added to that of groups 2, 3, and 4 no significant effect of silicon was found. Table 4.3 summarises the full range of variables used in analysis.

TABLE 4.3

Summary of the variables used to determine equation 4.16

		Minimum	Mean	Maximum
Carbon	%	0.04	0.1612	0.27
Silicon	%	0.07	0.2188	0.32
Manganese	%	0.25	0.7481	1.39
Nickel	%	0.01	0.2866	3.93
Chromium	%	0.01	0.0179	0.12
Oxygen	%	0.0006	0.0051	0.0380
N_{AlN}	%	0.0000	0.0035	0.0140
N_R	%	0.0000	0.0024	0.0095
Al_R	%	0.000	0.0208	0.195
N_{insol}	%	0.0000	0.0008	0.0034
Al_{insol}	%	0.000	0.0048	0.014
$d^{-\frac{1}{2}}(mm^{-\frac{1}{2}})$		4.12	8.3288	11.80
T_{20} (°C)		-107	-29.5932	26

CHAPTER 5.

DISCUSSION OF RESULTS.

5.1 The Regression Coefficient for Carbon:

From equations 4.15 and 4.16 it can be seen that an increase of 0.01% C will raise the ductility transition temperature (T_{20}) by 2.6°C. When the lowest carbon content steels (group 1) are excluded from the analysis, this increase in ductility transition temperature with .01% increase in carbon content becomes 2.8°C.,(equation 4.14). These figures compare well with data extracted from the work of Burns and Pickering[29] where 0.01% C raises the transition temperature (T_{20}) by approximately 2.9°C.

The work of Rinebolt and Harris[34] is also in good agreement with the figure predicted for carbon by equations 4.14, 4.15, and 4.16. These authors found that the 15ft-lb transition temperature was increased by 3.3°C. for steels of more than 0.30% carbon, and by 2.6°C. for steels of less than 0.30% carbon for each 0.01% increase in carbon. The figure for the low carbon range was however influenced by a larger than average grain size in their 0.01% carbon steel. When allowing some correction for this and plotting the best fit line through their complete carbon range these authors obtained a value of 3.0°C. per 0.01% carbon. In this case all the steels were normalised from 900°C.

Boulger and Hansen[26] used linear multiple regression analysis techniques to determine the effects of several elements on transition temperatures by NDT and Charpy Vee notch tests on $\frac{5}{8}$in. thick plate steel. For the 27 steels examined the NDT transition temperature was increased by 1.2°C. per 0.01% C, and the Charpy 15ft-lb, 25ft-lb, 30% and 50% shear fracture transition temperatures by 1.8°C., 2.5°C., 1.9°C., and 2.4°C., respectively per 0.01% C. Grozier[48] reported the 50% shear fracture transition temperature for sub-standard Charpy Vee notch specimens to be raised by 2.4°C. per % pearlite, or assuming the eutectoid composition equal to 0.8% C, by 3.0°C. per 0.01% C. Pickering and Gladman,[28] using the same definition of transition temperature, but for standard Charpy Vee notch specimens, computed a 2.2°C. rise in transition temperature per % pearlite, or based on the above assumption, a 2.7°C. rise per 0.01% C.

Although different criteria have been used as the transition temperature in determining the above increases in transition temperature with increased carbon content, the results are in general agreement with the coefficients of equations 4.14, 4.15, and 4.16.

Petch and Heslop[49] have shown that the equation for the lower yield point

$$\sigma_y = \sigma_o + k_y d^{-\frac{1}{2}}$$

can be extended to account for solid solution hardening in alloys of iron to give:-

$$\sigma_y = \sigma_o + k'(\% \text{ alloy}) + k_y d^{-\frac{1}{2}}$$

.....Eqn. 5.1

At constant temperature this equation can be rewritten in the form

$$\sigma_y = \sigma_o^{+} + \left[\sigma_o^{*} + k'(\% \text{ alloy})\right] + k_y d^{-\frac{1}{2}}$$

.....Eqn. 5.2

where $\sigma_o^{*} + k'(\% \text{ alloy})$ represents the temperature independent friction stress for solid solution alloys and k' is a constant.

This modified temperature independent friction stress can now be substituted into equation 2.10 to account for the effect of solid solution alloys on the ductility transition temperature. Although small variations in carbon content can have a large effect on this friction stress term in single phase iron alloys,[28] the main effect of carbon variation in the range considered here will be to alter the proportion of second phase (pearlite) present in the steel. For the normal range of heat treatments used in practice and in this investigation, the carbon in solid solution in ferrite probably remains fairly constant.

The variation in volume fraction pearlite is not directly accounted for in equation 2.10, since this equation is derived from theoretical considerations for a single phase material. Although the volume fraction pearlite has been shown to have no significant effect on the lower yield strength in steels of up to 0.2% carbon,[28] Burns and Pickering[29] have shown an increase in yield strength of approximately 22.0 tons/in.^{2} per 1.0% C in steels with the range 0.1% to 0.5% C. If this increase in yield strength is considered to be brought about by an increase in an "equivalent friction stress", this "equivalent friction stress" can be used in equation 2.10 to give a corresponding change in transition temperature.

The above authors[29] have shown that the initiation of cleavage cracks in pearlite appears to occur with relative ease, but that the propagation of these cracks through the pearlite occurs with apparent difficulty. They suggest that the increase in transition temperature with increasing carbon content could result from the initiation of cracks in pearlite due to one of the following reasons:-

i) a high dislocation density is produced in the pearlitic ferrite at low overall strain values resulting in local resistance to plastic deformation;

(i) the fracture of cementite lamellae leading to notch effects;

(ii) the creation of voids at ferrite-cementite interfaces resulting in the generation of dislocation at the interfaces and thus providing nuclei for cracks.

At first sight one is inclined to reject the first two suggested reasons, since equations 4.1, 4.15, and 4.16 suggest that carbon is equally effective in raising the transition temperature in quenched and tempered steels, where the carbide will be in small discrete particles. This may however be an erroneous conclusion since all the quenched and tempered steels have very similar carbon contents. Figs. 4-2 and 4-9 therefore only show predicted changes in transition temperature in the quenched and tempered steels due to variations in elements other than carbon.

Recent work[50] on fracture in pearlitic steels has shown that cracks develop in the cementite lamellae transversed by slip planes at overall strains of approximately 2%, lending support to the suggestions (ii) and (iii) above.

Although the data used to compute equations 4.1 and 4.16 was limited to 0.27% C maximum, the results from a high carbon experimental casts in two heat treated

conditions (1938A normalised from 830°C. and 1938B normalised from 950°C., see Table A7) are also shown in Figs.4-5 and 4-9. The agreement between the calculated and experimental values of T_{20} using equation 4.16 can be seen from Fig.4-9 to be excellent. Since grain size was difficult to determine on this high carbon steel, equation 4.4 was used to determine an equivalent value of $d^{-\frac{1}{2}}$ for substitution in equation 4.16.

5.2 The Regression Coefficients for $d^{-\frac{1}{2}}$ and N_{AlN}:

Equation 2.10 predicts that the ductility transition temperature should be proportional to $d^{-\frac{1}{2}}$, and that the coefficient for this grain size variable should be equal to $\frac{1}{\Sigma}\left(\frac{B_1 Y}{k_y} - k_y\right)$. However, the constant k_y and possibly also the surface energy term Y are proportional to the strength of dislocation locking,[47] so that this coefficient is not a constant but a variable, dependent on dislocation locking. Since locking in low alloy structural steels should under normal conditions be principally due to nitrogen,[47] the strength of locking is likely to be some function of the residual nitrogen content, i.e., the total nitrogen content minus the nitrogen combined as precipitates of aluminium and other nitrides. Consequently a large number of factors, other than the total nitrogen content, influence the strength of dislocation locking in structural steels, e.g., the Ti, V, Si and Al contents and the heat

treatment.[36,38 and 54] In addition to the above elements commonly found in steel, manganese is thought to have a large influence on dislocation locking through its interaction with nitrogen.[47 and 52] (This is discussed in section 5.3). This situation is further complicated by the precipitated aluminium nitride altering the grain size,[40] (see also equation 4.4).

Under the circumstances it is not surprising that the coefficient for $d^{-\frac{1}{2}}$ was found to vary between -15.5 and -9.65, depending on the N_R and Mn contents of the data included in the regression analysis, e.g., see equations 4.3 and 4.5. In general the smaller coefficient occurred with the steels of higher N_R content (stronger locking) and the larger negative coefficient with the low N_R content (weaker locking) steels, although this coefficient was also influenced by the Mn contents.

To overcome this difficulty a coefficient for the variable $d^{-\frac{1}{2}}$ was chosen which was representative of the average coefficient computed on data of group 2 + 3 + 4, and this coefficient was then used with the other data groups. Since this coefficient was now being considered as a constant, a further term had to be added to the regression equation which would satisfactorily represent the strength of dislocation locking. This variable, F', is discussed in greater detail in section 5.3.

The chosen mean coefficient for $d^{-\frac{1}{2}}$ had a value of -11.8, where d was the mean grain diameter in mm. Irvine et al[53] and Grozier[48] used multiple linear regression techniques to determine coefficients of -11.6(-2.3 $d^{-\frac{1}{2}}ins^{-\frac{1}{2}}/^{o}C.$) and -9.0 (-3.2 $d^{-\frac{1}{2}}ins^{-\frac{1}{2}}/^{o}F.$) respectively for this variable. Neither of the above authors recognised this coefficient as a variable dependent on the strength of dislocation locking, so that their coefficients represent average values for the strength of locking in the data examined. These coefficients are however consistant with equation 2.10 in that the smaller negative coefficient has occurred with data of high residual nitrogen content[48] (mean 0.0060%), and the larger negative coefficient has occurred with data from normalised or annealed steels containing aluminium nitride and therefore reduced residual nitrogen.[28] (Details of the mean and range of nitrogen content are not published in reference 28).

When the variable $d^{-\frac{1}{2}}$ was excluded from the regression analysis, it was found that the transition temperature could be adequately described by including a coefficient for the variable N_{AlN}, see equations 4.1, 4.2 and 4.15. Linear multiple regression analysis using $d^{-\frac{1}{2}}$ as the dependent variable confirmed a relationship between $d^{-\frac{1}{2}}$ and N_{AlN}, see equation 4.4. The significance level of this equation could probably have been improved by using the grain diameter d as the dependent variable,[40] but by sacrificing simplicity

of application.

When equation 4.4 (excluding the coefficient for C because of its low significance) is substituted in equation 4.16, the following expression is obtained for the normalised steels:-

$$T_{20} = 264(\%C) + 17(\%Mn) - 140{,}000(F') - 12(\%Ni) + 18(\%Cr) - 1980(\%N_{AlN}) + 3850(\%N_R) + 50(\%Al_R) + 68(\%Si_T) - 61$$

.....Eqn. 5.3

The above coefficients compare extremely well with those of equation 4.15, obtained by regression analysis of the original 52 sets of data. Exceptions are the coefficient for Si_T, of low significance in equation 4.16 and shown to be in error when the equation is used with the high Si_T data (see section 4.4,)and small differences in the coefficients for N_{AlN} and N_R. These differences probably result from inter-correlation between the N_{AlN} and N_R independent variables during the analysis of data for equation 4.15, and equation 5.3 is therefore probably more correct. Equation 5.3 can also be used on data from steels in the quenched and tempered condition, where there is some difficulty in determining ferrite grain size. The calculated constant for equation 5.3 now becomes - 108, compared with - 92 for quenched and tempered steels in equation 4.15. Although

equation 4.4 is not strictly applicable to data from quenched and tempered steels, the transition temperature of these steels is probably influenced by the austenite grain size, which is in turn a function of the aluminium nitride content.(54).

5.3 The Regression Coefficients for Mn and the Locking Strength Function $K_4F' + K_5(\%N_R) + K_c$:

The substitution of the dislocation locking strength variable in equation 2.10 with a constant regression coefficient for $d^{-\frac{1}{2}}$ necessitates the inclusion of a further variable in the regression equation to account for variability of dislocation locking strength. Since dislocation locking in structural steels is thought to be mainly by nitrogen,(47) and since the effectiveness of nitrogen locking is controlled by the Mn content,(52) it is necessary to consider the coefficients for Mn, N and F' together as shown in equation 4.6. The coefficient K_4 is of necessity a negative coefficient (confirmed by regression analysis) so that equation 4.6 can be rewritten as follows:-

$$T_{20} = K_3(\%Mn) + \left[- K_4(F') + K_5(\%N_R) + K_c \right] \quad \text{.....Eqn. 5.4}$$

where $F' = \dfrac{(\%Mn)\ (\%N_R)}{(\%Mn) + K_n(\%N_R)}$

Although the above combined variable has no theoretical basis, it satisfies the limiting conditions in that F' tends to zero as either N_R or Mn tend to zero; i.e., the locking strength variable (within the square bracket in equation 5.4) becomes proportional to the residual nitrogen content in the absence of manganese, and becomes a constant equal to K_c when locking is by carbon atoms only in the absence of residual nitrogen. In all cases there is also a positive coefficient for manganese (K_3) which is equal to the friction stress constant k' in equation 5.2. This represents the increase in transition temperature brought about by manganese in solid solution in the ferrite increasing the temperature independent friction stress.

Although the coefficients K_3, K_4 and K_5 were found to vary slightly on regression analysis of different sets of data (depending on the range of Mn and N_R in each data group), the values chosen for these coefficients in equation 4.16 appeared fairly consistantly when Mn and N_R were varied over a wide enough range, see equations 4.7, 4.8, 4.10, 4.11, 4.12 and 4.13. These coefficients, when used in equation 5.4, result in the curves shown in Fig. 5-1 when plotted to show the variation in transition temperature with manganese content for constant values of residual nitrogen. It can be seen from this figure that the transition temperature increases almost linearly with manganese content when the residual nitrogen content is low

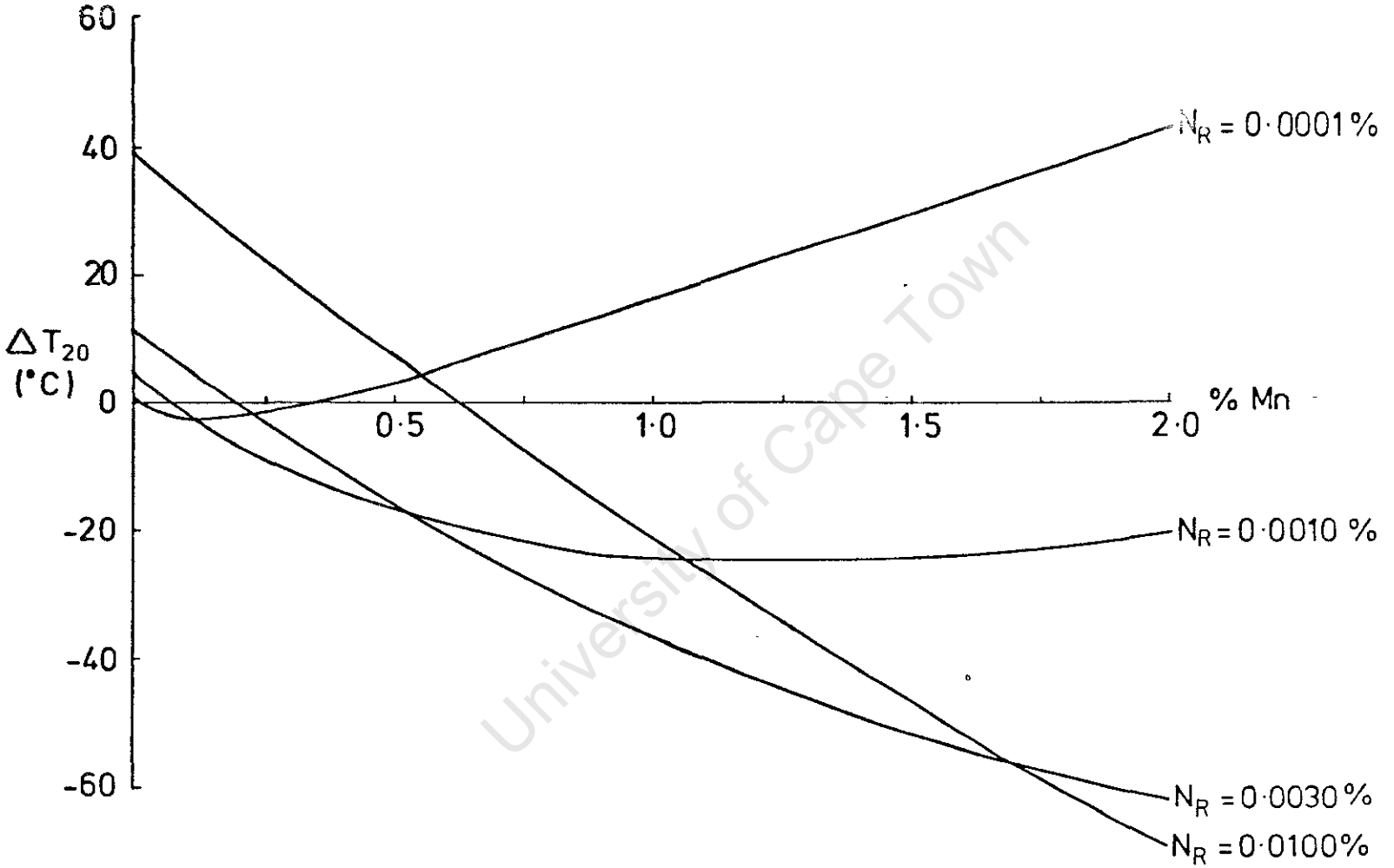

Fig.5·1 Change in transition temperatures with Mn constant given by equation 5.4 .

($< 0.0001\%$). On the other hand the transition temperature decreases almost linearly with manganese when the residual nitrogen content approaches 0.0100%; i.e., the transition temperature would appear on linear multiple regression analysis of data with high N_R contents to decrease linearly with increasing Mn content. This accounts for the negative coefficients obtained by Boulger and Hansen[26] (-35(%Mn)), Grozier[40] on steel with mean N_R = 0.0060%, (-38(%Mn)), and Rinebolt and Harris[34] (-56(%Mn)).

Analysis of the original 52 sets of data, see equations 4.1 and 4.2, also gave negative coefficients for manganese. When the $d^{-\frac{1}{2}}$ variable was included in the regression equation the coefficient for Mn was reduced to -32 (equation 4.3) and -30 (equation 4.5), showing that part of the reduction in transition temperature brought about by Mn was as the result of grain refinement, see equation 4.4. The mean N_R content of the data used for equations 4.3 and 4.5 was approximately 0.0030%. A curve for this nitrogen content is also shown in Fig.5-1, and for Mn contents up to 1.39% (Table 4.1) the curve can be seen to approximate to a linear relationship with a slope of approximately -35.

Fig. 5-1 can be replotted to show the variation in transition temperature with N_R content for constant values of Mn, see Fig.5-2. The reason for variability in the N_R coefficient with different data groups when regression

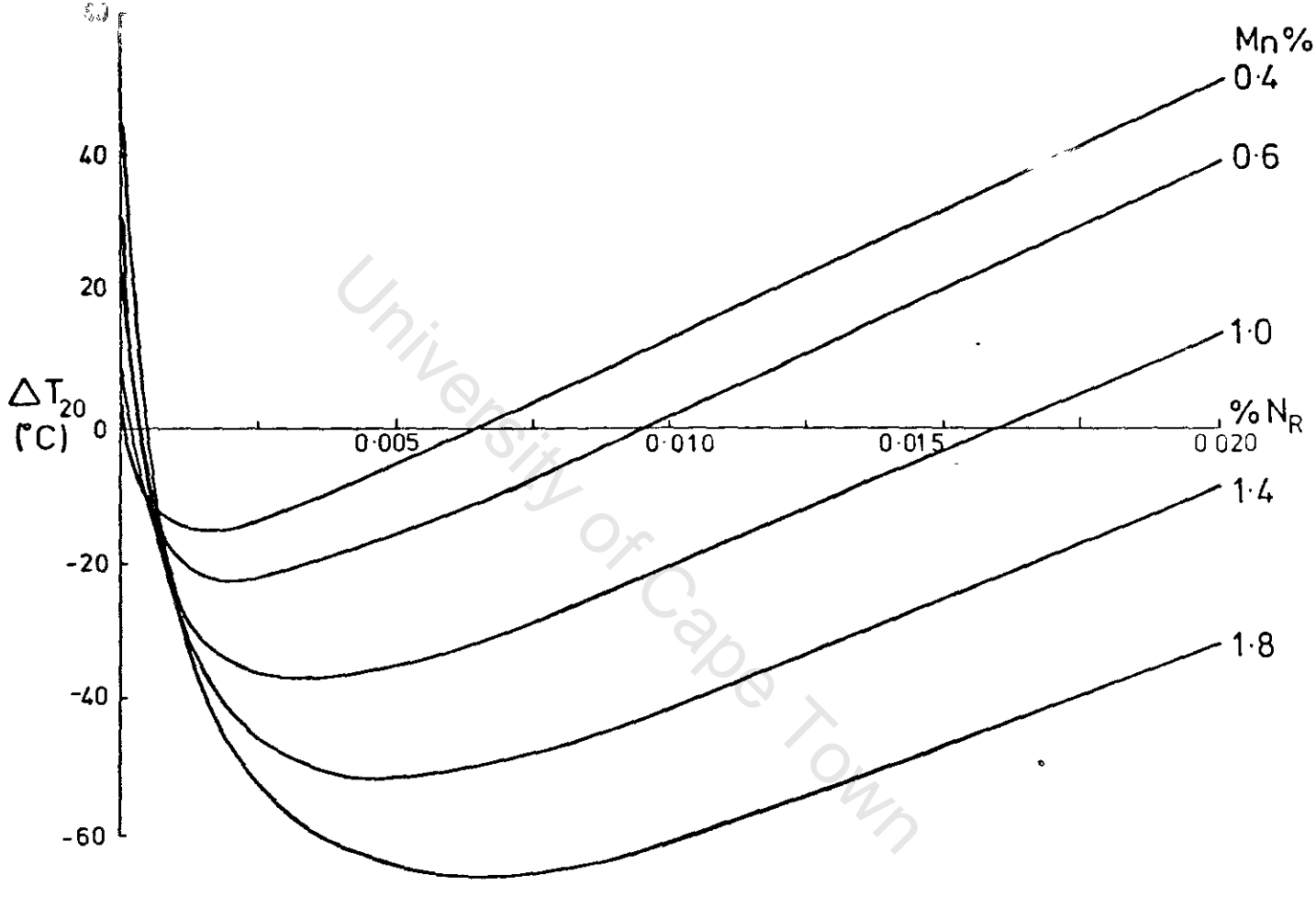

Fig.5·2 Change in transition temperature with N_R constant given by equation 5.4.

analysis is carried out with the variable F' excluded from the data can be seen from this figure, e.g.,

Table 5.1

Regression Group	Mean Mn	Mean N_R	Corrected for	Regression Coefficient N_R
1(low N_R)	1.00	0.0009	264(%C) -11.8($d^{-\frac{1}{2}}$)	-1,666
2(high N_R)	0.66	0.0059	264(%C) -11.8($d^{-\frac{1}{2}}$)	8,548
3(low N_R)	0.52	0.0005	264(%C) -11.8($d^{-\frac{1}{2}}$)	-21,618

The low values obtained for the N_R coefficients in equations 4.1, 4.2, 4.3, and 4.5 can also be explained from Fig. 5-2, e.g.,

Table 5.2

Equation No.	Mean Mn	Mean N_R	Regression Coefficient
4.1	0.6254	0.0032	1961(%N_R)
4.2	0.6254	0.0032	1239(%N_R)
4.3	0.6885	0.0032	Not significant
4.5	0.6988	0.0028	1577(%N_R)

When the mean N_R content lies to the left of the minimum in the curve for any particular (mean) Mn content, the regression coefficient for N_R on linear multiple regression analysis will be negative, and to the right of the minimum this coefficient will be positive. When the mean N_R content

lies near the minimum of the appropriate Mn curve in Fig. 5-2, the coefficient for N_R will approximate to zero and the significance level will become low.

The coefficient for N_R shown in equation 4.16 could be a slight underestimation, since this coefficient varied between 3500 and 4500 on regression analysis from group to group of the data. This coefficient could also be influenced by experimental errors in the determination of the N_{sol} and N_{insol} contents, since variations in time and temperature during initial chemical solution of the steel sample can dissolve more or less of the more stable nitrides.(55) This error could be especially large in the low nitrogen steels (regression groups 1 and 3). The coefficient for N_R is however unlikely to be as high as 8700, as reported by Irvine et al.(53)

If it is assumed that an increase of 1.0 tons/in.^{2} in in σ_o^* increases the transition temperature by approximately 5°C.(47) the coefficient for Mn in equation 4.16 represents an increase in σ_o^* of approximately 5.5 tons/in.^{2}/1.0% Mn. This compares reasonably with approximately 8 tons/in.^{2} at -196°C. and 4 tons/in.^{2} at 18°C. for the increase in σ_o per 1.0% Mn.(49) The exact increase in σ_o^* per 1.0%Mn is however likely to be difficult to determine, since manganese does not appear to form an ideal solid solution with ferrite. It has been

suggested that the manganese atoms form couples within the ferrite lattice,[52] providing preferential low energy sites for nitrogen atoms and thus weakening dislocation locking by the removal of nitrogen from the dislocations. The increases in σ_o^* with increasing Mn content is likely therefore to result from manganese couples, possibly associated with nitrogen atoms, as opposed to single manganese atoms.

No correction has been made in this analysis for manganese combined as sulphides or oxides. This correction may become necessary on commercial steels where the sulphur content may be considerably higher than that of these experimental steels, and where the steel may not be fully deoxidised by the addition of silicon.

5.4 The Regression Coefficients for Ni, Cr, Al and Si_T:

Although it is generally accepted that nickel lowers the transition temperature when alloyed with steel, its effect appears to be small. Equation 4.1 predicts a decrease in transition temperature of 1.8°C. for 0.10% nickel. This compares with approximately 1.7°C. per 0.10% nickel for the 15ft-lb energy transition temperature as determined by Rinebolt and Harris.[34] Manganese is therefore three times more effective in lowering the transition temperature of steels containing nitrogen.

It seems that there is no apparent increase in the lower yield stress of low carbon steels alloyed with nickel when compensating for changes in grain size and pearlite volume fraction,[28] thus nickel in solid solution would be expected to have little effect on the transition temperature. It would seem from the development of equation 5.3 that the small beneficial effect of nickel stems solely from its ability to refine the grain size, see equation 4.4, and this would account for the coefficient for nickel no longer being significant when the variable $d^{-\frac{1}{2}}$ was included in the regression analysis, see equations 4.3, 4.5 and 4.16.

A chromium addition of 0.10% can be seen from equation 4.1 to raise the transition temperature by approximately 2.9°C. and from equation 4.15 by approximately 1.8°C. However, only seven sets of the data had significant additions of chromium, and in all seven cases this addition amounted to approximately 1%. The coefficient for chromium is therefore to be considered with some caution, since these results can be seen to be grouped in Fig.4-1. This result is however in agreement with that published by Rinebolt and Harris[34] who found that 0.10% chromium raised the transition temperature by approximately 3.0°C.

The mechanism by which chromium raises the transition temperature is obscured by the fact that the chromium can exist in a number of forms in the steel, e.g., in solid

solution in the ferrite, as a carbide or as a nitride. It seems likely however that the increase in transition temperature arises mainly from the increase in the pearlite volume fraction brought about by the chromium addition, since the acid insoluble nitrogen content of these steels is less than the average for all the data, and there is apparently little if any increase in yield strength brought about by additions of chromium to ferrite.(56)

Aluminium not combined as aluminium nitride or as Al_2O_3 (Al_{insol}) is shown by equations 4.1 and 4.2 to raise the transition temperature by approximately 13°C. when the residual aluminium is increased by 0.10%. This is in excess of the 1 to 2°C. per 0.10% residual aluminium expected from the results of Lacy and Gersamer(56) if the increase in transition temperature is attributed wholly to an increase in the friction stress resisting dislocation movement. On the other hand, aluminium may alter the twinning propensity of the ferrite. This would raise the transition temperature since twinning has been shown also to initiate cleavage cracks.

Steels with high residual aluminium contents are also generally those in which nearly all the nitrogen is combined as aluminium nitride. In these steels manganese will no longer be able to play any part in the weakening of dislocation locking, and consequently only the effect of manganese on the friction stress would be operational, raising the

transition temperature. This is confirmed by equations 4.15 and 4.16 where the variable F' was added to the data for regression analysis so that the coefficient for Mn in these equations represents only the increase in transition temperature brought about by the increased friction stress due to manganese. The coefficient for Al_R is reduced in equations 4.15 and 4.16 so that 0.10% residual aluminium gives an increase in transition temperature of between $5^{\circ}C$. and $7^{\circ}C$. This is still in excess of that expected due to the increase in σ_o^*, so that the possibility of increased twinning propensity due to aluminium cannot be excluded.

None of the variables silicon, oxygen, N_{insol} or Al_{insol} proved significant, whether examined as a whole or after breaking into fractions, e.g.,

$$Si_T = Si_{SiO_2} + Si_{resid} + Si_{SiN}(N_{insol})$$

$$O_T = O_{Al_2O_3}(Al_{insol}) + O_{SiO_2} + O_{resid}$$

Although the coefficient for Si_T in equation 4.16 showed that a 0.10% increase in silicon content would raise the transition temperature by $6.8^{\circ}C$., this coefficient had a significance level of less than 20% and could be excluded from equation 4.16 without much alterations to the variance ratio for the equation. The addition of data from the high

silicon steels, group 5, lowered the significance level of the coefficient further, and when this data was used in conjunction with equation 4.16 the calculated transition temperatures were all higher than expected, see Fig. 4-9. That is, silicon either had a negative coefficient or a much smaller positive coefficient than shown in equation 4.16. Since a negative coefficient of almost equal magnitude occurred when analysing data for equation 4.15, it must be concluded that silicon has no significant effect in fully deoxidised steels and within the range of silicon content examined here. Silicon has, however, been shown to raise the transition temperature by 4.4°C. per 0.10% addition in some steels.(28) Although the oxygen content never proved to be significant in any of the regression equations it has been shown to raise the transition temperature and to produce intergranular fracture in ferrite in the absence of silicon or other strong deoxidisers.(33) The present regression analysis only occasionally indicated that oxygen raised the transition temperature, but even if this variable had been significant the coefficient was so small as to have a negligible effect in silicon killed steels.

5.5 Errors in Experimental Procedure:

Every effort was made to keep experimental errors to a minimum by keeping metallographic assessments to a minimum. Where possible metallographic assessments such as the % pearlite were substituted for by chemical analysis, and an energy criteria of transition temperature used instead of a macro fracture appearance criteria requiring estimations of the relative proportions of granular to shear fracture.

The measurement of grain size by metallographic techniques was however unavoidable. Two different techniques of grain size measurement were used, the first on steels from data groups 2,3,4 and 5, and the second on steels from data group 1. For the first technique the pearlite grains, usually much smaller than the corresponding ferrite grains, were ignored or simply counted as extensions of the ferrite grain boundaries. With steels from data group 1 the ferrite grain size in many of the specimens was considerably finer than those of the steels in groups 2, 3, 4 and 5, and in many instances approached the size of the pearlite grains. It was decided therefore to include the pearlite grains in this assessment of grain size, and to compensate for this difference in technique by an alteration in the value of the constant obtained in the regression equations, e.g., as for K_7 in equation 4.16. In addition to this there was the accumulation of errors associated with non-etching

primary and sub grain boundaries, variation from section to section and banding in the microstructure. Errors in the chemical analysis were in general minimal, except for those associated with analysis for N_{sol} and N_{insol}. The relative proportions of N_{sol} to N_{insol} are dependent on the temperature during solution and the time taken to dissolve the steel sample in sulphuric acid. This error would be largest in those steels of low total nitrogen content, and although every effort is normally made to keep procedure variables constant, some variations always occur.

The transition temperature T_{20} was taken from a line of best fit through the experimental points on graphs of Charpy energy versus temperature. In most instances the experimental results fell within a range of $\pm$ 10°C. of this line, but in a few cases the experimental results exceeded this range and were in some instances up to $\pm$ 30°C. from the best fit curve.

When the above errors are considered together, the 95% confidence limits of $\pm$ 25°C. for equation 4.16 seem quite reasonable. This means that in 95 cases out of every 100 the transition temperature is likely to be within $\pm$ 25°C. of that predicted by equation 4.16 from the chemical analysis and grain size. This range could be reduced to $\pm$ 20°C. if it was considered acceptable for 9 out of every 10 sets of data examined to fall within this range.

Fracture appearance assessments were made on all of the fractured specimens for comparison with the energy-temperature curve. In general these surfaces showed less than 5% shear, or 95% granular fracture, at the 20ft-lb energy transition temperature.

In some cases the fracture surface, although appearing granular, was uneven, as if a number of parallel cleavage cracks has propagated across the surface and had joined to complete the fracture. Electron fractography showed these surfaces to have small areas of microvoid coalescence fracture, see Fig. 1-2, despite the fracture appearing granular on a macro scale. For this reason a fracture appearance criteria was not used for the transition temperature.

CHAPTER 6.

APPLICATION OF EQUATIONS AND CONCLUSIONS.

6.1 Application of Equations 4.15 and 4.16 to Published Data:

Although a considerable amount of research has been carried out and published on the effect of metallurgical variables on the transition temperature, in most cases insufficient data is recorded to enable equations 4.15 or 4.16 to be used, i.e., in very few instances is data on N_{sol}, N_{AlN} and grain size for each test material published.

Data on the series of steels used by Irvine et al[53] has been obtained elsewhere,[57] and the calculated transition temperature from this data, using equation 4.16, is shown in Fig. 6-1 with the 95% confidence limits from the data used to derive equation 4.16. In this instance the data is complete except for data on N_{insol}, Al_{insol}, and O_T, but grain size measurements, total nitrogen, N_{AlN}, and total aluminium contents are given. The constant term K_7 was found to have a value 75.4 for this data series. This difference in constant is probably the result of differences in the techniques used for grain size measurement.

Although these results, shown in Fig. 6-1, show general agreement with equation 4.16, there is considerable scatter beyond the 95% confidence limits. This error occurs in part

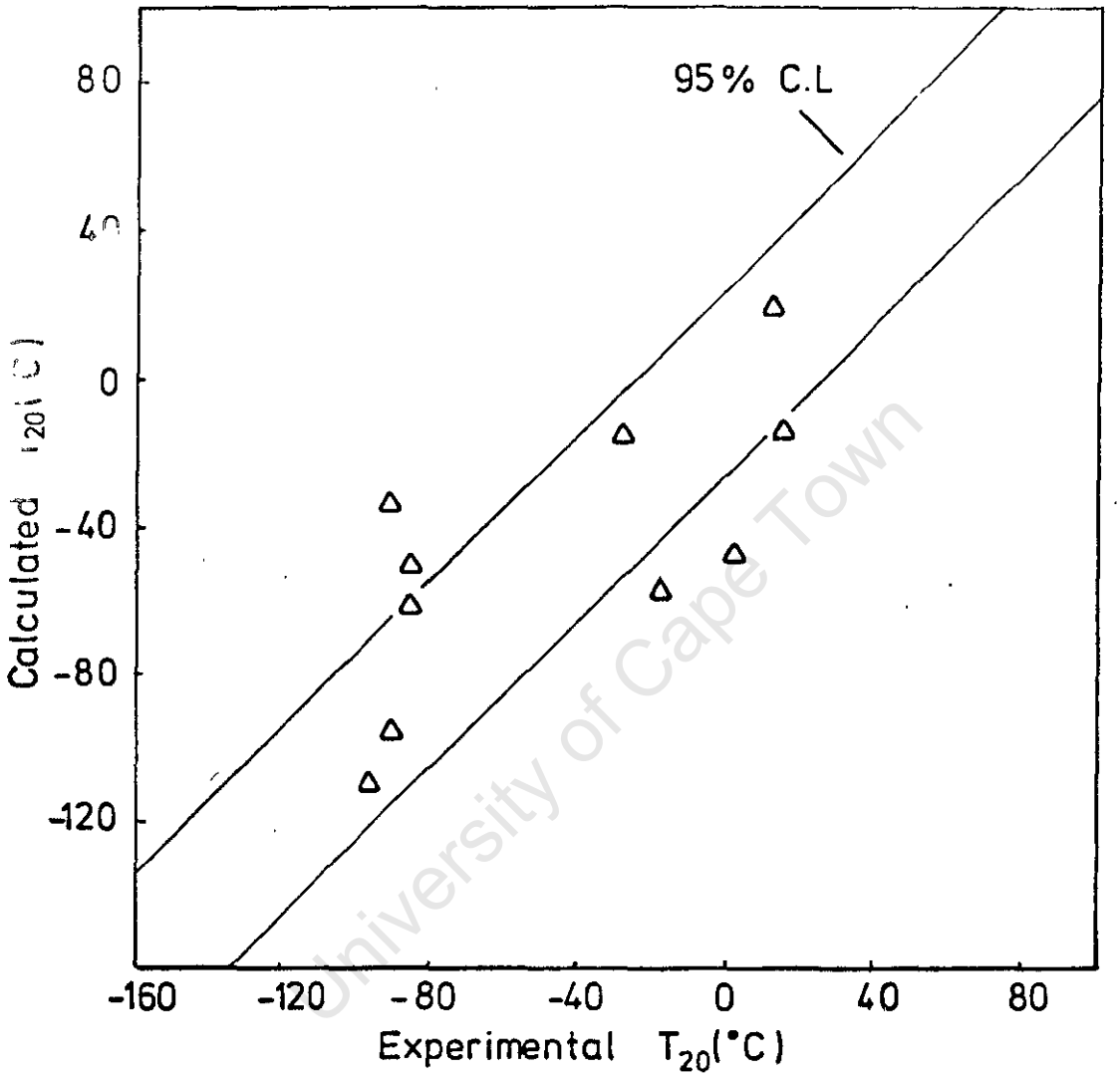

Fig.6·1 Published data from ref. 53 used with equation 4.16 .

due to these steels, except in two instances, containing very low Si_T contents so that they have not been fully deoxidised prior to the addition of aluminium. The positive coefficient for Si_T in equation 4.16 should not therefore be applied to this data, and it is more probable that any silicon in these steels would lower the transition temperature, (i.e. have a negative coefficient), since it would combine with oxygen to deoxidise the steel. It is emphasised again that the coefficient for Si_T in equation 4.16 has a low significance level and that the equation has been derived from fully deoxidised steels. If to counteract this effect the negative coefficient for Si_T from equation 4.15 is used, the corrected values for the calculated T_{20} show far better agreement with the experimental values, see Fig. 6-2.

Equation 4.16 can also be applied to a few of the results of Rinebolt and Harris[34] where data on the nitrogen content of their experimental steels is available. Since these nitrogen contents represent the total nitrogen content, data on steels containing strong nitride formers was not considered. Grain size measurements given in this data were obtained by comparison with A.S.T.M. charts and only the appropriate A.S.T.M. grain size number recorded. Some error is likely as a consequence since each A.S.T.M. grain size number covers a range of approximately 1.4 $d^{-\frac{1}{2}}$ ($mm^{-\frac{1}{2}}$) over the range measured.

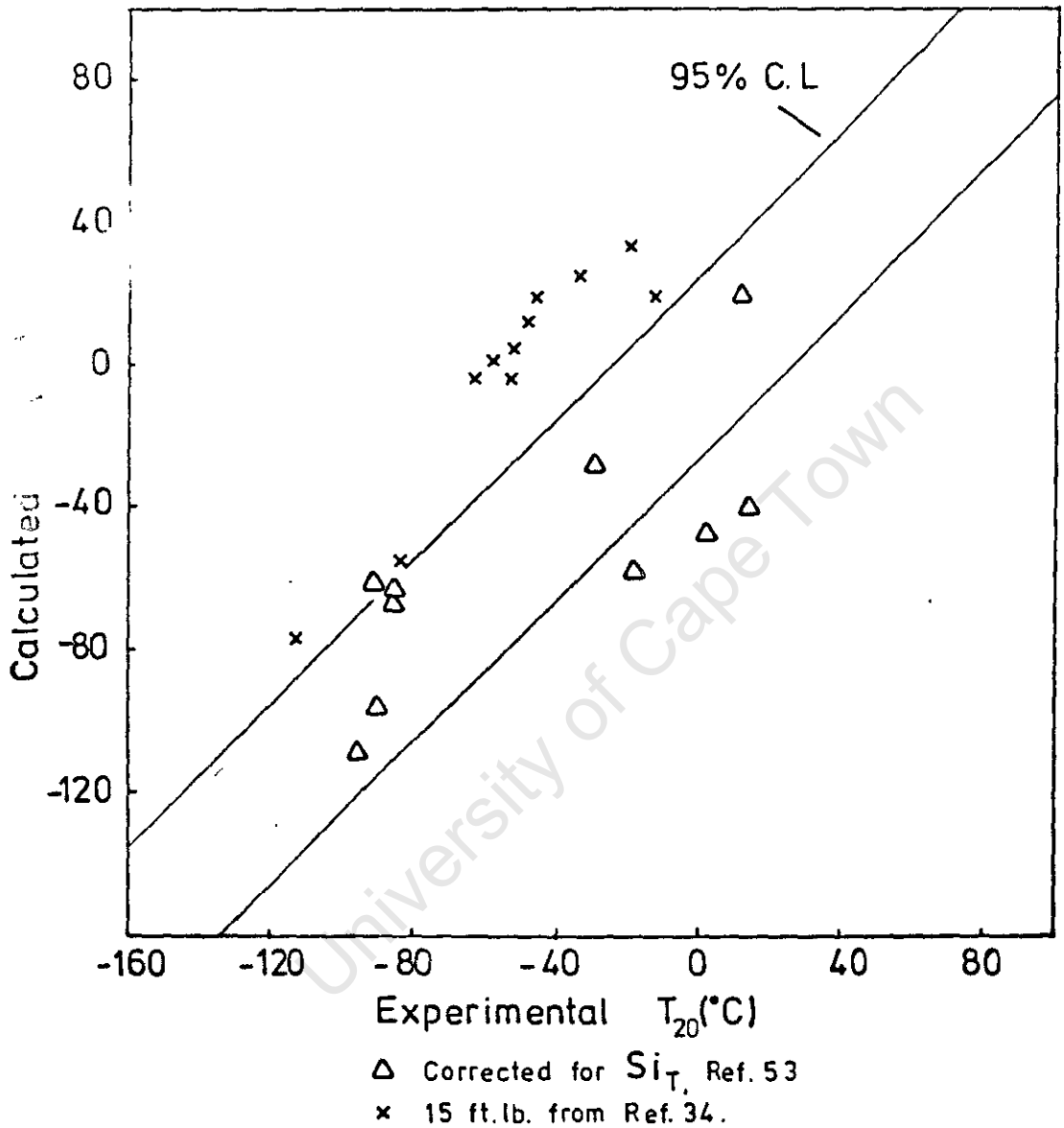

Fig. 6·2 Published data used with equation 4.16 .

The calculated transition temperature for the 20ft-lb energy level is compared in Fig. 6-2 with the experimental 15ft-lb energy transition temperature obtained by Rinebolt and Harris. These results, on silicon deoxidised steels, give an almost parallel line to that expected from equation 4.16, with the experimental 15ft-lb transition temperature lower than that calculated for the 20ft-lb energy level.

Both of the above sets of results compare reasonably with equation 4.16, or equation 4.16 modified for steels not fully deoxidised with silicon, i.e., by using the negative coefficient for Si_T from equation 4.15. By comparison a very poor correlation between the calculated and experimental transition temperatures is obtained, see Fig. 6-3, from data from regression groups 1, 2, 3, and 4 when used with the following equation derived by Irvine et al.[53 & 57]

$$I.T.T.(^{\circ}C.) = -7 + 44(\%Si) + 75(\%Al) + 8,700(\%N_R) + 275(\%C) - 11.6(d^{-\frac{1}{2}})$$

.....Eqn. 6.1

In the above equation the term 275(%C) has been substituted for the original 2.2(% Pearlite), and $-11.6(d^{-\frac{1}{2}})$ $(mm^{-\frac{1}{2}})$ for the original $-2.3(d^{-\frac{1}{2}})$ $(ins^{-\frac{1}{2}})$.

Even when the constant in the above equation is adjusted to compensate for differences in the techniques used to measure grain size, a satisfactory correlation

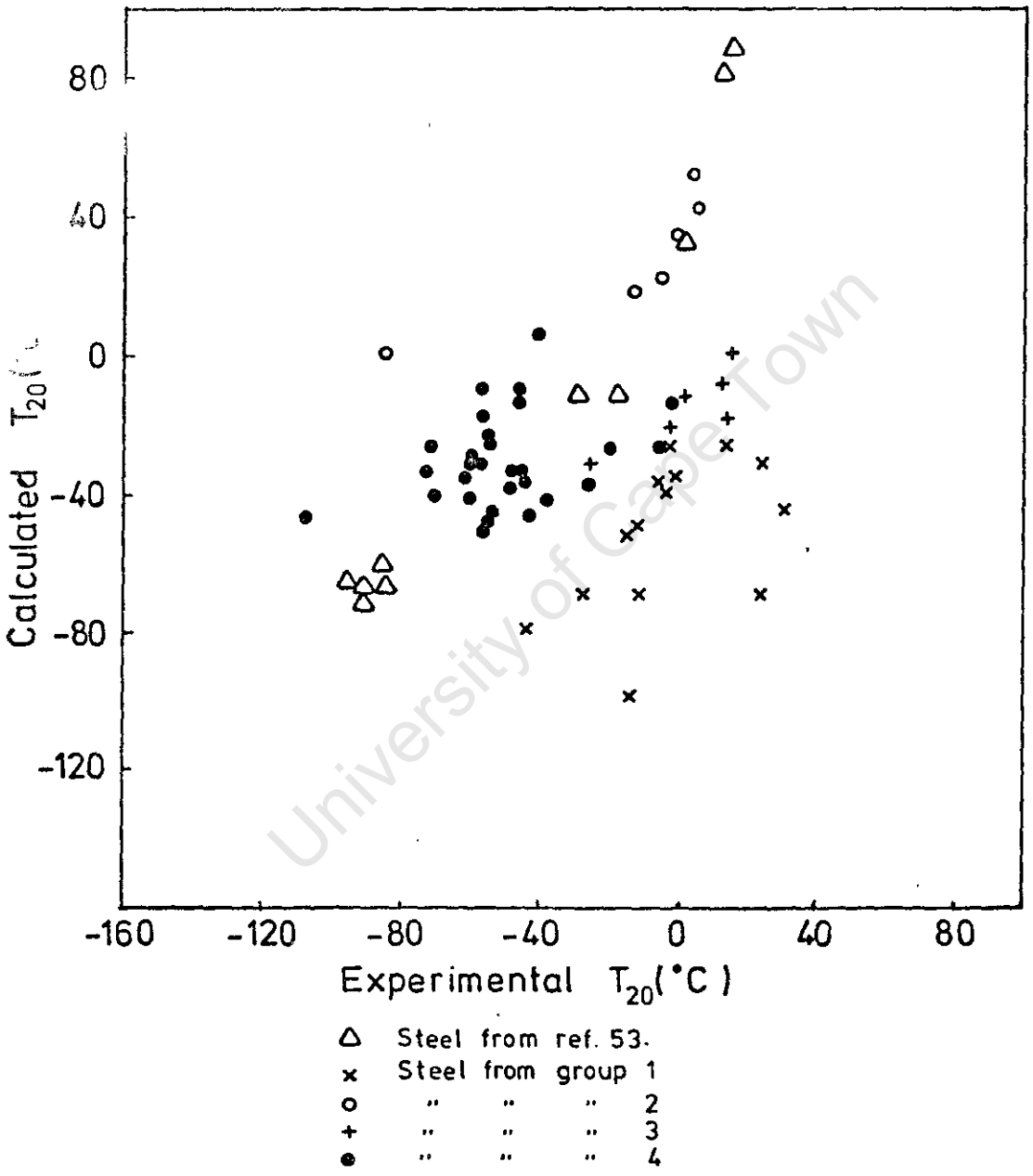

Fig. 6·3 Calculated and observed transition temperatures for experimental steels using equation 6.1 .

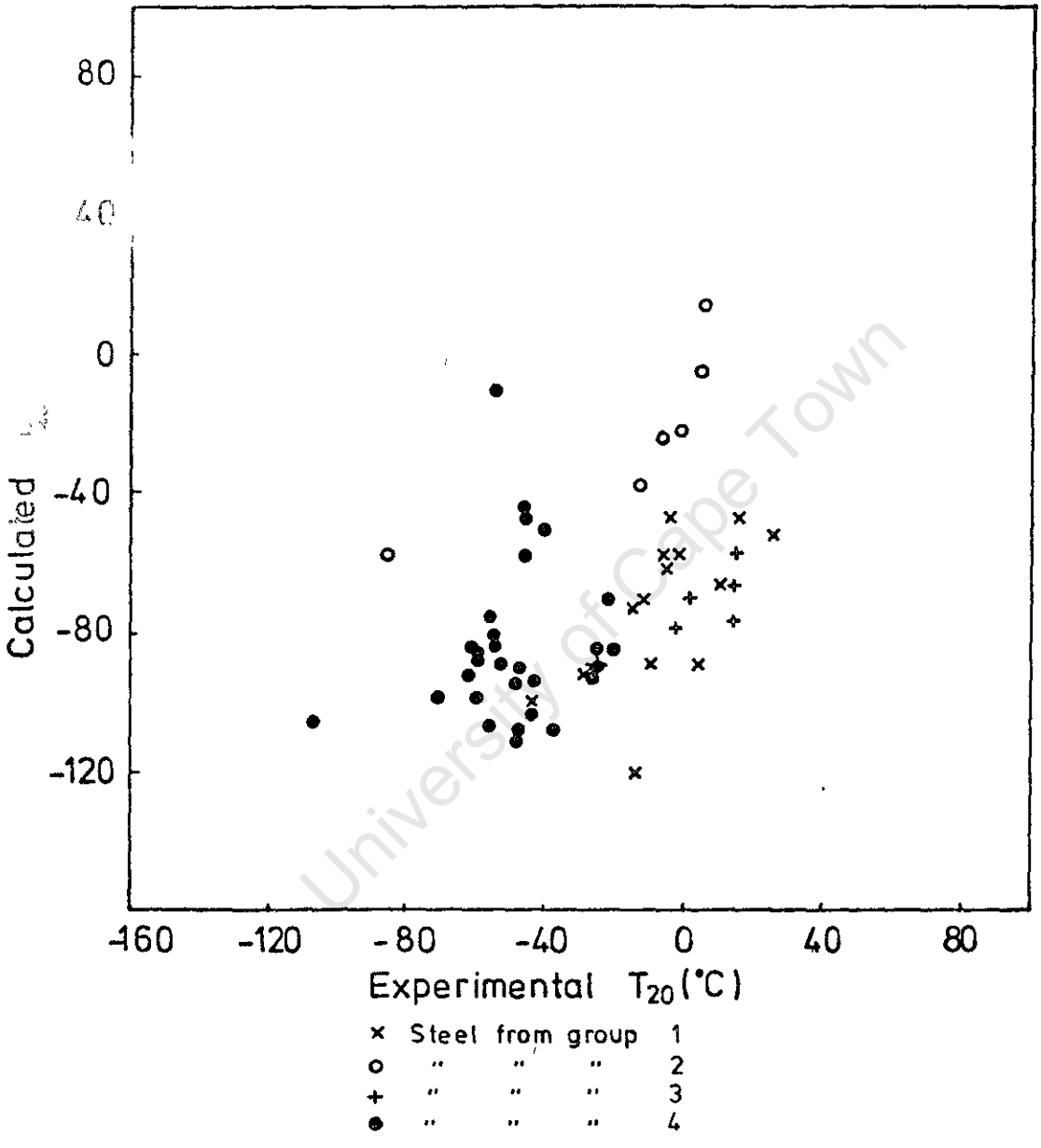

ig. 6·4 Calculated and observed transition temperature for experimental steels using equation 6.1 with corrected constant.

between the calculated and experimental 20ft-lb energy transition temperature is not obtained, see Fig. 6-4. Part of this error could be attributed to the fact that equation 6.1 was determined for the 50% brittle fracture appearance transition, using the standard Charpy test, but it is considered that the largest errors result from the coefficient for N_R in equation 6.1, and the lack of any variable to compensate for dislocation locking strength in this equation.

6.2 Application of Equations 4.16 and 5.3 to Commercial and Other Experimental Steels:

Data from four commercial 110-ton casts of carbon manganese steel, normalised from 900°C. as $1\frac{1}{4}$ in. diameter bar, (see Table A7 for analysis) was also examined. The experimental transition temperatures are compared in Fig.6-5 with those predicted from equation 5.2. These results can be seen to agree closely with the predicted transition temperatures. On the other hand, the four low nitrogen experimental casts, which showed ferrite-pearlite banding in the microstructure, and were therefore excluded from the regression analysis data (group 1) and included in Table A7, all show experimentally determined transition temperatures lower than that calculated from equation 4.16. Banding in the microstructure can probably be considered as a form of fibring with alternating hard and soft layers, so that a lower than expected

between the calculated and experimental 20ft-lb energy transition temperature is not obtained, see Fig. 6-4. Part of this error could be attributed to the fact that equation 6.1 was determined for the 50% brittle fracture appearance transition, using the standard Charpy test, but it is considered that the largest errors result from the coefficient for N_R in equation 6.1, and the lack of any variable to compensate for dislocation locking strength in this equation.

6.2 Application of Equations 4.16 and 5.3 to Commercial and Other Experimental Steels:

Data from four commercial 110-ton casts of carbon manganese steel, normalised from 900°C, as $1\frac{1}{4}$ in. diameter bar, (see Table A7 for analysis) was also examined. The experimental transition temperatures are compared in Fig.6-5 with those predicted from equation 5.2. These results can be seen to agree closely with the predicted transition temperatures. On the other hand, the four low nitrogen experimental casts, which showed ferrite-pearlite banding in the microstructure, and were therefore excluded from the regression analysis data (group 1) and included in Table A7, all show experimentally determined transition temperatures lower than that calculated from equation 4.16. Banding in the microstructure can probably be considered as a form of fibring with alternating hard and soft layers, so that a lower than expected

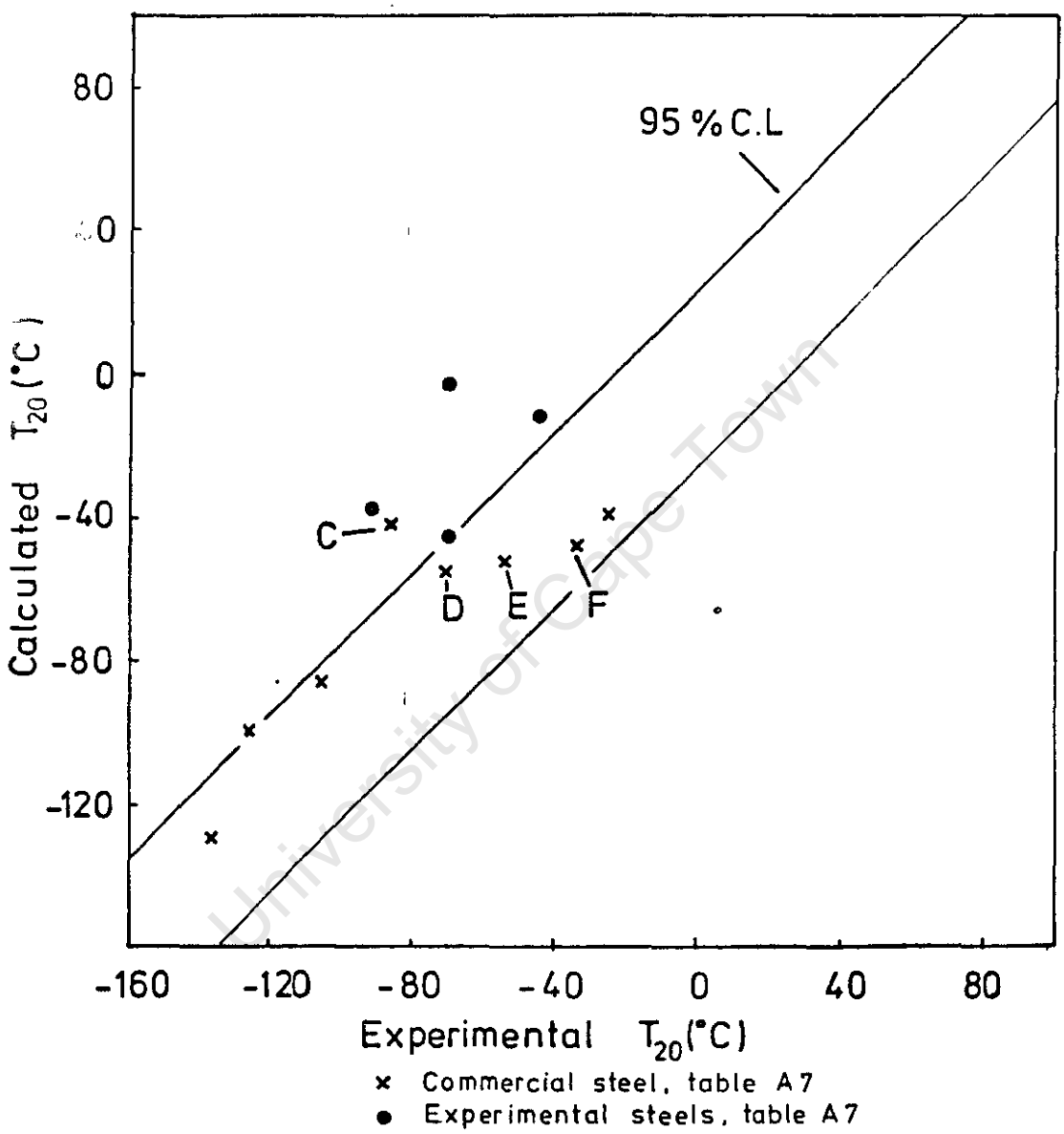

Fig. 6·5 Calculated and observed transition temperatures for steels from table A7 using equation 4.16 .

transition temperature would seem possible.

Four sample bars from a 110-ton commercial cast containing an addition of 0.022% niobium were also examined. These results are shown in Table A7 and Fig.6-5. The samples were (C) $1\frac{1}{4}$ in. diameter bar normalised from 900°C., (D) $\frac{7}{8}$ in. diameter normalised from 880°C., (E) $1\frac{1}{4}$ in. diameter bar in the hot rolled condition and (F) $\frac{7}{8}$ in. diameter in the hot rolled condition. It can be seen from Fig.6-5 that the niobium addition has not significantly affected the transition temperature except in the case of the $1\frac{1}{4}$ in. diameter bar cooled from 900°C. In this case there is a decrease in the transition temperature over that expected from equation 5.3. Since this equation is independent of grain size, and niobium is a known ferrite grain refiner,[57] the lower than calculated transition temperature for the normalised niobium steels can be assumed to result from a grain size smaller than calculated by equation 4.4.

6.3 Conclusions:

The brittle (cleavage) to ductile transition temperature of metals has been shown from theoretical considerations to approximate to the equation

$$T_c = \sigma_o^* + C - \left(\frac{\beta G \gamma}{k_y} - k_y\right) d^{-\frac{1}{2}}$$

(.....Eqn.2.10)

This equation can be further modified to include the effect of alloying additions by using equation 5.2 so that the above equation becomes

$$T_c = \left[\sigma_o^* + k' (\%\text{alloy})\right] + C - \left[\frac{\beta G \gamma}{k_y} - k_y\right] d^{-\frac{1}{2}}$$

.....Eqn.6.2

where the term in the first bracket represents an equivalent temperature independent friction stress which accounts for solid solution hardening brought about by the alloy addition, and the term in the second bracket represents the strength of dislocation locking.

Since both the strength of dislocation locking and the grain size, represented by $d^{-\frac{1}{2}}$, are varied in steels by the addition of certain alloys such as aluminium and manganese, and by the nitrogen content which is a function of the steelmaking process, the above equation requires further modification so that each term includes only one variable. This can be accomplished by using a constant, equal to the mean of the locking strength, with the variable $d^{-\frac{1}{2}}$, and by including a further variable in the equation which will account for variations in locking strength. This variable is likely to be a function of the residual nitrogen and the manganese contents in low carbon steels, since these elements appear to interact so that dislocation locking by nitrogen is weakened in the presence of manganese.

The suggested locking strength variable has the following form

$$- K_4(F') + K_5(\%N_R) + K_c$$

where $F' = \dfrac{(\%Mn)(\%N_R)}{(\%Mn) + K_n(\%N_R)}$

Equation 6.2 can now be modified to include this variable, so that for a low carbon steel with the normal range of alloying elements, the equation becomes

$$T_c = k_c(\%C) + k_{Mn}(\%Mn) + k_{Cr}(\%Cr) + - - - - - - - - - K_4(F') + K_5(\%N_R) - k_d(d^{-\frac{1}{2}}) + \text{constant} \quad \text{.....Eqn. 6.3}$$

Linear multiple regression analysis of data covering a wide range of elements normally found in low carbon, low alloy structural steels resulted in the following equation, similar to the above, for the ductility transition temperature

$$T_{20} = 264(\%C) - 11.8(d^{-\frac{1}{2}}) + 28(\%Mn) - 140{,}000(F') + 3850(\%N_R) + 18(\%Cr) + 50(\%Al_R) + 68(\%Si_T) + \text{constant} \quad (\text{.....Eqn.4.16})$$

where the constant K_n in the variable F' equals 1500.

It was found that this equation could be modified for steels in the normalised condition by virtue of a relationship between $d^{-\frac{1}{2}}$ and Mn, Ni and N_{AlN} (equation 4.4), so that the variable $d^{-\frac{1}{2}}$ was excluded and the equation became

$$T_{20} = 264(\%C) + 17(\%Mn) - 140,000(F^{\prime}) + 3850(\%N_R) + 18(\%Cr) + 50(\%Al_R) + 68(\%Si_T) - 12(\%Ni) - 1980(\%N_{AlN}) - 61 \quad (\ldots\ldots \text{Eqn. } 5.3)$$

This latter equation agreed closely with a similar equation obtained directly by regression analysis without the variable $d^{-\frac{1}{2}}$ included in the data (equation 4.15). The coefficient for Si_T in the above equations has a low significance level and is only applicable to fully deoxidised steels. In steels not fully deoxidised ($> 0.20\%$ Si_T) the negative coefficient for Si_T from equation 4.15 appears to be more correct, although still of low significance level.

The effect of nickel on the transition temperature was shown thus to be purely due to its effect on ferrite grain size.

When equation 5.4, representing locking strength, is differentiated with respect to N_R and equated to zero, the optimum manganese addition for any residual nitrogen content can be determined. This is shown in Fig. 6-6 for a

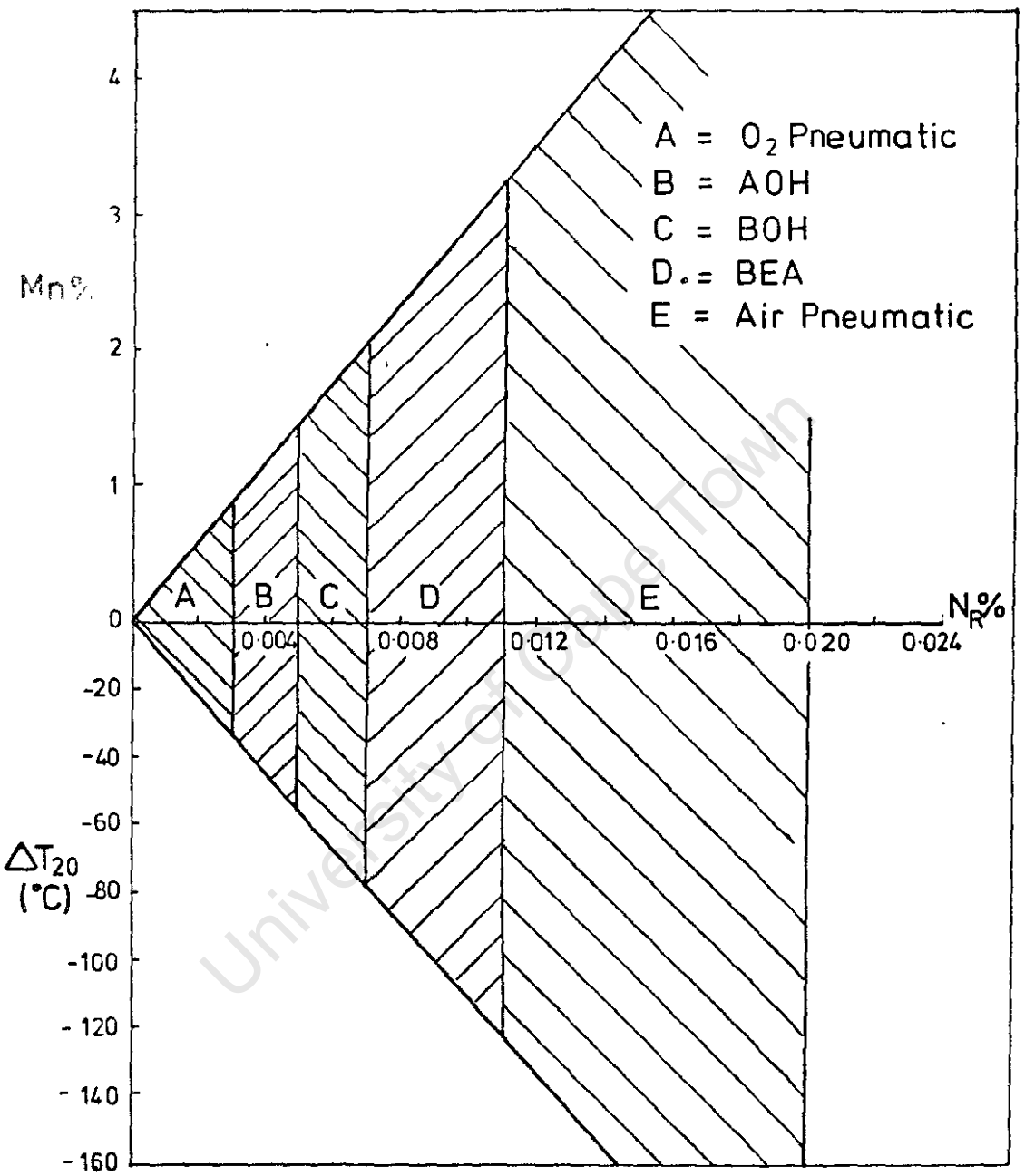

Fig. 6·6 Manganese addition required for optimum transition temperature with various steel manufacturing processes. (for constant grain size & not corrected for aluminium additions)

range of nitrogen contents covered by normal steelmaking practice. Also shown on this figure is the corresponding decrease in transition temperature brought about by this combined manganese-nitrogen content. In steels containing strong nitride formers such as aluminium, vanadium or titanium, an appropriate correction has to be made to Fig. 6-6 to compensate for any reduction in residual nitrogen content.

The above equations (4.16 and 5.2) have been shown to be applicable to published results, and to account for the variation in transition temperature observed in a limited number of commercial steels.

REFERENCES

1. GREENBERG, H. 1957, Metal Progress, vol.71, No.6, p.75

2. LAIRD, C. 1967, "Fatigue Crack Propagation", ASTM Special Tech. Publ. No.415, Philadelphia, Pa., p.131

3. McMILLAN, J.C. & PELLOUX,R.M.N., ibid, p.505

4. ERASMUS, L.A. 1970, "The Failure of Metals in Service", DSIR - Auckland University Symposium, P.57.1

5. PARKER, E.R. 1957, "Brittle Behaviour of Engineering Structures", John Wiley & Sons Inc., N.Y.

6. TIPPER, C.F. 1962, "The Brittle Fracture Story", University Press, Cambridge.

7. TETELMAN, A.S. & McEVILY, A.J. 1967, "Fracture of Structural Materials", John Wiley & Sons Inc., N.Y.

8. INGLIS, C.E. 1913, Trans.Inst.Naval Archit., vol.55, p.219

9. GRIFFITH, A.A. 1920, Phil.Trans.Roy.Soc.London, vol.221A, p.163

10. FELBECK, D.K. & OROWAN, E. 1955, Welding J.Res.Suppl., vol.34, p.570s

11. LOW, J.R. 1959, "Fracture", Ed.Averbach B.L., et al, M.I.T., Wiley, N.Y., p.68

12. IRWIN, G.R. 1958, Encyclopedia of Physics, vol.6, Springer, Heidelberg

13. LOW, J.R. 1953, "Relation of Properties to Microstructure", A.S.M., Novelty, Ohio, p.163

14. McCLINTOCK, F.A. & ARGON, A.S. 1966, "Mechanical Behaviour of Materials", Addison-Wesley, U.S.A., p.549

15. HAHN, G.T., et al 1959, Welding J.Res.Suppl., vol.38, p.372s

16. AVERBACH, B.L. et al 1959, "Fracture", M.I.T., Wiley, N.Y., pp 20 and 54.

17. PETCH, N.J. 1953, J.I.S.I., vol.173, p.25.

18. DINGLEY, D.J. & McLEAN, D. 1967, Acta Met., vol.15, p.885.

19. JOHNSTON, T.L. et al 1965, Phil.Mag., vol.12, p.305.

20. TWEEDDALE, J.G. 1964, "Mechanical Properties of Metals", Allen & Unwin Ltd., London.

21. 1959 British Standard Specification 131, Part 2.

22. HALL, W.J. et al 1967 "Brittle Fracture of Welded Plate", Prentice-Hall Inc., N.J.

23. WELLS, A.A. 1965, British Weld.J., vol.12, No.1, p.2.

24. FEARNEHOUGH, G.D. & HOY, C.J. 1964, J.I.S.I., vol.202, p.912.

25. WILSHAW, T.R. 1966, J.I.S.I., vol.204, p.936.

26. BOULGER, F.W. 1969, "Fracture", Ed. Liebowitz, H., vol.6, chap.4, p.204.

27. FEARNEHOUGH, G.D. & VAUGHAN, H.G. 1963, Welding J.Res. Suppl., vol.42, p.202s.

28. PICKERING, F.B. & GLADMAN, T. 1963, "Metallurgical Developments in Carbon Steels", I.S.I. Special Report 81, London, p.10.

29. BURNS, K.W. & PICKERING, F.B. 1964, J.I.S.I., vol.202, p.899.

30. HODGE, J.M. et al 1959, Trans.A.I.M.E., vol.215, p.745.

31. BOULGER, F.W. et al 1956, Welding Research Council Bulletin 26, N.Y.

32. SAGE, A.M. & COPLEY, F.E.L. 1960, J.I.S.I., vol.195, p.422.

33. REES, W.P. & HOPKINS, B.E. 1952, J.I.S.I., vol.172, p.403.

34. RINEBOLT, J.A. & HARRIS, W.J. 1951, Trans.A.S.M., vol.43 p.1175.

35. ALLEN, N.P. et al 1953, J.I.S.I., vol. 174, p.108.

36. ERASMUS, L.A. 1964, J.I.S.I., vol.202, p.32.

37. ERASMUS, L.A. 1967, Proc.First Australasian Conf. on the Mechanics of Structures and Materials., University of N.S.W., Australia.

38. ERASMUS, L.A. 1966, Iron & Steel, vol.40, p.477.

39. ERASMUS, L.A. et al 1970, University of Canterbury report Mech./MM/050/70, New Zealand.

40. IRVINE, K.J. & PICKERING, F.B. 1963, J.I.S.I., vol.201, p.944.

41. VOLK, W. 1958, "Applied Statistics for Engineers", McGraw-Hill Inc., N.Y.

42. WILLIAMS, E.J. 1959, "Regression Analysis", John Wiley and Sons Inc., N.Y.

43. I.B.M. 1968, "System 360 Scientific Subroutine Package", 360A-CM-03X, Version 3, H20-0205-3, 4th edition.

44. FISHER, R.A. & YATES, F. 1963, "Statistical Tables .....", 6th edition, Oliver & Boyd Ltd., London.

45. BEEGHLEY, H.F. 1949, Anal.Chem., vol.21, p.1513.

46. 1961 "Standard Methods of Analysis", The United Steel Co.Ltd., Percy Lund,Humphries & Co.Ltd., London.

47. PETCH, N.J. 1959, "Fracture", Ed.Averbach, B.L. et al, M.I.T. Wiley & Sons Inc., N.Y.

48. BUCHER, J.H. et al 1969, "Fracture", Ed.Liebowitz, H., vol. 6, chap.5, p.270.

49. PETCH, N.J. & HESLOP, J. 1957, Phil.Mag., vol. 47, p.649.

50. BARNBY, J.T. & JOHNSON, M.R. 1969, Metal Science Journal, vol.3, p.155.

51. ERASMUS, L.A. 1964, J.I.S.I., vol.202, p.128.

52. GLADMAN, T. & PICKERING F.B. 1965, J.I.S.I., vol.203, p.1212.

53. IRVINE, K.J. et al 1967, J.I.S.I., vol.205, p.161.

54. GLADMAN, T. & PICKERING, F.B. 1967, J.I.S.I., vol.205, p.653.

55. 1962 Report A3763/-/62, United Steel Co., R. & D.D. Sheffield, England.

56. LACY, C.E. & GENSAMER, M. 1944, Trans.A.S.M., vol.32, p.88.

57. IRVINE, K.J. et al 1964, Report P.M. 4635/14/64, United Steel Co., R. & D.D., Sheffield, England.

APPENDIX 'A'

Regression data:-

Tables A1 to A7

TABLE A1 - VACUUM MELTED PLAIN CARBON STEELS, NORMALISED FROM 89°C. (Element wt%)

Regression Group	Cast	C	Si	S	P	Mn	Ni	Cr	O	N_{sol}	N_{insol}	Al_{sol}	Al_{insol}	N_{AlN}	$d^{-\frac{1}{2}}$ ($mm^{-\frac{1}{2}}$)	T_{20} (°C)
2	329	0.09	0.20	0.006	0.006	0.63	0.03	0.02	0.0028	0.0076	0.0034	0.003	0	0.0020	6.30	-56
4	330	0.12	0.23	0.008	0.005	0.64	0.02	0.02	0.0010	0.0096	0.0026	0.015	0.004	0.0045	9.40	-60
4	331	0.16	0.22	0.007	0.006	0.60	0.02	0.02	0.0017	0.0122	0.0020	0.015	0.004	0.0086	9.40	-60
4	332	0.15	0.25	0.005	0.005	0.60	0.02	0.02	0.0023	0.0124	0.0022	0.021	0.014	0.0044	9.40	-40
4	333	0.16	0.20	0.006	0.006	0.62	0.02	0.02	0.0031	0.0142	0.0018	0.030	0.004	0.0082	9.40	-56
4	334	0.16	0.23	0 006	0.006	0.62	0.02	0.02	0.0028	0.0146	0.0014	0.038	0.003	0.0128	9.40	-54
4	335	0.15	0.22	0.008	0.007	0.62	0.01	0.02	0.0019	0.0120	0.0016	0.035	0	0.0093	8.20	-71
4	336	0.17	0.23	0.008	0.004	0.61	0.02	0.02	0.0015	0.0148	0.0022	0.051	0.003	0.0110	9.40	-55
4	337	0.17	0.23	0.005	0.005	0.62	0.02	0.02	0.0011	0.0140	0.0016	0.055	0	0.0131	9.60	-56
4	338	0.18	0.22	0.007	0.006	0.62	0.02	0.02	0.0010	0.0144	0.0022	0.062	0	0.0140	9.60	-48
4	339	0.15	0.20	0.005	0.008	0.61	0.02	0.02	0.0058	0.0178	0.0020	0.029	0.003	0.0091	9.40	-46
4	340	0.16	0.23	0.008	0.005	0.64	0.02	0.02	0.0010	0.0164	0.0014	0.096	0.003	0.0100	8.20	-46
3	343	0.19	0.22	0.006	0 006	0.39	0.01	0.02	0.0012	0.0006	0.0004	0.045	0	0	8.40	-28
3	344	0.22	0.22	0.006	0.005	0.61	0.01	0.02	0.0012	0.0008	0.0002	0.078	0.008	0	8.40	-3
4	345	0.16	0.21	0.007	0.005	0.63	0.01	0.02	0.0015	0.0068	0.0008	0.018	0.002	0.0058	9.17	-57
4	346	0.13	0.23	0.006	0.004	0.61	0.02	0.02	0.0015	0.0108	0.0010	0.029	0	0.0058	9.40	-55

TABLE A2 - AIR CAST PLAIN CARBON AND CARBON-MANGANESE STEELS, NORMALISED FROM 890°C. (Element wt%)

Regression Group	Cast	C	Si	S	P	Mn	Ni	Cr	O	N_{sol}	N_{insol}	Al_{sol}	Al_{insol}	N_{AlN}	$d^{-\frac{1}{2}}$ ($mm^{-\frac{1}{2}}$)	T_{20}(°C)
2	907	0.23	0.11	0.006	0.006	0.52	0.02	0.02	0.0221	0.0056	0.0002	0	0	0	5.96	5
2	908	0.25	0.11	0.007	0.006	0.51	0.02	0.02	0.0227	0.0050	0.0004	0.006	0.007	0	6.66	-1
2	909	0.24	0.12	0.007	0.007	0.52	0.02	0.02	0.0098	0.0056	0.0004	0.008	0.005	0	6.96	-6
2	910	0.22	0.17	0.005	0.005	0.53	0.02	0.02	0.0080	0.0044	0.0004	0.009	0.003	0	6.96	-13
4	911	0.24	0.16	0.008	0.008	0.49	0.02	0.02	0.0081	0.0056	0.0006	0.019	0.006	0.0046	8.93	-20
4	912	0.23	0.16	0.006	0.007	0.53	0.02	0.02	0.0078	0.0054	0.0004	0.038	0.005	0.0047	9.42	-27
4	913	0.23	0.16	0.007	0.007	0.52	0.02	0.02	0.0097	0.0058	0.0004	0.083	0.001	0.0060	9.17	-26
4	1919	0.13	0.15	0.010	0.007	0.51	0.02	0.01	0.0092	0.0046	0.0004	0.060	0.010	0.0042	7.67	-43
2	846	0.20	0.23	0.012	0.012	0.56	0.09	0.12	0.0183	0.0085	0.0010	0	0	0	7.58	4
5	1841	0.17	0.38	0.008	0.006	0.62	0.01	0.03	0.0046	0.0074	0.0010	0.170	0.010	0.0071	8.04	-50
4	2080 N	0.17	0.32	0.006	0.006	0.49	1.11	0.01	0.0052	0.0074	0.0002	0.043	0.009	0.0050	9.43	-73
2	2081 N	0.13	0.22	0.007	0.007	1.35	0.03	0.01	0.0058	0.0074	0.0020	0.009	0.004	0.0012	7.94	-85
4	2082 N	0.13	0.22	0.007	0.007	1.39	0.01	0.01	0.0046	0.0076	0.0002	0.036	0.009	0.0054	9.26	-107
4	2083 N	0.14	0.27	0.007	0.008	1.27	0.01	0.01	0.0042	0.0072	0.0002	0.069	0.003	0.0069	9.43	-94
4	2084 N	0.13	0.18	0.008	0.006	0.92	0.01	0.01	0.0056	0.0076	0.0002	0.024	0.002	0.0041	9.43	-71
5	3256	0.24	0.65	0.007	0.004	0.56	0.01	0.01	0.0051	0.0080	0.0002	0.025	0.003	0.0055	8.81	-43
5	3257	0.24	0.43	0.006	0.005	0.57	0.02	0.01	0.0072	0.0066	0.0004	0.048	0.007	0.0055	8.28	-43

TABLE A3 - AIR CAST CARBON-MANGANESE AND NICKEL STEELS, SLOW COOLED FROM 890°C. (Element wt%)

Regression Group	Cast	C	Si	S	P	Mn	Ni	Cr	O	N_{sol}	N_{insol}	Al_{sol}	Al_{insol}	N_{AlN}	$d^{-\frac{1}{2}}$ ($mm^{-\frac{1}{2}}$)	T_{20}(°C)
4	2076 F	0.18	0.21	0.009	0.005	0.50	3.92	0.02	0.0057	0.0060	0.0004	0.013	0.001	0.0034	9.26	-58
4	2077 F	0.17	0.21	0.007	0.006	0.50	3.93	0.01	0.0051	0.0070	0.0004	0.035	0.005	0.0037	9.90	-62
4	2078 F	0.17	0.21	0.007	0.006	0.42	3.91	0.01	0.0047	0.0066	0	0.066	0.003	0.0038	9.90	-44
4	2079 F	0.18	0.07	0.008	0.006	0.32	2.05	0.01	0.0132	0.0060	0.0004	0.013	0.014	0.0024	9.00	-6
4	2080 F	0.17	0.32	0.006	0.006	0.49	1.11	0.01	0.0057	0.0070	0	0.044	0.009	0.0044	7.94	-2
4	2081 F	0.13	0.22	0.007	0.007	1.35	0.03	0.01	0.0060	0.0084	0.0002	0.009	0.003	0.0055	6.99	-56
4	2082 F	0.13	0.22	0.007	0.007	1.39	0.01	0.01	0.0045	0.0076	0.0002	0.036	0.013	0.0054	8.69	-60
4	2083 F	0.14	0.27	0.007	0.008	1.27	0.01	0.01	0.0049	0.0076	0.0002	0.068	0.004	0.0065	8.20	-49
4	2084 F	0.13	0.18	0.008	0.006	0.92	0.01	0.01	0.0053	0.0078	0.0002	0.026	0.010	0.0064	7.94	-38

TABLE A4 - AIR CAST CARBON-NICKEL AND En 36 STEEL QUENCHED FROM 890°C AND 850°C RESPECTIVELY AND TEMPERED AT 680°C.(Element wt%)

Regression Group	Cast	C	Si	S	P	Mn	Ni	Cr	O	N_{sol}	N_{insol}	Al_{sol}	Al_{insol}	N_{AlN}	$d^{-\frac{1}{2}}$ $(mm^{-\frac{1}{2}})$	T_{20}(°C)
11	837	0.17	0.20	0.026	0.012	0.38	3.39	0.87	0.0285	0.0070	0.0006	0	0	0	...	-88
11	838	0.15	0.21	0.022	0.013	0.35	3.33	0.86	0.0177	0.0068	0.0010	0.004	0.008	0	...	-81
11	839	0.16	0.20	0.025	0.015	0.40	3.39	0.99	0.0064	0.0068	0.0010	0.008	0.009	0	...	-96
11	840	0.16	0.23	0.028	0.015	0.43	3.40	0.99	0.0067	0.0072	0.0008	0.014	0.012	0.0016	...	-91
11	841	0.15	0.29	0.027	0.014	0.43	3.37	0.96	0.0055	0.0072	0.0008	0.077	0.008	0.0074	...	-91
11	842	0.17	0.19	0.028	0.015	0.36	3.37	0.90	0.0045	0.0070	0.0008	0.043	0.008	0.0065	...	-100
11	843	0.16	0.24	0.026	0.012	0.40	3.35	0.96	0.0050	0.0066	0.0008	0.208	0.008	0.0065	...	-72
11	2076 0	0.18	0.21	0.009	0.005	0.50	3.92	0.02	0.0045	0.0060	0.0004	0.009	0.003	0.0040	...	-126
11	2077 0	0.17	0.21	0.007	0.006	0.50	3.93	0.01	0.0050	0.0070	0.0004	0.034	0.002	0.0057	...	-143
11	2078 0	0.17	0.21	0.007	0.006	0.42	3.91	0.01	0.0061	0.0066	0.0002	0.063	0.004	0.0056	...	-137
11	2079 0	0.18	0.07	0.008	0.006	0.32	2.05	0.01	0.0152	0.0060	0.0004	0.014	0.011	0.0029	...	-75
11	2080 0	0.17	0.32	0.006	0.006	0.49	1.11	0.01	0.0053	0.0070	0.0001	0.043	0.006	0.0060	...	-98

TABLE A5 - VACUUM MELTED LOW NITROGEN CARBON STEELS NORMALISED FROM 900°C. (Element wt%)

Regression Group	Cast	C	Si	S	P	Mn	Ni	Cr	O	N_{sol}	N_{insol}	Al_{sol}	Al_{insol}	N_{AlN}	$d^{-\frac{1}{2}}$ ($mm^{-\frac{1}{2}}$)	T_{20} (°C)
5	903 V	0.10	0.33	0.006	0.008	0.56	0.01	0.01	0.0017	0.0008	0.0008	0.009	0	0.0005	7.45	17
3	905 V	0.25	0.26	0.006	0.005	0.54	0.01	0.01	0.0013	0.0010	0.0006	0.035	0	0.0005	5.77	-7
3	906 V	0.25	0.22	0.005	0.007	0.58	0.01	0.01	0.0018	0.0004	0.0006	0.062	0	0.0004	8.15	14
3	907 V	0.17	0.24	0.006	0.004	0.58	0.01	0.01	0.0021	0.0010	0.0008	0.013	0	0.0006	7.90	26
3	908 V	0.26	0.23	0.006	0.005	0.55	0.01	0.01	0.0019	0.0012	0.0012	0.033	0	0.0006	8.15	1
3	909 V	0.27	0.23	0.005	0.009	0.40	0.01	0.01	0.0015	0.0012	0.0006	0.068	0	0.0007	7.45	15
5	975 V	0.24	0.35	0.007	0.006	0.84	0.01	0.01	0.0015	0.0028	0.0014	0.027	0.004	0.0017	7.88	-43
3	977 V	0.22	0.27	0.006	0.006	0.51	0.01	0.01	0.0014	0.0016	0.0004	0.089	0.003	0.0011	7.29	13

TABLE A6 - VACUUM MELTED PLAIN CARBON LOW NITROGEN STEELS, NORMALISED FROM 890°C. (Element wt%)

Regression Group	Cast	C	Si	S	P	Mn	Ni	Cr	O	N_{sol}	N_{insol}	Al_{sol}	Al_{insol}	N_{AlN}	$d^{-\frac{1}{2}}$ ($mm^{-\frac{1}{2}}$)	T_{20}(°C)
1	1179	0.08	0.23	0.008	0.007	0.25	0.01	0.01	0.0380	0.0026	0.0008	0	0	0	6.38	15
1	1180	0.12	0.24	0.005	0.007	0.25	0.01	0.01	0.0014	0.0006	0.0008	0	0	0	6.28	25
1	1181	0.04	0.23	0.005	0.007	0.45	0.01	0.01	0.0024	0.0006	0.0008	0	0	0	5.54	10
1	1182	0.10	0.23	0.010	0.007	0.47	0.01	0.01	0.0010	0.0004	0.0008	0	0	0	6.37	-5
1	1183	0.14	0.23	0.008	0.007	0.67	0.01	0.01	0.0009	0.0008	0.0010	0	0	0	6.43	-4
1	1184	0.11	0.24	0.004	0.008	0.64	0.01	0.01	0.0029	0.0012	0.0008	0	0	0	6.98	-6
1	1185	0.14	0.23	0.005	0.007	0.86	0.01	0.01	0.0011	0.0010	0.0012	0	0	0	7.40	-2
1	1187	0.14	0.26	0.006	0.007	1.13	0.01	0.01	0.0022	0.0008	0.0008	0	0	0	8.60	-12
1	1189	0.13	0.28	0.004	0.007	1.32	0.01	0.01	0.0067	0.0014	0.0010	0	0	0	9.05	-15
1	1190	0.05	0.25	0.010	0.007	1.31	0.01	0.01	0.0010	0.0006	0.0006	0	0	0	7.88	-10
1	1191	0.14	0.25	0.005	0.007	1.49	0.01	0.02	0.0007	0.0006	0.0012	0	0	0	10.12	-28
1	1194	0.09	0.25	0.005	0.007	1.76	0.01	0.01	0.0017	0.0012	0.0004	0	0	0	10.20	-44
1	1195	0.12	0.22	0.007	0.007	1.60	0.01	0.01	0.0013	0.0002	0.0006	0	0	0	9.10	3
1	1196	0.07	0.24	0.009	0.007	1.89	0.01	0.02	0.0007	0.0002	0.0008	0	0	0	10.67	-14

TABLE A7 - COMMERCIAL AND OTHER CARBON MANGANESE STEELS NORMALISED FROM 900°C. (Element wt%)

Regression Group	Cast	C	Si	S	P	Mn	Ni	Cr	O	N_{sol}	N_{insol}	Al_{sol}	Al_{insol}	N_{AlN}	$d^{-\frac{1}{2}}$ ($mm^{-\frac{1}{2}}$)	T_{20}(°C)
9	3/1431	0.11	0.29	0.026	0.013	1.40	0.15	0.07	0.0048	0.0090	0.0002	0.027	0.005	0.0062	...	-137
9	1/1443	0.10	0.27	0.032	0.011	1.42	0.23	0.12	0.0026	0.0108	0.0006	0.029	0.002	0.0080	...	-125
9	1/2381	0.12	0.30	0.038	0.011	1.44	0.17	0.12	0.0085	0.0072	0.0006	0.012	0.010	0.0043	...	-105
9	S A 1	0.11	0.23	0.027	0.015	0.54	0.01	0.01	0.0082	0.0042	0.0006	0	0	0	...	-24
9	1/2109 C	0.19	0.30	0.036	0.019	1.15	0.16	0.10	0.0089	0.0060	0.0006	0.026	...	0.0052	...	-85
9	1/2109 D	0.20	0.28	0.029	0.016	1.14	0.17	0.09	0.0074	0.0074	0.0002	0.026	...	0.0052	...	-70
9	1/2109 E	0.18	0.30	0.029	0.019	1.13	0.16	0.10	0.0104	0.0062	0.0004	0.029	...	0.0006	...	-58
9	1/2109 F	0.20	0.28	0.029	0.016	1.14	0.17	0.09	0.0074	0.0062	0.0004	0.026	...	0.0006	...	-34
9	1938 A	0.53	0.17	0.005	0.007	0.60	0.02	0.02	0.0118	0.0086	0.0008	0	0	0	...	60
9	1938 B	0.53	0.17	0.005	0.007	0.60	0.02	0.02	0.0118	0.0080	0.0002	0	0	0	...	74
9	1186 V	0.16	0.25	0.006	0.007	0.91	0.01	0.01	0.0015	0.0010	0.0008	0	0	0	8.60	-44
9	1188 V	0.17	0.25	0.009	0.007	1.12	0.01	0.01	0.0009	0.0008	0.0008	0	0	0	8.42	-70
9	1192 V	0.10	0.25	0.007	0.007	1.49	0.01	0.01	0.0010	0.0010	0.0010	0	0	0	9.46	-91
9	1193 V	0.13	0.28	0.005	0.007	1.70	0.01	0.01	0.0006	0.0014	0.0010	0	0	0	10.00	-70